UNIVERSITÀ DEGLI STUDI DI CATANIA

Faculty of Engineering

PhD in Electronic Engineering,
Automation and Control of Complex Systems

Doctoral Thesis

INSECT BRAIN MODELING FOR COGNITIVE ROBOTICS

Tutor:
Prof. P. ARENA

Supervisor:
Prof. L. FORTUNA

Student:
PIETRO SAVIO TERMINI

ACADEMIC YEAR 2011-2012

Ai miei genitori,
per avermi sopportato in questo lungo percorso.

Introduction

During his history, man has always tried to imitate nature, to better know and understand himself. Thanks to the improvement of electronic technologies, the instruments with which he has followed this target have been improved, with results more and more realistic. Trying to artificially reproduce what nature has slowly realized and time tested, humans find amazing problems and solutions, that give a contribution to their life quality. Robots are the way humans try to reproduce animals, and study their interaction with the environment. Robots help to better know animals and animals help to create efficient robots. Analyzing animal brains leads to new control systems that could allow robots to be able to orient themselves, to take decisions, to survive alone, to complete dangerous missions, to be completely autonomous. Robot implementation could also lead to predictions, for basic science, deriving from emergent properties of models. The goal of this work is to design and simulate a simplified model of the brain of the *Drosophila melanogaster*. Fly has a small brain that shows a wealth of complex behaviors. Genetic techniques allow to remove parts of the Drosophila brain and the analysis of mutants behavior can lead to hypotheses about the functions of every single brain part. The bio-inspired models have been implemented in robotic structures and in robot simulators, in order to make comparisons between the real fly and the modeled one. This PhD research has been oriented toward two main lines: the first one has been directed to the insect brain modeling; the second line has been oriented to the simulation and the implementation of the model in robotic structures and then to the analysis of the behavior of the robots in order to obtain comparative results with real flies as well as predictions about the behavior of the real flies under particular circumstances.

This thesis is divided in seven chapters. The first four chapters describe an original robotic architecture inspired by the fruit fly *Drosophila melanogaster*. In the last three chapters, instead, one peculiar part of the insect brain, the Mushroom Bodies, is analyzed and modeled. This structure presents a lot of interesting capabilities and it deserves attention and investigation. Biological

details will be given step by step, in order to emphasize the link between biology and models.
Many people have worked with me during the redaction of this thesis. I want to thank them all, because the passion they demonstrated for their work has deeply contributed to my human and professional growth.

Contents

Chapter 1

An insect brain computational model: the architecture

The fruit fly *Drosophila melanogaster* is an extremely interesting insect because it shows a wealth of complex behaviors, despite its small brain. Nowadays genetic techniques allow to knock out the function of defined parts or genes in the *Drosophila* brain. Together with specific mutants which show similar defects in those parts or genes, hypothesis about the functions of every single brain part can be drawn. Following these experiments, a computational model of the fly *Drosophila* has been designed with a view to its robotic implementation.

1.1 Introduction

Robots can be used to reproduce animal behavior in order to study their interaction with the environment. Robots help to improve the understanding of animal behavior and animals help to create efficient robots. The study of animal brains leads to new control systems that could allow robots to be able to orient themselves in complex environments, to take decisions, to accomplish dangerous missions, in other words to be completely autonomous. Robot implementation of biological systems could also lead to predictions for basic sciences, e.g. when investigating the emergent properties of models. Several attempts are present in the literature related to algorithms or bio-inspired networks able to mimic the functionalities of parts of the brain. A lot of work has been done in several animal species belonging to mammals, molluscs and insects [1]. Looking into the insect world different research groups around the world are trying to design models which are able to reproduce interesting behaviors shown by insects: cooperation mechanisms in ants [2], navigation

strategies in bees [3], looming reflex in locusts [4], homing mechanisms in crickets [5], central pattern generator and obstacle climbing in cockroaches [6], [7], reflex-based locomotion control in the stick insect [8], just to cite some examples. It is evident that the effort is focused on specific peculiarities associated with the different insect species that can be also useful for robotic applications. Nevertheless, a more challenging task consists of trying to model the main functionalities of an insect brain, looking from an higher level, trying to identify the mechanisms involved in the sensing-perception-action loop.

In this chapter a model of the *Drosophila melanogaster* brain, amenable to a robotic implementation, is described. This fly has a small brain that brings about a great variety of complex behaviors. Moreover, genetic techniques allow to remove or to inactivate parts of the *Drosophila* brain, creating mutants. The analysis of mutant behaviors can lead to hypotheses about the functions of the single brain parts. Moreover, the so-called *partial rescue* technique, allows to activate genes needed for a structure or a biochemical pathway only in a selected part of the brain, whereas the rest of the fly is still mutant for that gene. This technique is used to definitely establish the one-to-one correlation between that brain part and the behavior it is responsible of. Biological experiments on the fly Drosophila have been conducted and analyzed by Strauss et al. [9]. Neurobiological functional models are being discussed there. Following the functional, neurogenetic and behavioral analysis of the *Drosophila* brain, a general computational architecture has been designed and implemented in a robot simulator. This important step allowed starting to compare some of the main behaviors met in the real fly with the simulation. The *Drosophila melanogaster* brain structures responsible for perceptual and motor control capabilities, namely the Central Complex and the Mushroom Bodies, are briefly described in Paragraph 2. Paragraph 3 is related to the presentation of a computational model of the fruit fly brain, while Paragraph 4 introduces the model implementation on real and simulated robots. Finally, the chapter draws the conclusions. In the following chapter the simulation results about the validation of the model and a possible application in a real-life scenarios will be presented.

1.2 Biological Background

The *Central Complex* and the *Mushroom Bodies* are the most striking structures of the *Drosophila melanogaster* brain, located in the *protocerebrum*. The *Drosophila* brain is estimated to contain about 100 000 neurons. The *ventral ganglion* might add another 20 000 neurons.

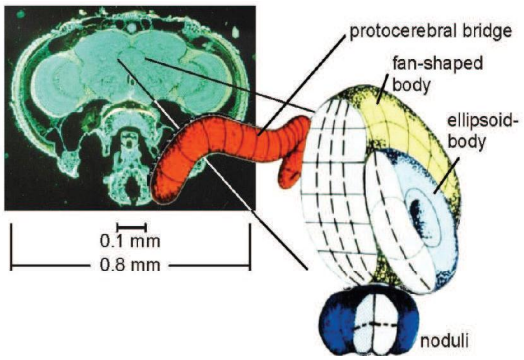

Figure 1.1: *Drosophila* Central Complex, after Strauss 2002 [10]. The CX is composed by four major regions, the *fan-shaped body*, the *ellipsoid body*, the *noduli*, the *protocerebral bridge*. The input into the CX seems to be highly preprocessed because there are no known projections from primary sensory areas.

1.2.1 Central Complex

The Central Complex (CX) resides in all insect brains at the midline of the brain between the protocerebral hemispheres. It is composed of different regions, as shown in Fig. 1.1, and it has been studied anatomically using Golgi analysis [11]. The *fan-shaped body* (FB) is the largest neuropil which possesses eight fans in the latero-lateral extent, six layers in the dorso-ventral direction and four shells in the anterior-posterior direction. The *ellipsoid body* (EB) has a perfect toroid shape and possesses 16 segments and it has two radial zones. The paired *noduli* reside ventral to the fan-shaped body just dorsal to the oesophagus. The *protocerebral bridge* (PB) is a rod-like neuropil composed of a chain of 16 glomeruli just posterior to the fan-shaped body. There are no evident direct tracts from any sensor systems which bring unfiltered information from sensors to the Central Complex. There are, however, two accessory areas of the CX. The *lateral triangles* are the starting point of input into the ellipsoid body, and the *ventral lobes* are a major input and output region for the fan-shaped body. Because there are no known projections from primary sensory areas to the CX, the input into the CX seems to be highly preprocessed. Experimental evidence from *Drosophila* and many different insect species demonstrate that primarily visual information is processed in the CX [12], [13]. In *Drosophila melanogaster*, the CX is composed of about 2000 to 5000 neurons. Details can be found in [9].

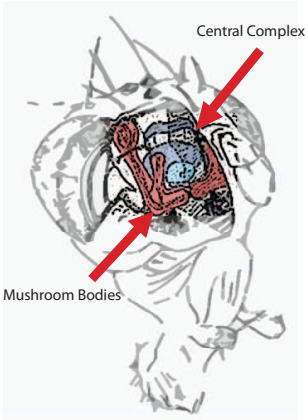

Figure 1.2: *Drosophila* Central Complex and Mushroom Bodies. The MBs frame the CX without known direct connections.

1.2.2 Mushroom Bodies

The *Mushroom Bodies* (MBs) are a paired structure of the insect protocerebral hemispheres spreading out in three dimensions. The MBs "frame" the CX without known direct connections (Fig. 1.2). The most important constituents of the MBs are the 2500 Kenyon cells per side which run in parallel from the *calyx* through the *peduncle* and to the *lobes*. In flies, there is a prominent olfactory input from the antennal lobes into the calices. Input from other sensory modalities is not obvious in *Drosophila*, but tasks of the MBs related to vision are described for flies. In honeybees, MBs receive prominent visual [14], gustatory, and mechanosensory [15] input. In flies and bees, the MBs lobe region receives information on sugar reward (via octopaminergic neurons) or electric shock (via dopaminergic neurons). There is an output of the MBs to pre-motor areas of the brain. Inside the MBs the flow of information is through the Kenyon cells from the calyx towards the lobes.

The MBs in *Drosophila* can be conveniently ablated chemically [16]. The method is not universally applicable to other neuropils because those do not usually have a unique time window for their neuroblasts to divide.

1.3 Computational architecture

The main parts of the insect brain have been modeled and integrated into a computational architecture. This global computational model inspired by the *Drosophila* brain is presented in Fig. 1.3. It has been designed in order to be directly linked to a robotic implementation.

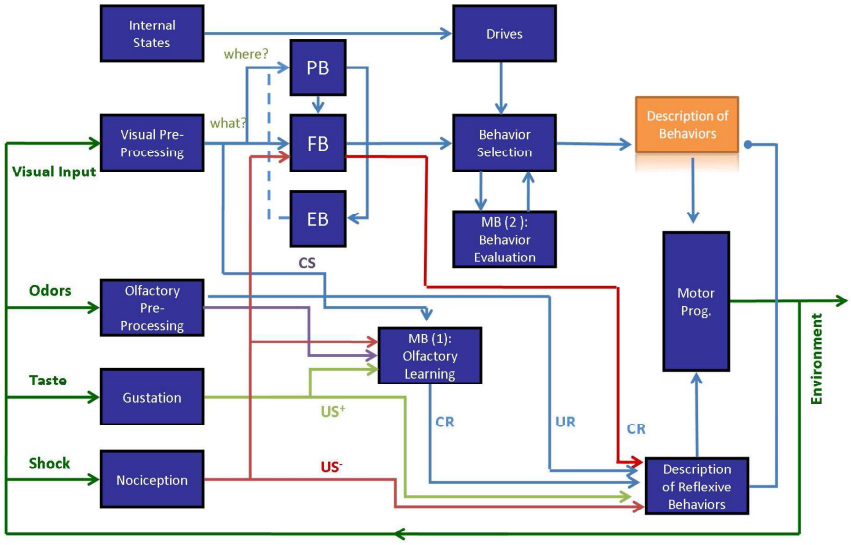

Figure 1.3: Computational architecture of the *Drosophila melanogaster* brain. The olfactory and the visual pathways are modulated by drives in order to select the winning behavior. Learning is present in the MBs and FB blocks and it gives to the model its plasticity. The reflexive pathways allow the fast realization of the most basilar behaviors, like escaping reactions.

The main parts of the whole architecture are described in the following.

1.3.1 Sensorial pathways and internal states

In the model, it is possible to distinguish four main sensorial pathways; the olfactory and the visual pathways allow to percept the environment while the gustation and the nociception are indispensable to obtain information about the goodness or badness of the current situation. The learning is obtained using mechanisms based on classical conditioning. Moreover, the own state can be monitored through a set of virtual proprioceptive sensors, that could be chosen according to the application.

1.3.2 Drives and Behavior Selection Network

Every living being has to know both the external and its internal states to survive in the environment. An internal state is supposed to be directly related to drives: hunger, thirst, the will to sleep etc. are used by animals to know their state and to adapt the behavior accordingly to it. These kinds of drives can be easily transferred to robots: the need for power supply is the most evident

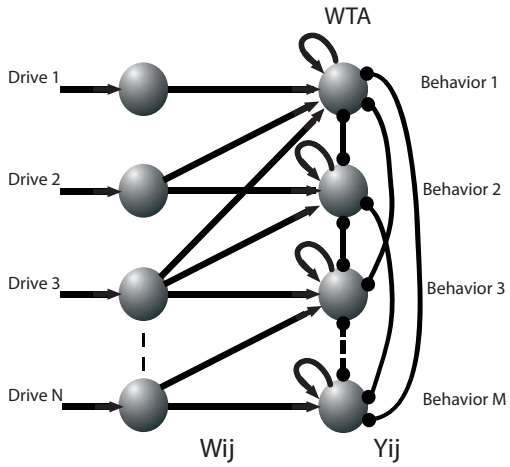

Figure 1.4: Spiking network used to simulate the Behavior Selection functionalities. Drives are represented by input currents. Each drive can excite more than one behavior. Synaptic efficiencies between the input layer and the WTA layer represent the influence that each drive has in each behavior. Only the most excited behavior can win the competition and can be selected.

example. In order to satisfy its needs, the robot has to choose a behavior from a pre-defined number of available behaviors. Behavior is meant, for the time being, like a sequence of programmed actions. Each behavior is oriented to satisfy one or more drives. Even if there are not specific experiments that can demonstrate the existence of such a network in the *Drosophila* brain, an artificial Behavior Selection Network (BSN) was supposed and implemented. The BSN was thought as a two layers neural network, in which each unit is an Izhikevich Class I spiking neuron [17], having the following equation:

$$\begin{aligned} \dot{v} &= 0.04v^2 + 5v + 140 - u + I \\ \dot{u} &= 0.02(-0.1v - u) \end{aligned} \tag{1.1}$$

with the spike-resetting

$$\texttt{if } v \geq 0.03\texttt{, then} \begin{cases} v \leftarrow -0.055 \\ u \leftarrow u + 6 \end{cases} \tag{1.2}$$

where v is the membrane potential of the neuron, u is a recovery variable and I is the synaptic current. In Fig. 2.10 an example of BSN is shown. The number of neurons in the first layer matches the number of drives the robot has to satisfy. The number of neurons in the second layer corresponds to the number of available behaviors. Every drive is represented by a current, that

is then converted in a spike-rate by the corresponding first layer neuron. The efficiencies of the synapses connecting the first and the second layer neurons are chosen according to the capacity of each behavior to satisfy each drive. Synaptic weights W_{ij} represent the importance of drive i for the behavior j. Synaptic efficiencies are fixed: no learning is considered at this step. The second layer is a Winner Takes All (WTA) network; during every simulation step the neurons in the second layer are competing and only one neuron can win the competition: the behavior represented by the winning neuron is the selected behavior for the next robot step. To avoid a continuous switching among the selected behaviors, an auto-excitatory synapse has been introduced in each neuron of the second layer of the BSN. In this way, if a behavior has been selected during a simulation step, the probability to be selected again is increased at the next step the robot takes. Synaptic weights Y_{ij}, i≠j , represent the inhibitory synapses between neuron i and j in the WTA layer. Synaptic weights Y_{ii} represent the auto-excitatory synapses of neuron i in the WTA layer. The last point to clarify is how to transform drives in an input current. Let's imagine having the drive "recharge", the robot analogue to "sleep", strongly connected to an internal sensor that measures voltage in batteries. It is possible to implement a transfer function that takes as input the battery level and gives as output a numerical evaluation of the "sleep" drive. Other methods for behavior selection have been used in literature, in particular for sequence learning [18]. The proposed approach could be modified in order to implement sequence learning, but up to now there are no biological evidences about the capabilities of *Drosophila* in learning sequences of behaviors.

1.3.3 Central Complex model

Protocerebral bridge model

Object detection and distance estimation are functions related to the PB in fruit flies. Mronz and Strauss proposed a simple model based on parallax motion [19] that can be used to model these functions and a hardware implementation for an autonomous roving robot has been proposed in [20]. However, it is possible to use a generalized PB model, made of a cascade of three simple blocks:

- *Object Detection Block*. This block takes input from the visual system and is used to detect the presence of an object.
- *Distance Estimation Block*. When an object has been detected, this block estimates its distance from the robot. In real flies, distance is estimated using a parallax motion approach.

- *Object Position Block*. It is possible to reproduce fly behavior assuming as interesting objects those standing in the compartments ranging from the frontal direction to ±100 degrees in the two lateral sides and repulsive ones those standing in the compartments from ±100 degrees to ±160 degrees on the rear part of the robot. Objects at angles exceeding 160 degrees cannot be seen.

Fan-shaped Body model

The fan-shaped body model has been designed as a cascade of two sub-blocks, a feature extraction and a feature evaluation element.

- *Feature Extraction*. Once an object has been detected, the Feature Extraction Block classifies it by using a series of features. As underlined in focused experiments with flies [12], the following features can be considered:
  - *Color*. Using a HSV representation, it is assumed to consider only the Hue value.
  - *Orientation*. Orientation is meant as the angle between the vertical direction and an axis that represents the direction in which an object is mainly distributed.
  - *Size*. Size is meant as the portion of total visual area of the robot occupied by the object, normalized with respect to the distance from the robot.
  - *Center of Gravity*. This feature is given by the height of the center of gravity normalized with respect to the vertical dimension of the visual area and the distance from the robot.
  - *Wideness*. Wideness is meant as the maximal horizontal extension of the object, normalized with respect to the total horizontal dimension of the visual area and the distance from the robot.
  - *Height*. Height is meant as the maximal vertical extension of the object, normalized with respect to the total horizontal dimension of the visual area and the distance from the robot.

- *Feature Evaluation*. The robot collects features and is able to associate features to punishment or neutral situations. Every feature has a *punishment value*: if this value exceeds a threshold, the robot escapes every time it meets an object with that feature. The punishment value of a

feature decreases if the robot is not punished when that feature is encountered. When the robot meets an object, it evaluates its Escaping Value: this is a weighted sum of the punishment values of the features of that object. When the Escaping Value is high enough, the robot escapes from the object, even if not punished. This is the simplest way to implement a classifier. Other, more performing and sophisticated algorithms, either bioinspired, or more information theory-bases, like the Neural Gas [21], could be implemented to add plasticity to this simple, starting point model.

Ellipsoid body model

Neuser [13] described the role of the *Drosophila* ellipsoid body in the visual short term memory. That functional analysis leads to the implementation of a model able to create a spatial memory in a robot. By using polar coordinates to code the robot position in the environment, it is possible to design neural architectures inspired by the ant's path integration [22]. However other solutions could be based on a mathematical implementation of a polar path-integration algorithm and this kind of approach (easier and more robust) has been taken into consideration at this stage. A scheme describing the path integration mechanism is shown in Fig. 1.5. Supposing $\Delta s << r$, defining λ as the direction of the current robot movement and $\delta = \lambda - \nu$, the approximation of the current robot position is recursively given by:

$$r_{n+1} = r_n + \Delta r_n = r_n + \Delta s_n cos(\delta_n) \tag{1.3}$$

$$\nu_{n+1} = \nu_n + \Delta \nu_n = \nu_n + \Delta s_n sin(\delta_n / r_n) \tag{1.4}$$

where Δs_n is the length of the robot step of index n and r and ν are the coordinates that represent the position of the robot with respect to the object that is supposed to be the origin of the polar coordinate system.

1.3.4 Mushroom Bodies model

The MBs are a key structure of the insect brain. Mushroom Bodies are primarily involved in olfactory learning [23],[24] and in a more complex function that will be called *behavior evaluation* [25]. Because experiments are not able to demonstrate the connection between the two functions, two uncoupled models were implemented.

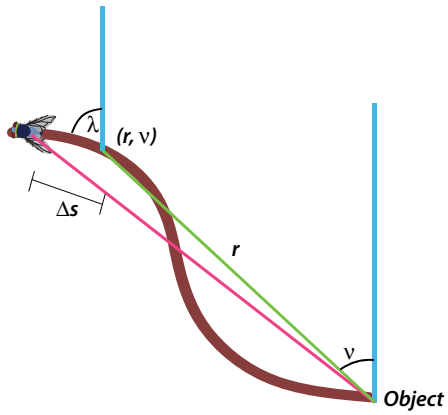

Figure 1.5: Path Integration scheme (modified after [22]). The values of r and ν represent the position of the robot from the object. Every robot step r and ν are updated according to the last robot movements, in direction λ by a path increment Δs.

Olfactory learning model

A two layer spiking neural network was designed and implemented to model the olfactory learning function. The Spike Timing Dependent Plasticity (STDP) has been applied as learning algorithm [26], [27]. This algorithm can reproduce Hebbian learning in biological neural networks. The algorithm works on the synaptic weights, modifying them according to the temporal sequence of spikes occurring. The algorithm is represented by the following formula:

$$\Delta W = \begin{cases} A_+ \exp\left(\Delta t/\tau_+\right), & \texttt{if } \Delta t < 0 \\ -A_- \exp\left(\Delta t/\tau_-\right), & \texttt{if } \Delta t > 0 \end{cases} \tag{1.5}$$

where Δt is the time delay between pre and post synaptic spikes. In this way the synapse is reinforced if the pre-synaptic spike happens before the post-synaptic one, it is weakened in the opposite situation. Parameters τ_+ and τ_- represent the slope of exponential functions, while positive constants A_+ and A_- represent the maximal variations of the synaptic weight.

Each neuron is modeled by an Izhikevich Class I neural model [17]. A scheme of the neural model is shown in Fig. 2.1. The Shock (Punishment) Neuron takes as an input a current proportional to the value of the robot punishment, while the Good (Reward) Neuron takes as an input a current proportional to the reward. In experiments with *Drosophila*, the punishment could be represented by an electrical shock, while the reward is represented

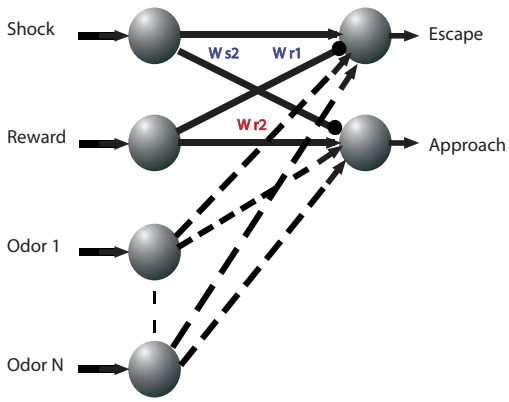

Figure 1.6: Olfactory Learning Model. Solid line (dashed) connections correspond to fixed (plastic) synapses; arrows (bullet) correspond to excitatory (inhibitory) connections. The model here presented can be easily extended to the desired number of odors.

by sugar. Each of the remaining neurons of the first layer takes as an input a current proportional to the odors the robot can detect in the environment. Each odor has a corresponding receptor and a neuron that converts the current in a spiking-rate if the current is high enough above the threshold for the Class I Izhikevich model. In a real robotic implementation odors can be substituted with other sensorial inputs, according to the application. Specific neural network composed by Izhikevich neurons and STDP learning were already implemented to realize approaching or escaping behaviors. They are here omitted for simplicity [28]. In the present implementation, synapses between the Shock and the Reward Neuron and the output layer have a fixed value. Outputs of the second layer neurons are connected to a Motor Program block. The robot escapes from the actual position if the Escape Neuron is firing, while it begins an approaching algorithm if the Approach Neuron is firing. Synapses between unconditioned stimuli (i.e. shock and reward) and motor neurons are fixed and represent the inherited knowledge whereas connections between conditioned stimuli (i.e. odors) and the motor system are subject to learning, according to the STDP rule. If not reinforced, the efficiency of a synapse decays with time.

Behavior Evaluation model

When a behavior is selected, the robot defines a setpoint to be reached. A setpoint is meant as a desired value for a vector of physical quantity linked to the definition of the drives: to satisfy its needs, the robot has to minimize the error between this setpoint and its actual state. For example, let us assume

that the robot has a low battery voltage and that a charging-station is present in the environment. In this situation the robot could choose to go to the base station whereas the desired battery level would be the setpoint. If the selected behavior is not able to allow the robot to satisfy its needs, that behavior has to be inhibited: in the opposite situation, if the selected behavior leads to satisfying its needs, that behavior has to be excited. The Behavior Evaluation block inhibits or excites the actual behavior depending on the amount of time already spent and the amount of success reaching the setpoint. Inhibition or stimulation is easily implemented sending a current to the neuron of the WTA layer in the BSN associated to the ongoing behavior. Maybe some additional plasticity could be implemented into the Behavior Selection Network through the Behavior Evaluation model. In particular, the synapses between the neuron related to the selected behavior and drives that represent the setpoint could be reinforced (or weakened) if the last selected behavior has been able (or not) to reach the last setpoint. However, there are no biological evidences about this point.

1.3.5 Motor Programs and Description of Behaviors

The Motor Program block describes all the possible elementary actions that the robot can perform. Motor learning is not considered up to now, although it is envisaged to be investigated and added in the near future.

1.3.6 Reflexive Behaviors

When the robot is punished in some way it needs to escape as fast as possible from the object responsible for the shock. The *Description of Reflexive Behaviors* is a simple high level block that allows the robot to take the right direction in the case it is punished.

1.3.7 Complex Behaviors

The *Description of Behavior* block is a high level part of the complete model that describes the available behaviors that the robot can follow. The choice of the possible behaviors the robot can exhibit depends on the robot applications. Applying a searching strategy to find a charging station could be an example of a typical behavior. The description of each behavior, however, could depend on the robotic structure and the embedded sensorial system.

1.4 How to Simulate Drives and Behaviors

The implementation of drives and behaviors on a real robot strongly depends on the field of application in which that robot is involved. The simulation of the general model of an insect brain requires a simulated environment, where behaviors and drives, which the robot has to satisfy, need to be defined. Drives and behaviors that could be chosen for a simulation of the whole model are presented in the following. The focus is to simulate the model in a context that can present analogies with the *Drosophila* real experimental set-up, in order to obtain the experimental validation of the model.

1.4.1 Drives

A brief description about the suggested drives and their analogies with real fruit flies is presented here.

- *Sleep.* The drive Sleep is assumed to be the need for a robot to charge its batteries. In real fruit flies sleep is indispensable for learning [29]. In common robots we can quantify the drive sleep using a function of the battery level:

$$I_{drive} = K_{drive} \tanh(\Lambda - \chi) + \psi \tag{1.6}$$

  where K_{drive}, Λ, χ and ψ are the parameters of the function. Through these parameters it is possible to set the maximum and the minimum value of the current and the optimal battery level. An example is shown in Fig. 1.7. The optimal battery level is represented by the point in which the drive Sleep is equal to zero. If the battery level exceeds the optimal point, the drive becames negative, in order to inhibit a battery charging. In order to simulate the battery level, it is convenient to implement a virtual sensor. The output of such sensor is the estimated battery level. The battery level must decrease each step in which the robot is far from the charging station, and reaches the Max Battery Level after a given time spent in the charging station area. A sleep drive is indispensable for every time it is necessary to have a completely autonomous robot, which must be able to find power supply sources and use them to move for a long time.

- *Hunger.* The need of food can be reproduced putting inside the environment objects or landmarks that the robot should periodically find and/or visit. The drive Hunger could be thought as proportional to the time the robot left the object. This drive is indispensable to obtain a

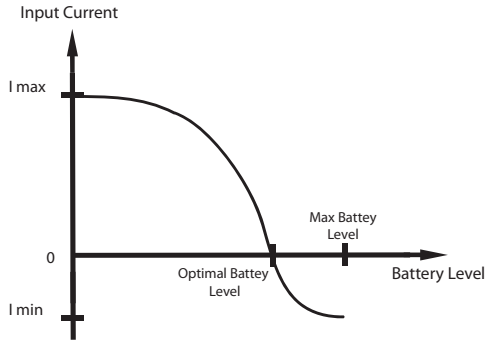

Figure 1.7: Example of the transfer function used to model the sleep drive. A low battery level leads to a high value of the current related to the *Sleep* drive. The optimal battery level is represented by the point in which the drive *Sleep* is equal to zero. If the battery level exceeds the optimal point, the drive became negative, in order to inhibit a possible dangerous battery charging.

behavior that can match with reality but also to force the robot to find objects that can be periodically useful. The drives Hunger and Sleep have some similarities; their differences would be remarked according to the application.

- *Shelter.* When in danger, a fly looks for a safe place. A fly in open spaces often has the tendency to protect itself, typically aiming to approach and follow walls. Shelter can be related the distances of the robot to the walls.

- *Curiosity.* The drive Curiosity allows a fly to search for other resources when the other drives are satisfied. Curiosity can be quantified with a constant value. From a robotic point of view, curiosity leads the robot to explore the environment and to acquire information about the objects it meets.

1.4.2 Behaviors

To make the robot able to satisfy its drives, the following behaviors could be implemented. They would constitute the output of the Behavior Selection Network, that will be further discussed.

- *Exploration.* During an exploration behavior the robot tries to find new resources. In flies, the environment exploration is characterized by an increase of the mean-free path algorithm [30]. As in the real flies, during an exploration behavior it is possible to distinguish two behaviors [31]:

  - Sitter larvae behavior: short path length and tight turning angles.
  - Rover larvae behavior: long path length and wide turning angles.

  Exploration can be thought as a default behavior: the robot could choose this behavior when no particular drives are enabled. Usually curiosity is the drive that mainly influences the choice of an exploration behavior. The implementation of the exploration behavior requires also the management of the obstacle avoidance and object detection. Moreover, the robot must be able to update its position at each step; in our case, the ellipsoid body model is involved.

- *Homing.* The homing behavior is meant as the return to the charging station, from where the robot usually initiates the simulations. Of course, the position of the Home must be known and updated every step. An obstacle avoidance algorithm has to be implemented during the homing behavior. Homing behavior is needed to have an autonomous robot, able to charge its battery before its autonomy is compromised.

- *Landmark Recalling and Achievement.* During the navigation the robot meets objects: if some objects are associated to food, the robot must remember their position in order to reach them when it is needed. The biological plausibility of this behavior is evident. The robot must use the path integration system to update its position from each interesting object.

- *Centrophobism.* A centrophobic behavior has been found in flies [32]. From a biological point of view, centrophobism in flies could be a consequence of the increase of mean-free path in the exploration behavior. A fly uses centrophobic behavior to protect itself in dangerous environments. Shelter is the drive that mainly influences the choice of a centrophobic behavior.

1.5 Remarks and Conclusions

A simplified computational model of the *Drosophila melanogaster* brain has been designed. Two main centers of the insect brain have been considered: the Mushroom Bodies and the Central Complex.

The Mushroom Bodies model has been splitted into an olfactory learning model and a behavior evaluation model, following the actual neurobiological evidence. The olfactory learning model is a two layer spiking neural network

and the STDP algorithm has been used for the learning implementation. Concerning the CX, it has been divided into several blocks. The fan-shaped body has been modeled as a feature extraction block followed by a classifier, while the protocerebral bridge model allows the robot to detect interesting objects. An orientation memory has been implemented into the ellipsoid body model. Moreover a Behavior Selection Network is used by the robot that autonomously chooses the most suitable behavior able to fulfill its drives (i.e. internal motivation mediated by external stimuli). Behaviors allow the robot to satisfy drives. Finally, a list of drives and behaviors has been suggested with a view to the implementation of the model in real robots or robotic simulators.

Chapter 2

An insect brain computational model: simulation results

The computational model of the *Drosophila*, described in the previous chapter, has been tested and implemented on a robot simulator. Moreover, the normal capabilities of the fly have been extended in order to have an useful robot-oriented model. Results about a possible application in a real-life scenario of the whole model of the *Drosophila* brain are here reported.

2.1 Introduction

In the last years animals have considerably influenced robotics. Robotics can improve the research in biology [33] and, moreover, without any doubts results in neurobiology helped the design of robotic structures and control systems [34], [35], [36]. In particular, insects attract the interest because the relative small number of neurons in their brain contrasts with their behavioral complexity. Insect strategies in problem solving have been analyzed and adapted to the implementation in mobile robots [22], [37]. In this way, the modeling of insects brain functionalities seems to be really useful in order to develop efficient robots.

The fly *Drosophila melanogaster* has become the reference point in the insect brain modeling, thanks to the genetic techniques that allow a deep functional analysis of its brain neuropils. Brain structures and functionalities of this fly have been modeled and implemented on real robots [19], [20]. Moreover, the *Drosophila* behavior inspired control systems useful for robotic applications [38].

This Chapter presents the results of simulations and tests on the computational architecture presented in Chapter 1. The proposed approach shows

the advantage to be potentially improved and generalized to be useful for real robotic applications.

2.2 Simulation Setup

Details about the robotic simulator and the implementation of the simulation environment are presented in this paragraph.

2.2.1 The robot and the simulator

The robot used in the experiments is a Pioneer P3-AT differential-drive roving robot. The platform operates as a server in a client-server environment; the onboard PC is used to host the control architecture. The robot dimensions are 50cm x 49cm x 26cm and its weight is 9 Kg.

MobileSim is the software used for simulating the Pioneer P3-AT roving robot in a virtual 2D environment. This simulation environment, that is extremely realistic (e.g. odometry errors are taken into consideration), has been used to evaluate the performance of the proposed control system.

2.2.2 Simulation of odors, punishments and rewards

In order to implement olfactory classical conditioning it is necessary for the robot to have sensors that can detect odors and that can monitor rewards or punishments given to the robot. In a simulation environment it is convenient to implement virtual sensors. For instance, if an object releases an odor called Odor1, it is convenient to assume the output of the olfactory sensor as a Gaussian function of the distance d from the robot to that object:

$$f_{od}(d) = K_{od}e^{-d/\tau_{od}} \tag{2.1}$$

where K_{od} is a constant gain and τ_{od} represents the decay of the sensor output when the robot moves away from the object.
It is possible to use a similar strategy to determine the output of a punishment sensor and the output of a reward sensor:

$$f_{pun}(d) = K_{pun}e^{-d/\tau_{pun}} \tag{2.2}$$

$$f_{rew}(d) = K_{rew}e^{-d/\tau_{rew}} \tag{2.3}$$

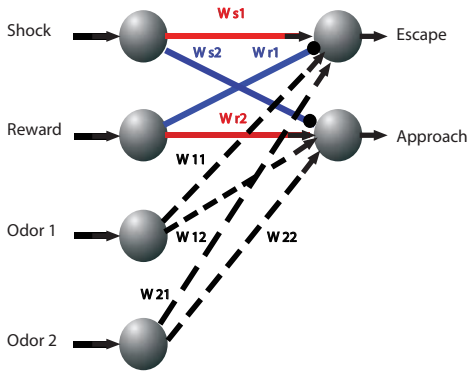

Figure 2.1: Olfactory Learning Model. solid line (dashed) connections correspond to fixed (plastic) synapses; arrows (bullet) correspond to excitatory (inhibitory) connections.

The values of the constants can be determined in order to obtain a tighter Gaussian function for the output of the punishment and reward sensors: in this way, if the robot is approaching the object, it will first detect the odor and then it will be rewarded or punished if that object is not neutral.

2.3 Simulation Results

The experiments made in order to validate each model of the general computational architecture of the *Drosophila melanogaster* brain are here presented.

2.3.1 Mushroom Bodies and olfactory learning

The following simulation shows how the MBs model for odor learning works. This model is shown in Fig. 2.1. Each neuron is an Izhikevich Class I spiking neuron [17]. The simulation of the model has been done using the Euler integration method with a constant integration time of 20 milliseconds. The synapses time constant is 800 milliseconds and synaptic weights are initialized to the value of 0.05. A priori known information is codified in the fixed synaptic weights that have been initialized to the value of 10 (excitatory) and -3 (inhibitory). A decay rate has been introduced: every 100 simulation steps all synaptic weights are decreased by 1% percent of their value. The implemented network is the same as shown in Fig. 2.1. This simulation was performed to verify the capability of the MBs model to make the right associations between

Object	Odor	P/N/R
Object A	Odor 1	Punishment
Object B	Odor 2	Reward
Object C	Odor 2	Punishment
Object D	Odor 2	Neutral

Table 2.1: Summary of the characteristic of the objects in the MBs model test.

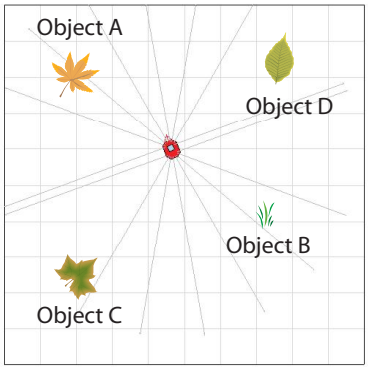

Figure 2.2: Simulation environment used for the MB model test.

odors and rewards or punishments in a complex environment. The robot is introduced into a square arena, 10m x 10m, in which four objects are present. There is an odor spreading out from each object in the environment. In particular, Eq. 2.1 has been used. Two different odors are associated to these objects and a reward or a punishment is given to the robot when one of the objects is reached, following the association reported in Table 2.1.

Exploring the environment shown in Fig. 2.2, the robot has to learn that there is a strong association between the Odor 1 and the punishment: in a testing phase, the robot will be able to escape when detecting that odor, before the shock occurs. The behavior of the network neurons during the simulation is shown in Fig. 2.3 while Fig. 2.4 presents the trend of the synaptic weights during the simulation. The network evolves for 100 simulation steps for each robot action. At the end of the simulation, the robot has explored the environment completely and it is able to make the right association. Other experiments were performed, obtaining similar results.

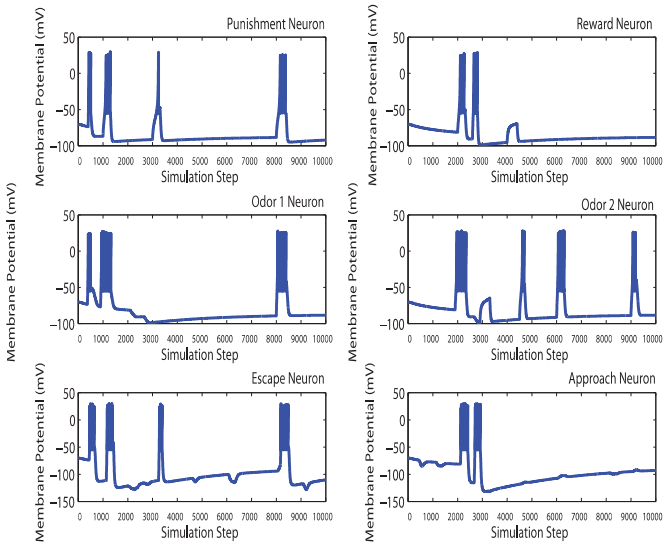

Figure 2.3: Simulation results of the olfactory learning model: behavior of the neurons membrane potential during simulation. The implemented network is shown in Fig. 2.1.

2.3.2 Protocerebral bridge and fan-shaped body

Through a functional analysis of the *Drosophila* protocerebral bridge and fan-shaped body, it is possible to suppose that object detection and distance estimation are mainly performed by the PB, while the FB is related to feature extraction and classification. In the following experiments, the properties of the PB and FB models and the capabilities of the robot in terms of visual learning are presented.

In particular, the proposed simulation is inspired by the experiment designed by Liu and collaborators on real flies [12] about visual learning and object recognition. The robot has to explore a square arena, (10m x 10m), in which four objects are present. Even if these objects are different, they can have some similar features. The objects used in this simulation are shown in Fig. 2.5. Every time the robot meets an object, it tries to recognize that object, extracting features and comparing them with the stored ones. If the robot meets an object for the first time, it extracts and stores the new features. It has been assumed to consider six features: color (in the Hue Saturation Brightness representation, here only the Hue value is considered), orientation, size, center of gravity position, wideness and height. The PB model has been set so that the robot is able to detect objects in a range of four meters. Objects

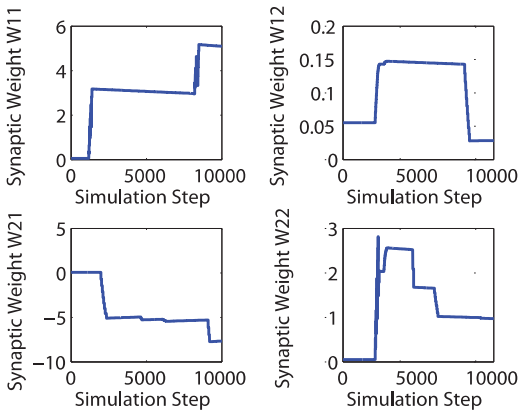

Figure 2.4: Simulation results of the olfactory learning model: trend of the synaptic weights during the simulation. The implemented network and the meaning of the parameters are illustrated in Fig. 2.1.

triggering punishment shock the robot if its distance from these objects is less than 2.7 meters. In this experiment the color "green" is a bad feature: the robot will be punished every time it tries to approach a green object. Therefore the robot has to learn to avoid green objects. The arena and the simulation results are shown in Fig. 2.6. At the beginning of the simulation, the robot tries to approach every object standing in its visual range. If punished, the robot increases the *punishment value* of the features of the approached object. If an object is neutral, the punishment value of the features associated to that object decreases. If the escaping value of an object reaches a threshold, the robot will escape when that object is detected. In this simulation the robot learns correctly to avoid green objects. Fig. 2.7 shows also the punishment value of the bad feature (green color) and the punishment value of a neutral feature, the wideness, that is the same for all the objects. In order to implement a hysteric response, when the punishment value exceeds 2, it is simply raised to 7. In this way the robot will remember this bad feature association for a long time, even if the learning is not reinforced. If the robot detects an object, the punishment value of all the features that do not belong to that object will remain the same. A time-dependent decay rate could also be introduced. In a second experiment, the robot has to learn to avoid each "T" object. Color is now neutral for the robot. Even if the shape is not a feature, a T is different from an inverted T because of the different center of gravity. This experiment leads to the same conclusion of the first experiment; the robot is able to recognize bad features and to avoid them.

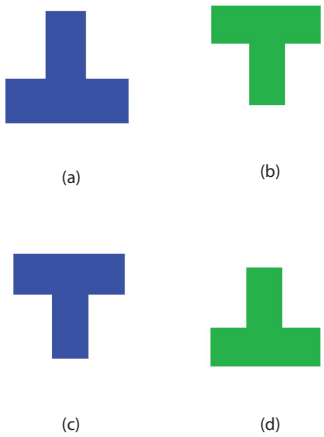

Figure 2.5: Objects used in the fan-shaped body model simulation. (a) blue inverted T-shape; (b) green upright T-shape; (c) blue upright T-shape; (d) green inverted T-shape.

2.3.3 Ellipsoid body

In real fruit flies, the ellipsoid body is necessary for a visual short-term memory and orientation [13]. A polar path integration system is present in the architecture to model the ellipsoid body. Supposing that an object (in our case the home) is the origin of the polar reference system, the distance of the robot to the object is indicated with r, while the position of the robot is represented by the angle ν.

In the following simulation the behavior of the EB model while the robot is moving around the environment is evaluated. In the simulated environment an odometry error has been introduced, to make the results more realistic. In this first experiment we want to show how the ellipsoid body model works: the robot must be able to orient and update its position while moving into a square arena (8m x 8m). The robot starts from the Home position and moves randomly in the arena: its capability to update its relative position with the Home is analyzed. Of course the coordinates stored into the robot memory will be different from the real ones, because of the odometry errors and the approximation of the path integration method. Fig. 2.8 shows an example of trajectory and the response of the ellipsoid body. The same test has been repeated many times, in order to make a better analysis of the model.

In order to test the capability of the model in real situations, it is convenient to simulate the robot behavior and the EB response in more complex arenas. In the following experiment the robot has to explore a large arena, in which

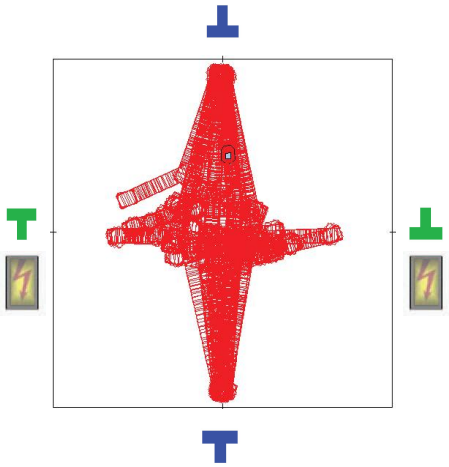

Figure 2.6: Robot trajectories obtained during the testing of the fan-shaped body model. After being punished enough times, the robot is able to isolate the dangerous feature (the green color) and escape when a green object is found.

several objects are present. The robot starts from the Home and initially it moves randomly: this behavior is created to simulate a typical escape reaction of real flies when newly introduced into an arena.
After that, the robot starts an Exploration behavior. If the robot meets objects it is able to learn about their danger or neutrality, thanks to the MBs model. During the exploration, the robot updates its position from the Home. An obstacle avoidance mechanism was also implemented. During this experiment two behaviors are available: Exploration or Homing. The level of the battery decreases while the robot explores the arena. A virtual battery sensor has been implemented. If the level of the battery is too low, the BSN switches the selected behavior to the Homing behavior. If the stored position is correct, the robot must be able to return to the Home position. Obstacle avoidance is used also during the Homing behavior. Simulation results are shown in Fig. 2.9. The robot starts to move and, after the escaping reaction implemented to match the biological experiments with real flies, it begins an exploration (a). The escaping reaction from the Home position to position (a) is not outlined for clarity reasons. After fifteen exploration steps, the battery level is low and the robot starts its homing behavior (b). Using an obstacle avoidance algorithm, the robot is able to return to the Home (c).

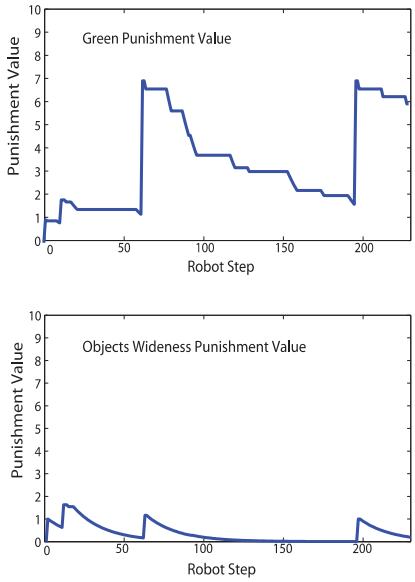

Figure 2.7: Comparison between the punishment value of the dangerous feature and the punishment value of a neutral feature, the wideness. Using the punishment value algorithm the robot is able to discriminate the dangerous feature. The decreasing of the Punishing Value of the dangerous feature is due to the steps in which the robot can detect a green object but is not so near to be punished.

2.3.4 Behavior Selection

In order to allow the robot to choose the "right" behavior, the Behavior Selection Network has been introduced into the model. This network is shown in Fig. 2.10. The BSN has been tested and its properties have been analyzed. In a real implementation of the model the drives are the inputs of the first layer of the network.

In the following simulations hypothetic drives have been simulated in order to study the response of the BSN in different possible situations. This experiment shows how the Behavior Selection Network works. It has been assumed to have four drives and to represent these drives with four input currents. In this first example the following synaptic weights have been used: $W_{12} = W_{21} = W_{31} = W_{32} = W_{43} = 1.5$; $W_{11} = W_{22} = W_{33} = W_{44} = 10$; $Y_{12} = Y_{13} = Y_{14} = -3$; $Y_{21} = Y_{23} = Y_{24} = -3$; $Y_{31} = Y_{32} = Y_{34} = -3$; $Y_{41} = Y_{42} = Y_{43} = -3$; $Y_{11} = Y_{22} = Y_{33} = Y_{44} = 3$. (see Fig. 2.10 for the network topology). A random Gaussian noise has been added in the input currents (σ =2). Fig. 2.11 presents the behavior of the neurons of the network.

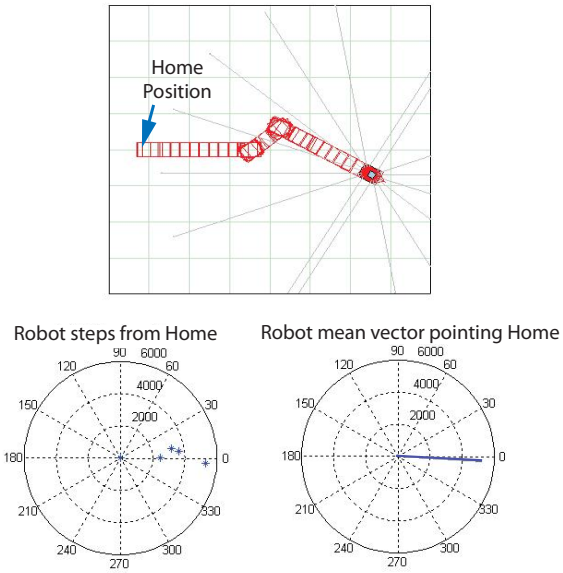

Figure 2.8: EB results. The relative position of the robot with respect to the Home is represented in polar coordinates and it is indicated in millimeters (distance) and degrees (angular position). In this case the current robot position is $r = 5730$ mm, $\nu = -12.23$ degrees.

When a second layer (WTA layer) neuron is firing faster than the others, the respective behavior is selected. The network has been simulated for ten thousand simulation steps, with an integration step of 20 milliseconds. During a short transient, all the WTA neurons are firing: this situation is due to the response of the synapses between WTA neurons. After this transitory period, only one neuron can win the competition.

2.4 Real life scenario application

Previously a model of the main parts of a fly brain computational model has been tested. Herewith the capability of the model to solve real useful problems is shown. By modifying the behavior repertoire but maintaining the conceptual structure of the general model we can obtain a versatile robot that is able to learn about the environment, to make choices and to face potentially dangerous situations. The experiment presented in the following is only one example of the real applications of the insect brain model, and it could be easily modified or generalized.

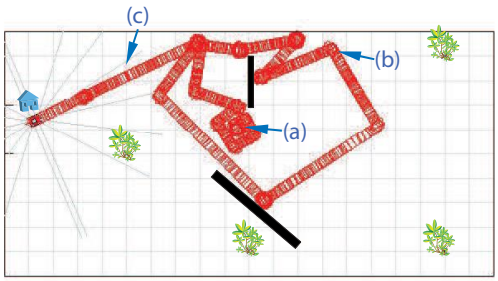

Figure 2.9: The robot starts to move and, after the escaping reaction implemented to match the biological experiments with real flies, it begins an exploration (a). The escaping reaction from the Home position to position (a) is not outlined for clarity reasons. After fifteen exploration steps, the battery level is low and the robot starts its homing behavior (b). Using an obstacle avoidance algorithm, the robot is able to return to the Home (c). In order to have a more complex simulation, some objects have been also introduced into the arena, but these did not influence the results.

2.4.1 Description of the experiment

Let us imagine to have a critical situation in which, after a disaster (e.g. earthquake, fire) it is necessary to rescue people trapped in a place. Often situations like this are very dangerous both for survivors and people who try to help them. Now let us image to have a smart robot able to explore the environment and which can learn, recognize people and remember their position. Such a robot could manage a critical situation acquiring the information needed to solve it. In the present experiment an environment that can represent a place after a disaster has been implemented into a robot simulator. The robot has to explore the environment, find some good objects that it is able to recognize, remember their position and learn about all kinds of danger present in the environment. At the end of the exploration, the robot must escape from the environment and give all the information useful for humans to know the position of the survivors and organize a safe rescue. In order to solve this problem, the behavior repertoire of the robot has been limited to two possible behaviors, exploration (*rover* type) and homing. In the same way, two drives are considered, *Curiosity* and *Sleep*, the latter indispensable for the robot to understand when to leave the environment and return home; for this, a virtual battery level sensor is used. The MBs model was also simplified: only the olfactory learning model will be considered. The synaptic weights, the synapses time constant and the integration step are the same of the previous simulations. To make the simulation light, every robot step of the

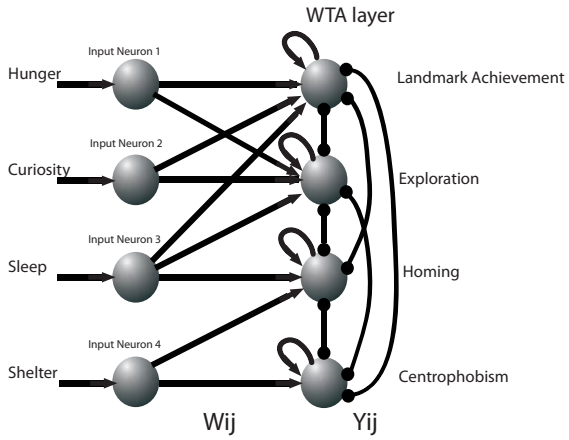

Figure 2.10: Spiking network used to simulate the Behavior Selection functionalities. Drives are represented by input currents. Each drive can excite more than one behavior. Synaptic efficiencies between the input layer and the WTA layer represent the influence that each drive has in each behavior. Only the most excited behavior can win the competition and can be selected.

robot includes only one hundred simulation steps of the MBs and BSN neural networks.

The arena implemented for the simulation and the results are shown in Fig. 2.12. The Home represents the starting point for the robot exploration and the point the robot has to reach at the end of the simulation. S_1 and S_2 represent the position of the targets: let us assume the robot considers them as interesting objects and, after an approach, it is able to recognize them. Let us assume that the targets are a blue T-shaped object and a blue inverted T-shaped object. Also present are Obj_1, Obj_2 and Obj_3, which are identical among one other. The robot cannot see them, but can sense them thanks to another sensorial system (i.e. olfactory). The robot is punished every time it tries to approach them. In the environment, two other objects are present, a green upright T-shaped object and a green inverted T-shaped object. The robot can detect them with the visual system. The robot is punished only when it tries to approach the first one, while the second one is neutral.

After a long exploration, the robot must be able to detect the targets, learn to avoid as soon as possible the objects Obj_1, Obj_2 and Obj_3, understand that the green upright T-shaped object is dangerous and finally reach the Home and give the position of the targets at the end of the exploration. Mushroom Bodies model will be used for the learning involving Obj_1, Obj_2 and Obj_3; the protocerebral bridge model will be used for the detection of the objects and

the fan-shaped body model for the visual learning; the ellipsoid body model is indispensable for homing and remembering the position of the targets. For this simulation, the capabilities of real flies have been extended, for instance, improving the performances of the EB that is now able to store multiple target information in a long term memory. This is an example of how the elementary functions of the *Drosophila* brain that allows the insect to face with its world can be easily extended in a modular way to make a robot able to fulfill more complex tasks, not affordable for the real fly. The Behavior Selection Network is useful to select the homing behavior if the battery level is too low. The parameters of the model have been set so that the robot can sense odors if its distance is lower than three meters away from the nearest odor source, while it is punished if its distance from that source is less than one meter. In the same way, the visual system of the robot can detect objects if they are closer than 2.5 meters. It is punished if an object is closer than 1.5 meters. The arena used for the simulation is 28m long and 15m wide.

2.4.2 Results

Experimental results from one of the simulations are shown in the following, discussing step by step the behavior of the robot. Only the most relevant robot steps are depicted in Fig. 2.12, for the sake of clarity. Besides, Fig. 2.13 shows the MBs model response during the whole simulation.

At step 1 the robot starts the simulation from the Home position. At the second step the robot enters the arena and begins an exploration behavior. The ellipsoid body model updates the position of the robot. Neurons of the MBs model are not stimulated and they lie in their silent state. At the following step (step 5, not shown), the robot uses the increase of the mean free path algorithm. The EB model updates the position of the robot. During the exploration, the robot must find objects and sense odors. At step 9, the robot senses $Odor_1$, but it is not punished, because it is not close enough to Obj_1. In the following step the robot continues its exploration following the increase of the mean free path algorithm, while the EB model updates the position it has stored.
At step 11 (not shown), the robot detects the green T-shaped object. The FB model extracts features from this object and the robot tries to approach it. While the robot is approaching the new object, it is punished (step 12).
After being punished, the robot escapes from the green upright T-shaped object (step 13). It experiences an unexpected situation: the robot sensed $Odor_1$ but was punished after two subsequent steps, due to the punishing visual input, and not for the odor. So, even if not planned in this way, the robot has made an association between $Odor_1$ and Punishment. This situation is

plausible and is a natural consequence of the correlation implementation of the STDP learning. As a consequence, the association between $Odor_1$ and the need to escape is reinforced. While it is escaping, the robot again detects Obj_1, senses $Odor_1$, is punished and escapes again in the opposite direction (step 14, not shown), reaching once more the green inverted T-shaped object (step 15). The robot is then punished for the third time. At step 16 (not shown), the robot is escaping again. At step 20 and 21 the robot is sensing $Odor_1$ again, without being punished. It is very interesting to analyze how the MBs model responds to this contradictory situation. Studying the firing of each neuron of the MBs model, it is possible to see that at a first time the robot was punished immediately after sensing $Odor_1$, while at a second time it senses $Odor_1$ but it is not punished. In this way, at a first time the robot made an association between punishment and $Odor_1$, but at a second time this association was weakened. However, the synaptic weight between the $Odor_1$ neuron and the Escape neuron of the olfactory learning model was not high enough to make the robot escape when sensing again $Odor_1$, without being punished. Now the robot continues its exploration of the arena. At step 22 the robot is near Obj_2, it is sensing $Odor_1$ again but it is not close enough to be punished. The association between punishment and $Odor_1$ must decrease again. While exploring, the robot detects the first target (step 27). The fan-shaped body analogue extracts the features of the object, the robot recognizes the target and tries to approach it. The EB model stored the position of the robot. The target S_2 is now reachable in the future. The robot leaves the object and begins another exploration.

After many steps, the robot detects and reaches the target S_1 and stores its position (step 41). After leaving the second target, the robot begins another long exploration. At step 55, the robot is into the area of detection of the green T-shaped object, but in this case the PB model leads the robot to consider this object repulsive because it is standing in the rear of the robot, therefore the robot leaves the object. The robot continues its exploration and, detecting Obj_3, the robot senses $Odor_1$ again at step 59. At step 63, the robot is close enough to Obj_3 to be punished. Because of the position of the robot, the punishment is not so strong, but the robot is sensing $Odor_1$ and it is recalling the association with punishment: even if the Punishment neuron only spikes once, the robot escapes.

Analyzing MBs response and the synaptic weights at step 64, it is evident how the robot reinforced the association between $Odor_1$ and Punishment, as shown in Fig. 2.14. Learning allowed the robot to escape fast, without strong punishment. After escaping, at step 65, the robot meets again the green T-shaped object. While the robot tries to approach it, the low output of the virtual

battery sensor determines the behavior and initiates homing behavior. The EB model is involved to remember the Home position. The response of the EB model at step 65 is shown in Fig. 2.15. At steps 67, 69 (not shown) and 71 the robot tries to return to the Home position. At the end of the simulation, the robot can communicate the approximated position of the targets. Moreover, the robot is aware of the association between an odor and a danger. Nevertheless, in this simulation, the robot was not able to safely associate a visual feature with reward or punishment, because it has been punished only once while approaching a landmark.

2.5 Remarks and Conclusions

A computational model inspired by the *Drosophila melanogaster* brain has been implemented within a robot simulator. The olfactory learning model is a two layer spiking neural network and the STDP algorithm has been used for the learning implementation. This algorithm allows the robot to make associations involving odors in complex environments. The orientation memory has been tested through the simulation of the ellipsoid body model. The Behavior Selection Network has been simulated with hypothetic drives. Moreover, the whole architecture has been simulated in an application useful for real life scenarios. The reported results demonstrate that the proposed computational model can be successfully applied to real robots to solve tasks in complex environments.

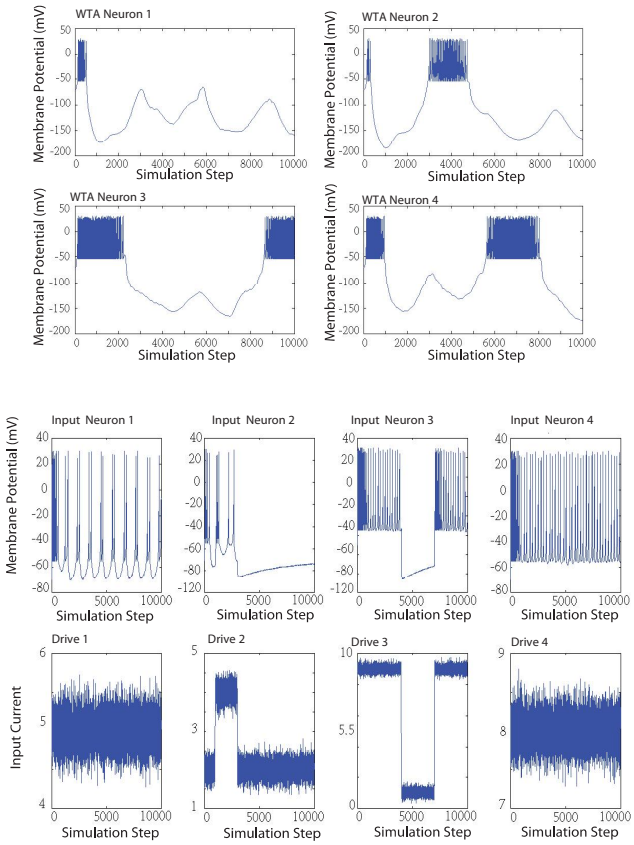

Figure 2.11: Results of the simulation of the BSN. After a short transient in which all the WTA neurons are firing, only one neuron can win the competition. The transient is a consequence of the time response of the synapses between WTA neurons. Variation of the drives could also lead to new transient, in which the WTA neurons compete. A low value of the auto-excitatory synapses weights in the WTA layer can cause a continuous switching of the selected behavior, while a too high value leads to a conservative behavior selection.

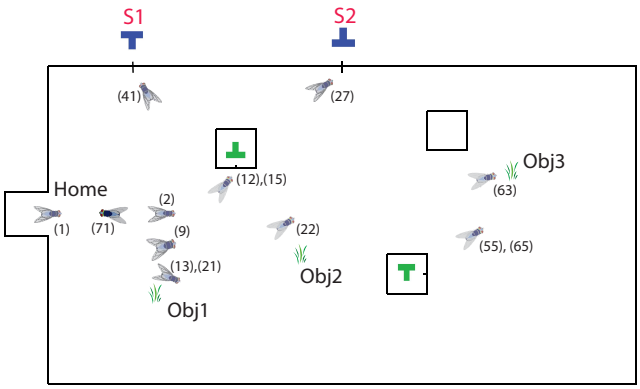

Figure 2.12: Most relevant robot steps of the proposed simulation. After the exploration of the environment the robot returns to the Home and gives the position of the target S_1 and S_2. Moreover, information about the dangers in the environment are stored in the FB and the MBs model.

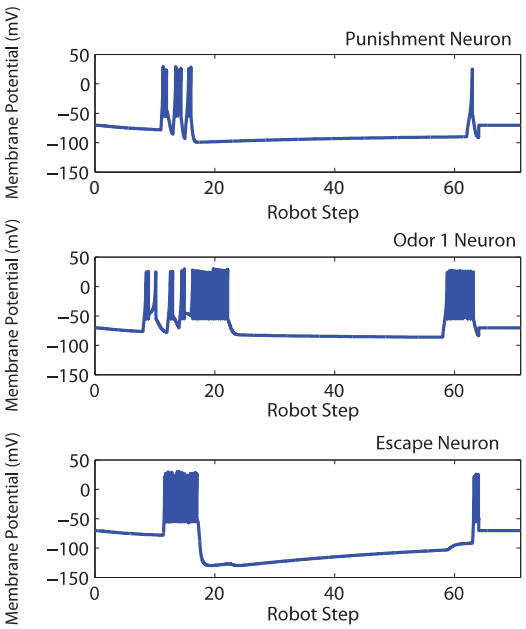

Figure 2.13: Mushroom Bodies model response obtained during the simulation.

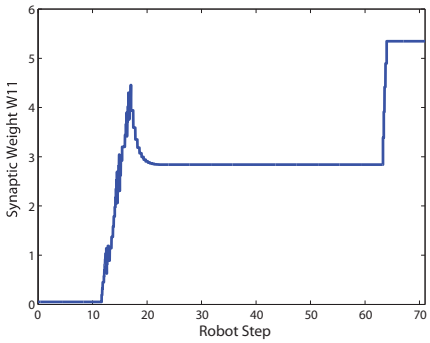

Figure 2.14: Trend of the synaptic weight of the synapses between the $Odor_1$ receptor neuron and the Escape neuron, in the pre-motor area. The synaptic weights of the MBs olfactory learning model are subject to STDP learning. The higher the value of the weight is, the faster the robot will escape if punished while sensing that odor. If the weight exceeds a certain threshold, the robot sensing that odor will escape even if not punished at all. For clarifications about the parameters, the model implemented is shown in Fig. 2.1.

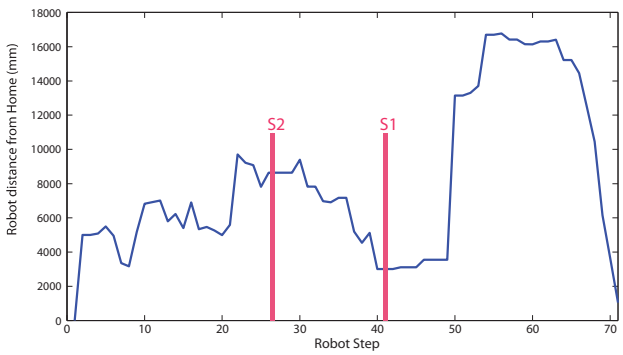

Figure 2.15: During the simulation, the EB model estimates the distance of the robot from the Home position. Errors in the position are due to the simulated odometry error and to the path integration method approximations.

Chapter 3

Visual learning in Drosophila: application on a roving robot

Visual learning is an important aspect of fly life. Flies are able to extract visual cues from objects, like colors, vertical and horizontal distributedness, that can be used for learning to associate a meaning to specific features (i.e. a reward or a punishment). Interesting biological experiments show trained stationary flying flies avoiding flying towards specific visual objects, appearing on the surrounding environment. Wild-type flies effectively learn to avoid those objects but this is not the case for the learning mutant rutabaga defective in the cyclic AMP dependent pathway for plasticity. A bio-inspired architecture is here proposed to model the fly behavior and experiments on roving robots were performed. Statistical comparisons have been considered and mutant-like effect on the model has been also investigated.

In an interesting paper Liu and coauthors [12] trained flies to avoid flying towards specific visual objects appearing on a surrounding white cylinder. If flies approached such an object a heat beam was automatically activated punishing the on-going behavior. Wild-type flies effectively learn to avoid those objects but this is not the case for the learning mutant rutabaga defective in the cyclic AMP dependent pathway for plasticity. The dangerous and the harmless objects shown on the cylinder were characterized by distinct visual features: their height over ground, their angular orientation or their size. Interesting biological experiments using a partial rescue technique for localizing the memory in the fly brain show that the object features are stored in the fan-shaped body (i.e. part of the Central Complex). Using the currently known information available through the experiments a model of the part of the Central Complex involved in visual learning has been designed.
Experiments on a roving robot were performed to evaluate the proposed architecture. The artificial insect brain model has been implemented in order to

control the behavior of the robot. The experimental set-up includes an arena where some objects are present. These objects are different but they also have common features. We assume to consider dangerous one of the possible features (for example, the green color). Every time the robot tries to approach a green object, it will be punished. Every time the robot detects an object, it switches the behavior in order to approach the selected object. The Fan-shaped Body will work as a classifier increasing or decrease the weights relative to each feature of the detected objects. In this way the robot learn to avoid dangerous objects and to recognize the dangerous features.

3.1 The artificial model

The development of an insect brain model is a complex task that can be handled and then evaluated considering several different prospectives. The research was principally directed towards the fly *Drosophila melanogaster* and the neural blocks identified and modeled are often tuned in the fly direction. The direction followed in the architecture evaluation process, consisted into comparing the results obtained by neurobiologists in fly experiments with the robot behavior when performing the same tasks.
Biological experiments that involves flies are mainly based on behavioral analysis; this approach motivates the use of statistical analysis of the insect behaviors in order to obtain the relevant key parameters filtering out noise and the fact that only few variables are considered in each experiment discarding the other intrinsic internal variables. These results have been replicated on the robot obtaining a good match between fly and robot behaviors. Moreover another interesting useful aspect for the model evaluation consists in the analysis of the mutant fly behavior. Several experiments concerning fly can be replicated using, instead of Wild type exemplars, genetically modified lines where either specific blocks of the brain or basic learning mechanisms are altered (e.g ablating neural assembly in the brain or using gene expressed toxins that can modify specific learning cascades making the fly deficient in specific behaviors). Experimental results obtained with mutant flies can be obtained also by using the insect brain model following the same alteration that neurobiologists perform on real insects. This is an added value that can be used to further justify the feasibility of the developed structure.
The general block diagram of the implementation of the insect brain architecture has been presented in Chapter 1 and it is reminded in Fig. 3.1. It is possible to notice, however, that another block, namely MB3 , has been added to the model. The role of this block will be discussed deeply in the next chapter.

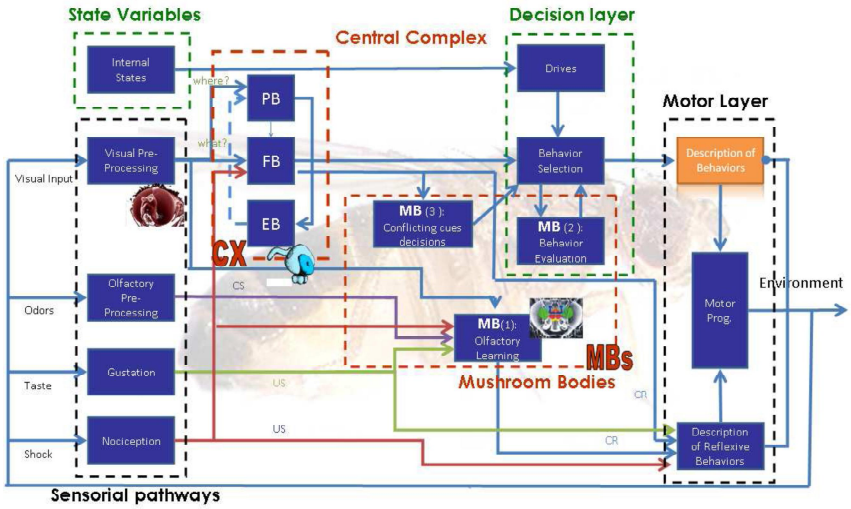

Figure 3.1: Block diagram of the insect brain model.

The Central Complex is the brain structure mainly involved in visual tasks; it is composed by three neuropils, namely the Protocerebral Bridge [19], the Ellipsoid Body [13] and the Fan-shaped Body. In particular, The Fan-shaped body model allows the robot to implement a visual conditioning. This model and its connection with the rest of the insect brain have been upgraded with respect to the first implementation, how it will described in the following section.

3.2 Experimental Results

3.2.1 Robotic Environment

The experiments were performed both in simulation and on real robots. The developed SW/HW framework includes a 2D simulation environment useful for roving robots (see Fig. 3.2 (a)) and a 3D dynamic simulator based on ODE, where legged and hybrid robots can interact with objects in a virtual arena (see Fig. 3.2 (b)). Different robotic platforms used during the experiments are: the roving robot equipped with an on-board PC (Fig. 3.2 (c)), two different prototypes of the hybrid robot Tribot (see Fig. 3.2 (d)) and a six-legged robot called Minihex (see Fig. 3.2 (e)).

The framework developed to test the insect brain, includes a graphical interface that allows to identify the different active blocks while the robot is performing the experiment as shown in Fig. 3.3.

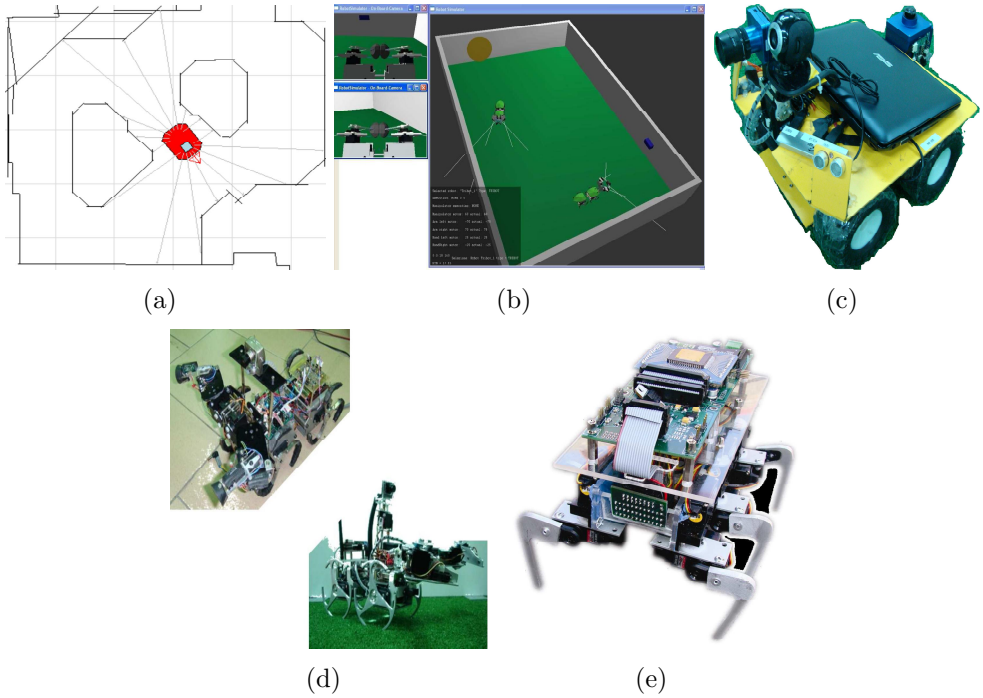

Figure 3.2: The experiments have been performed both in simulation, using a 2D simulation environment (a) and a 3D dynamical simulator (b) and by using robotic prototypes: (c) a rover, (d) hybrid robots (Tribot I and II) (e) and a hexapod (MiniHex).

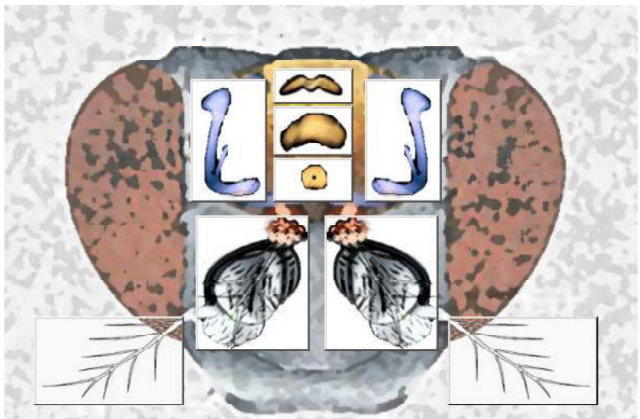

Figure 3.3: Graphical interface where the active elements of the insect brain are visible during the experiments.

3.2.2 Results

Experiments carried out on visual learning show the fly capability to associate either attractive or repulsive behaviors to specific objects or even single features if a training stage is performed using a reward or punishment-based procedure.
The proposed model inside the insect brain to demonstrate these cognitive processes, is mainly related to the Central Complex (CX) block. In particular the Protocerebral Bridge (PB), the Fan-shaped Body (FB) and the Ellipsoid Body (EB), are able to support this new process. The objects placed just in front of the robot are segmented and all the relevant features are extracted. The visual preprocessing phase, that mainly involves the optic lobe, has been performed both using standard libraries developed inside the framework and by means of the Eye-Ris visual system. Concerning the Fan-shaped body, the relay station role performed during the visual orientation, is now integrated and augmented with storing capability together with learning mechanisms. The FB model is a multi-network architecture in which each subnetwork is a spiking structure as shown in Fig.3.4 where unconditioned stimuli (i.e. reward and punishment) are used to trigger a spike timing dependent plasticity (STDP)[26] based learning. Each subnetwork manages a particular feature (i.e. color, shape).
The first layer of the network receives in input the visual pre-processed signals and is connected to a second layer with two neurons associated to the two main behaviors that can be elicited at this level: escaping and approaching. In particular, analyzing the synaptic connections, we can underly that the shock neuron is connected through an excitatory synapsis to the escaping neuron and inhibits the approaching neuron. This is justified because in presence of a dangerous condition the robot escapes without taking into account the other sensory signals. The depicted connections are fixed (not subject to learning) because represent the basic level of a priori-knowledge present in the system for safety reasons.
The other sensing neurons that receive information about the visual features of the object, are connected to both the second layer neurons through excitatory synapses subject to learning. The initial values have a bias toward the approaching behavior giving to the robot an initial preference (i.e. curiosity) to be attracted from the objects in the scene. However the escaping behavior, when elicited, is able to inhibit the object approaching. Similar structures can be replicated for different features in a modular way. Each subnetwork is devoted to handle specific visual features that concur to the behavior selection process through a third layer as shown in Fig.3.5. The third layer transfers the information processed through the CX to the Behavior Selection Network (BSN), where the merging with the other sensory modalities occurs.

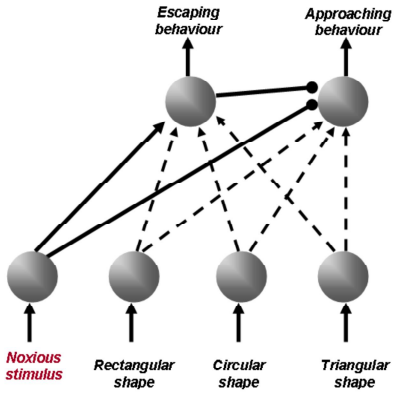

Figure 3.4: Elementary block of the FB structure. Unconditioned stimuli (e.g. an electric shock) guide the learning of a spiking network that associates a meaning to visual features extracted in the FB. The example refers to shapes, solid lines represent fixed synapses whereas dashed lines indicate plastic connections subject to learning through STDP.

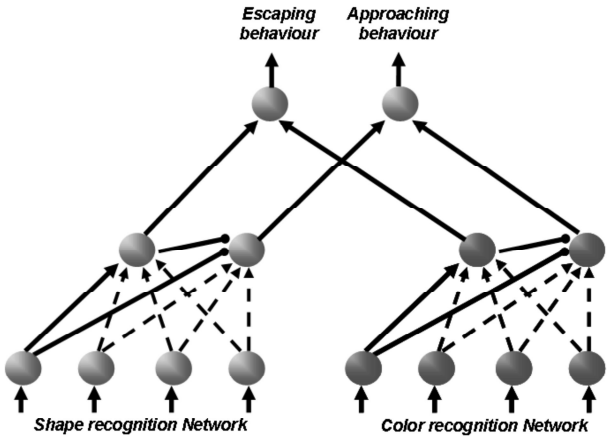

Figure 3.5: Multiple Elementary blocks of the FB structure can be connected each other through a second layer where visual features are combined.

In Fig. 3.6 the robot behavior when four attractive objects are placed in the arena is shown. In this simulation the robot is able to extract the object features for learning. The final behavior depends on the fact that the robot has been rewarded when reaching all the targets. In contrast, if during the simulation a pair of targets is considered dangerous the final behavior is depicted in Fig. 3.7 where the robot safely reach the left and right targets while after a series of punishments in the downside one, learn to avoid both the bottom and upper side targets that have the same visual features.

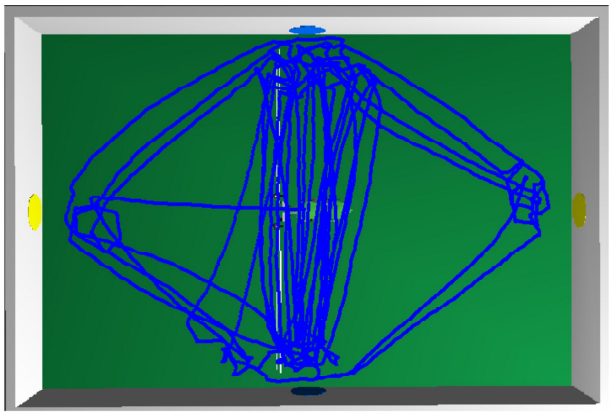

Figure 3.6: Visual learning experiment. The simulated robot trajectories show the emerging behavior when the robot is rewarded for reaching the targets placed on the center of the walls. The patrolling between the two targets on the farther walls does not emerge due to the preference in reaching the nearest target among the visible ones.

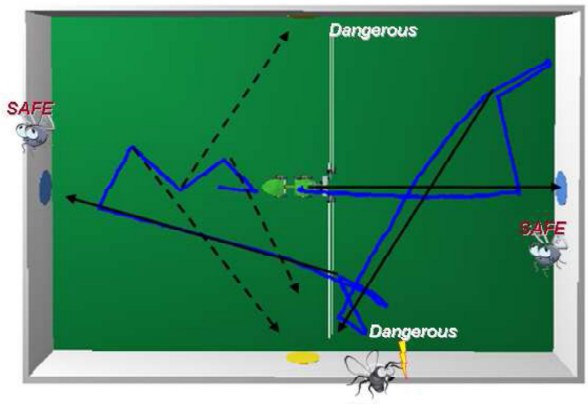

Figure 3.7: Visual learning experiment. The robot safely reaches the left and right targets (see the solid arrows) whereas is punished when the downside object is reached. The learning process allows the robot to avoid the objects and visual features associated to dangerous events, in this case the bottom and upper side ones (dashed arrows).

In the following preliminary tests on a roving robot are reported which are currently under evaluation for further optimization. The same set-up used in the dynamic simulator environment has been replicated in the arena for the robot experiments. Two yellow circles have been projected in the screens in

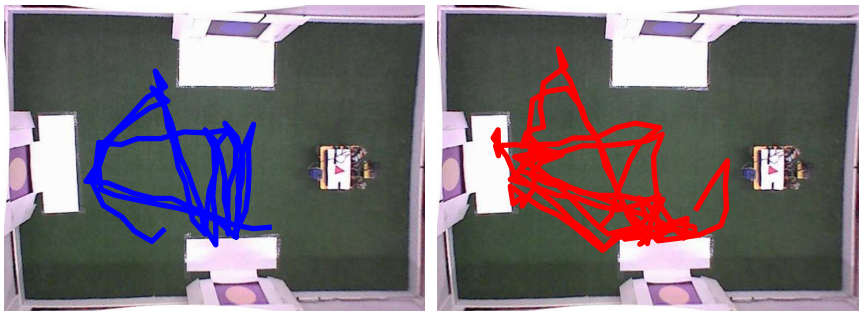

(a) (b)

Figure 3.8: Trajectory followed by the robot for the first 100 steps (a) and for other 150 (b). The robot initially attracted by the blue landmark, after several punishments learns to avoid it.

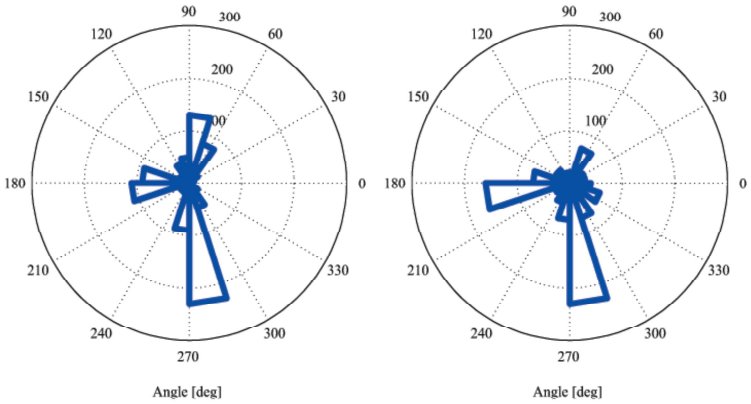

(a) (b)

Figure 3.9: Gaze direction for the first 100 steps (a) and for other 150 (b).

the left and right side walls whereas a blue circle is shown in the upside of the arena. The Rover, exploring the arena, is attracted by these targets and is punished when the blue circle is reached. the trajectory obtained during the experiment are reported in Fig. 3.8. The robot is initially attracted by all the landmarks (Fig. 3.8 (a)) and then avoids the blue circle (upper wall) due to the punishment signals (Fig. 3.8 (b)). The changes in the robot behavior are also evident in Fig. 3.9 where the gaze direction for the first and second part of the experiment is reported.

The level of punishment associated to each feature is shown in Fig.3.10 where the escaping value for each object is also shown.

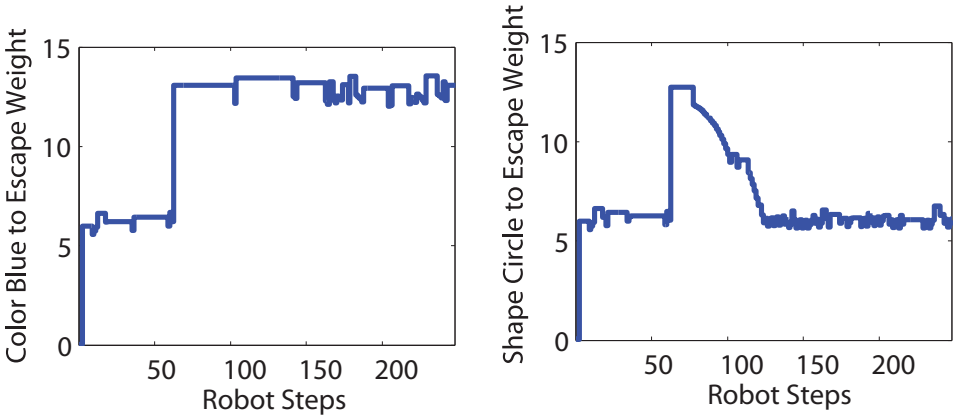

Figure 3.10: Temporal evolution of the synaptic weights that associate the blue color (left) and the circle shape (right) to the escaping behavior. After 100 steps the robot is able to discriminate the blue circle as dangerous.

3.3 Conclusions

The insect inspired spiking neural architecture has been designed and implemented both in software and hardware robotic environments. This structure has been tested in a biological-like experiment of visual conditioning on roving robots. The STDP paradigm applied to the fan-shaped body network allows the robot to extract dangerous features from objects and modulate behavior of the robot in order to avoid dangerous objects in the environment.

Chapter 4

Modeling the decision making process in fruit fly

A decision making process has been identified in the flies that have been trained to avoid objects with specific visual features. In presence of a conflict the fly has to decide which features are the most relevant to make a choice. The decision making strategy seems to be guided by a pre-wired hierarchical categorization of the features that, for instance, leads the fly to give more importance to color with respect to shape. The bio-inspired architecture of the *Drosophila* brain is here upgraded to model the fly behavior and experiments on roving robots are reported. Statistical comparisons have been considered and mutant-like effects on the model has been also investigated.

4.1 Introduction

Visual learning is an important aspect of fly life. Flies are able to extract visual cues from objects and associate a meaning to them depending on other proprioceptive and exteroceptive stimuli [12].
Decision making is an interesting aspect of the insect brain. The number of experiments related to this process are limited due to the complexity of the set-up that needs to exclude a multitude of possible concurrent variables to perform a correct analysis of the results. However an interesting experiment was performed by Tang and Guo (2001) [39], they trained stationary flying flies, using a heat beam, to avoid a visual pattern in a choice situation where two times two pairs of objects are presented. One pair of objects was green and had an upright-T shape and the other pair was blue and had an inverted T-shape. In the test situation the colors were switched between objects. This feature mixture creates a conflicting situation for the flies. Is the predictor of heat the

form or the color of the previously punished object? Wild-type flies took their decisions to avoid the previously punished objects based on the color of the objects, showing a strong preference in following the color information. An interesting behavior arises when the level of color saturation decreases during the experiments. The dilemma is therefore created not only switching the colors between the landmarks, but also fading the level of saturation. Below a certain threshold for color saturation wild-type flies suddenly and consistently select the shape instead of the color of the objects to be avoided. There was always a clear decision in all flies of the population. Mushroom Bodies-less flies had no clear decision point at which they would switch from color to shape. Rather their population average started with short preference for the color at full saturation and then gradually shift towards shape as the color fades. Therefore Mushroom Bodies (MBs) can be considered as a relevant center for visual-based decision making processes. A bio-inspired architecture has been proposed to model the fly behavior and experiments on a dynamic simulation environment were performed.

4.2 Model Description

In insects and in particular in flies, MBs are a key neural assembly for decision making. Visual information are mainly processed through the Central Complex (CX) [12], [19], [13] but interesting experiments on the fly show that even if no direct connections have been till now discovered between CX and MBs, the latter is responsible for decision making processes also in relation to visual inputs. The role of MBs for generalization with foreground/background separation and in presence of contradictory cues has been demonstrated in different experiments. How it has been shown in Chapter 3, modeling the Fan-shaped body, an important element of the CX, it is possible to replicate on a robotic platform the visual conditioning biological experiments carried out on the fly [40]. The proposed model for solving decision making problem in visual-related experiments in flies is shown in Figure 4.1. The visual information acquired through the fly's compound eyes is elaborated in the CX to be used for the final behavior selection. Beside this direct path a secondary one through the Mushroom Bodies is established. Only a limited number of relevant information are acquired from the visual preprocessing layer to be used to modulate the CX response. The MBs works as a gateway that using control gains can unbalance the response of the CX. This mechanism is not important for tasks like visual learning nevertheless is fundamental in presence of contradictory visual cues to solve a dilemma. The part of the MBs block devoted to this process, that we called MB3, is important to solve con-

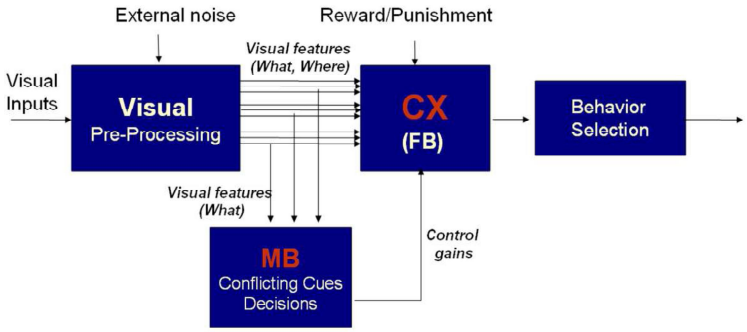

Figure 4.1: Block diagram of the elements of the insect brain involved in the decision making process in presence of contradictory cues in the processed visual field.

tradictory situations, as will be shown, but it is not essential for the visual orientation, targeting and learning. As depicted in Figure 4.1, the direct path through the CX and the indirect path through the MB goes to the Behavior Selection Network (BSN) that does not correspond to a real physical structure of the brain but a block where all the distributed functionalities related to the final behavior choice have been glued. The current implementation of the BSN consists of a two layer spiking network implementing a Winner Takes All - like behavior.

The role of MBs in handling visual information is up to now limited to two specific circumstances: in presence of contradictory cues and for foreground/background separation allowing a generalization process. In the following the model proposed to deal with the decision making process in presence of contradictory cues is reported and the structure has been modeled on the basis of the experimental results reported in [39]. The so-called MB3 network works as a gateway that modulates the information that from the FB are directed to the BSN depending on specific input signals. The key information processed at this level is the color saturation that allows to sharply decide the most convenient behavior to be performed. The network consists of two neurons that receive an input current related to the color saturation value of the segmented object. One of the neurons is sensible for high level and the other for low level of saturation. The output of these neurons inhibit the output of the two subnetworks of the FB (i.e. shapes and colors). These connections guarantee that when the color saturation level is high, the color network will lead with respect to the others and viceversa. The MB3 network receives inputs from the FB, in particular the escaping and approaching signals are used to understand if a dilemma is present, due to the presence of contradictory cues. When both the neurons are active, the MB3 block inhibits one of the

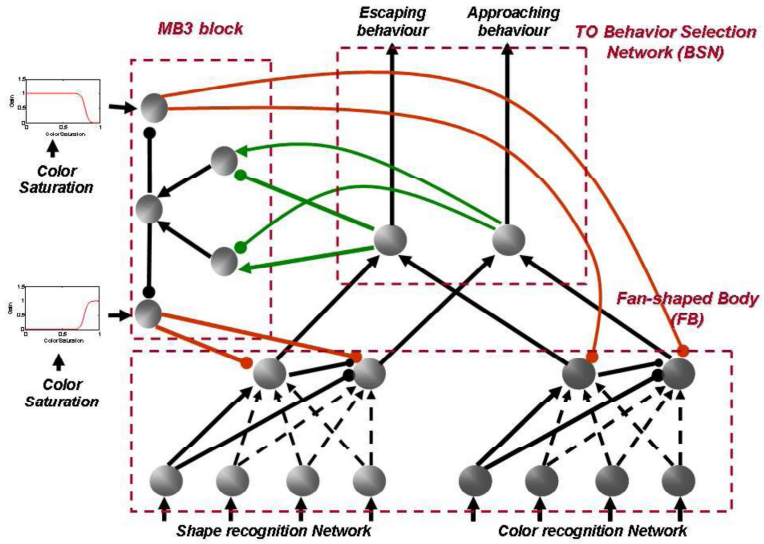

Figure 4.2: Interaction between the FB, MB3 and BSN blocks, the presence of MB3 is important for the final behavior selection as part of the decision making process.

output of the FB subnetworks solving the dilemma depending on the level of color saturation, otherwise the MB3 is silent and does not interact with the process. Figure 4.2 shows the whole network including FB, MB3 and part of the BSN. The visual preprocessing block is able to extract the relevant features from the segmented objects present in the scene and the FB associates a meaning to the visual data depending on the rewarding or punishing signals coming from the environment. Finally the acquired information compete at the behavior selection block in choosing the final robot behavior. The role of MBs in this control chain consists in modulating the information coming from the FB depending on the value of specific visual features that in the proposed experiments, in accordance with experiments in the fly, correspond to the level of color saturation. In summary, the experiments were performed both in simulation and on real robots using a SW/HW framework that allow to perform dynamic simulation on a 3D environment [41].

4.3 Simulation Results

To evaluate the performance of the proposed control system, a virtual arena similar to that one used for the biological experiments has been considered. The rectangular arena contains two pairs of landmarks placed on the opposite walls. The simulated robot, depending on the received punishment signals,

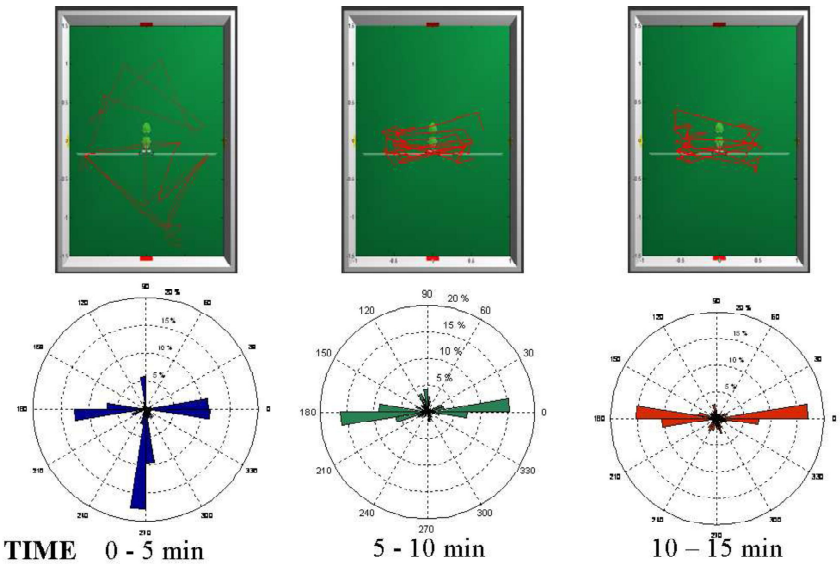

Figure 4.3: The behavior of the robot in terms of followed trajectories and gaze distribution, is acquired in windows of 5 minutes. The red squared landmarks in the bottom and upper part of the arena are dangerous and the robot learns to avoid objects with these features.

modifies its behavior as shown in Figure 4.3, where the robot activity is summarized in windows of 5 minutes for a total of 15 minutes of simulations. The robot trajectories, together with the gaze direction for each time window are reported. The robot, during an initial exploration phase, learns to avoid the red squares that are associated to a punishment.

The FB network, where meanings are associated to visual features, evaluates, depending on the received signals, a punishment value for each feature. The time evolution of the gaze direction distribution is shown in Figure 4.4 where it is evident that in a few minutes the simulated robot learns to avoid the red square. A very similar behavior is reached also when the information about the object shape is missing (e.g. all the objects have the same rectangular shape) as shown in Figure 4.5 where the gaze direction in time is similar to the previous case. In Figure 4.6 the evolution of the punishment values is also reported, it is evident that the dangerous feature is now represented only by the yellow color while the square shape is no longer considered dangerous in this scenario.

Another interesting case is obtained when the shape is the only distinct feature between the landmarks, for instance putting in the arena red circles and squares. Only the square objects produce a punishment to the robot. The

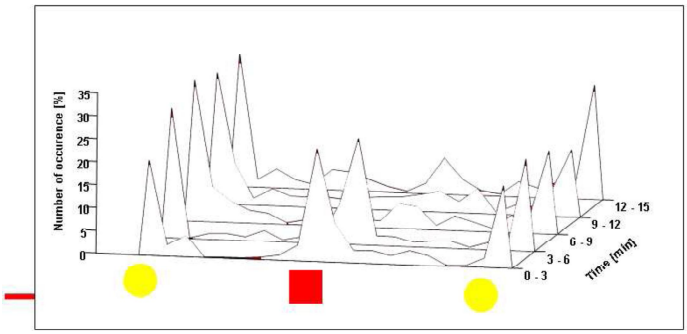

Figure 4.4: Evolution of the gaze distribution in time. After a few punishment events, the robot avoids to direct its attention to the red squared object.

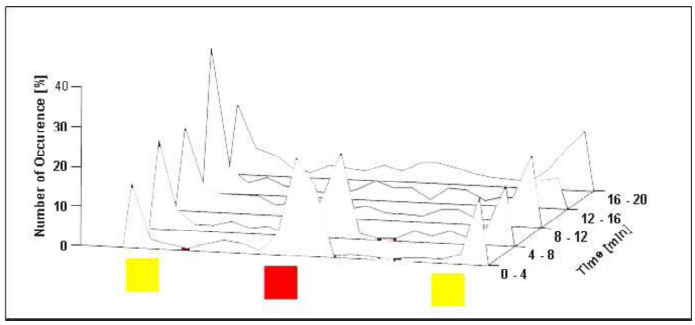

Figure 4.5: Evolution of the gaze distribution in time when the objects have the same shape but different colors.

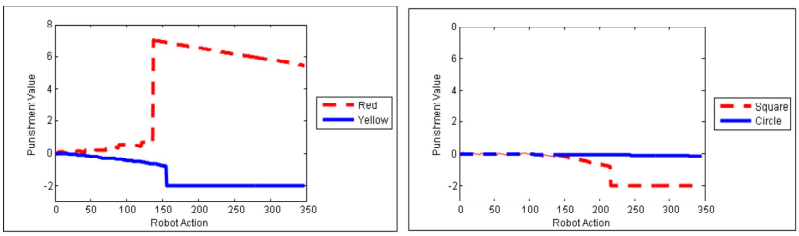

Figure 4.6: Evolution of the punishment value when the objects have the same shape but different colors.

gaze direction is reported in Figure 4.7 and the behavior is similar to the other illustrated cases, whereas the trends of the punishment values associated to the visual features reported in Figure 4.8 show, for the red feature, series of oscillations not visible in the previous case (for the square shape) that depend on the detection sequence during the simulation and on the general preference for the color feature with respect to the other cues that was implemented in

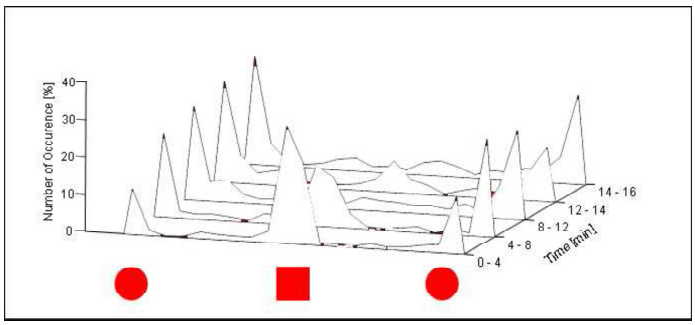

Figure 4.7: Evolution of the gaze distribution in time when the objects have the same colors but different shapes.

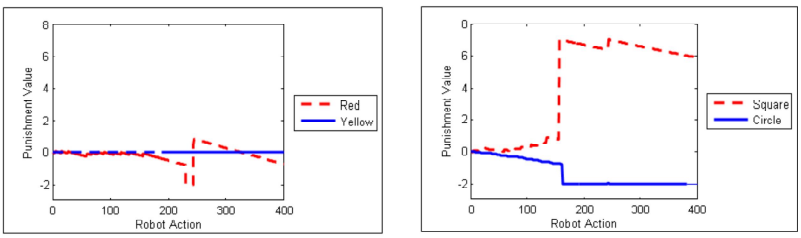

Figure 4.8: Evolution of the punishment value when the objects have the same colors but different shapes.

resemblance with the biological case.

Eventually the role of the MB3 block, that works as a gateway modulating the information generated by the FB, is evident in the case of a dilemma. The robot after learning in the arena shown in Figure 4.3, is facing a new scene where the visual features associated to the objects are contradictory if compared with the first arena, in fact a yellow square and a red circle are now present: the color was switched with the shape. In Figure 4.9 the behavior of the robot is shown through the gaze direction obtained in three different simulations that differ for the value of the color saturation. When the saturation is high ($CS = 1$) the robot has a preference for the color (i.e. red), decreasing the saturation ($CS = 0.8$) the robot has no preference and tries to escape from the objects, finally for low level of color saturation ($CS = 0.5$) a preference for the shape arises. Going deeper in details analyzing the critical case of $CS = 0.8$, it is possible to evaluate the temporal evolution of the robot behavior as shown in Figure 4.10. During the first 5-10 minutes the robot has no preference for the objects while, thanks to a forgetting factor, during time the robot starts to approach objects with square shapes and later on also red objects if the punishment signal is no longer present in the environment.

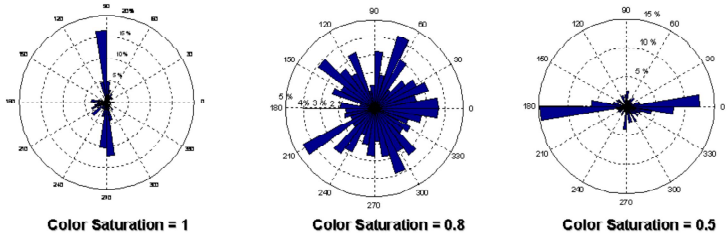

Figure 4.9: Dilemma test in presence of the MB block. After a learning phase performed in the arena in Figure 4.3, a testing is performed changing the color feature between the two objects. When the color saturation is high, the robot has a remarked preference for the color, reducing the color saturation (CS=0.8) no preference appears whereas further reducing the color saturation (CS=0.5) a preference for the shape appears.

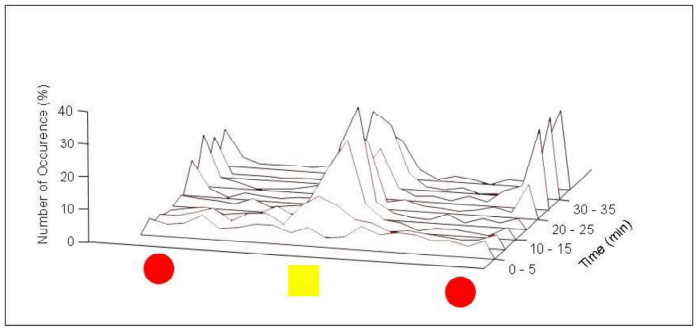

Figure 4.10: Dilemma test in presence of the MB block. When the color saturation is about CS=0.8, the robot shows no preference but due to a forgetting factor a preference for the shape appears in time and persists if the punishment signal is removed

A very interesting result obtained in [39] consists in replicating the Dilemma experiment in a mutant fly with defects in the MB block. The results obtained while changing the level of color saturation are given in Figure 4.11, in our case the block MB(3) is not active it is interesting to analyze that while for low level of saturation the behavior is very similar, when the color saturation is high the robot is not able to decide which feature is dangerous with respect to the other and tries to avoid both without solving the dilemma. To summarize the results and compare the behavior of wild type and MB-defective robots, a preference index has been considered. The index is similar to that one used in the biological experiments in [39], and is calculated considering the time spent

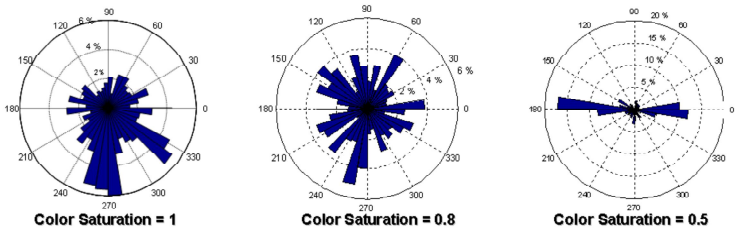

Figure 4.11: Dilemma test after ablating the MB block. The presence of an high color saturation is not enough to force the robot to make a choice.

observing each object compared with the entire simulation time:

$$PI = \frac{t_{YS} - t_{RC}}{t_{tot}} \tag{4.1}$$

where t_{YS} is the time spent observing the yellow squared object t_{RC} is the time spent observing the red circular object and t_{tot} is the duration of the experiment. Figure 4.12 shows the trend of the Preference index for both the simulation campaign. The index is obtained performing a set of 10 simulations of 5 minutes for the different levels of color saturation. The results show that the robot controlled with an insect-like brain structure is able to make a clear decision among the two objects depending either on the color (for $CS > 0.8$) or on the shape ($CS < 0.8$) while the mutant robot, where the effect of the MB block on the decision process is missing, is not able to decide in case of high level of color saturation. Finally also in the mutant experiment when the degradation of the color is high enough, the preference for the shape takes the lead.

4.4 Conclusion

Flies are able to extract visual cues from objects, like colors, vertical and horizontal distributedness, and others, that can be used for learning to associate a meaning to specific features. In presence of a conflict the fly has to decide which features are the most relevant to make a choice. A bio-inspired model of the *Drosophila* brain centers involved in this task has been proposed to model the fly behavior and experiments on roving robots were performed. Results have been compared to biological data.

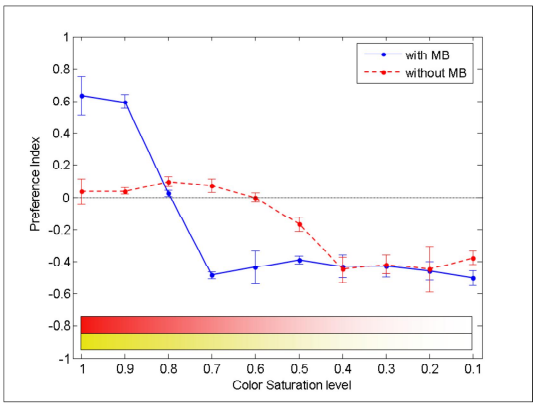

Figure 4.12: Representation of the robot behavior through the preference index in presence of a dilemma in the proposed simulations. See [39] for biological details and comparisons. Significative differences are visible when the MB block is eliminated from the control loop.

Chapter 5

A model for expectation in insects

In this chapter a neural model inspired by the insect olfactory system, with particular attention to the fruit fly *Drosophila melanogaster*, is proposed. This architecture is a multilayer spiking network: each layer is inspired by the structures of the insect brain mainly involved in olfactory information processing, namely the Mushroom Bodies, the Lateral Horns and the Antennal Lobes. In the Antennal Lobes layer olfactory signals lead to a competition among sets of neurons, resulting into a pattern which is projected to the Mushroom Bodies layer. Here a competitive reaction-diffusion process leads to a spontaneous emerging of clusters. The Lateral Horns have been modeled as a delayed input-triggered resetting system. Using plastic recurrent connections, with the addition of simple learning mechanisms, the structure is able to realize a top-down modulation at the input level. This leads to the emergence of an attentional loop as well as to the arousal of basic expectation behaviors in case of subsequently presented stimuli. Simulation results and analysis on the biological plausibility of the architecture are provided and the role of noise in the network is reported.

5.1 Introduction

The enhanced tools recently adopted in insect Neurophysiology have allowed to shed light on the details of neural signal processing in some specific parts of insect brain responsible for complex behaviours like attention. The insect brain areas responsible for these processes are the *Mushroom Bodies* (MBs) that, together with the *Lateral Horns* (LHs), are primarily devoted to olfactory learning. The spatio-temporal olfactory information coming out

from a neural structure named Antennal Lobes (ALs), is processed and stored in spatial patterns [42, 23]. MBs are well known for their capability to perform associative learning for odor conditioning [43]. Recently neural models inspired by the *Drosophila melanogaster* and locust brain anatomy were proposed using roughly the same number and connectivity as the olfactory biological counterpart. The spatio-temporal coding in such neural structures has been investigated in [44], where a model for codifying spatio-temporal patterns into spatial patterns was implemented. In that paper the structure exploited autonomous clustering capabilities and no learning algorithms were taken into consideration. In order to include specific learning capabilities into the system, the proposed architecture is based on models of spiking networks where characteristics like visual features, learning, recalling and forgetting were considered [45, 46]. These structures were successfully applied to enhance the capabilities of an autonomous robot, but they were really far from the skills of insects, which are able to show other interesting capabilities like attention and expectation-based behaviors. Novel tools from Neurophysiology are continuously advancing the knowledge about neural activity even in such small brains as the fruit fly. In particular, in [47] interesting clues of the presence of attention processes were found analyzing the registered local potential field (LPF) within the fly brain. The author was able to show increased LPF activity when the fly is positioned in a rotating cylinder with two alternating different objects, whereas no LPF variation was observed when displaying twice the same object in the same setup. Moreover learning mutants in the cAMP cascade, showing deficits in short-term memory, did not show such neural evidence. Of course specific tests excluded that such behavior was due to a lack of visual cues responsiveness. To host such skills, the traditional model, mainly based on feedforward connections from the sensory to the classification layer, should also include other kinds of feedback connections, able to affect the input sensitivity to particular expected sensory features. Recently feedback connections from MBs to the ALs have been found [48]. Here a functional role of such connections in filtering input information is hypothesized and proposed in the developed model. This new interesting feature allows to refine the models previously presented, adding new capabilities to the system.

Starting from the already introduced neurobiological findings, a new artificial model of the insect olfactory system with enhanced capabilities is here introduced. This model could explain how sophisticated attention and expectation mechanisms arise in insects when they facing with complex environments. Learning to know in advance which incoming input stimulus is correlated with the actual one is a fundamental ability in living beings, useful to take the appropriate action, sometimes life-saving. The possibility to make predictions

and to modulate sensorial inputs through expectations is the key point of the model introduced in this work. The proposed model is a multi-layer spiking neural network basically inspired to [44], and including the recent findings in [48]. The first layer represents the Antennal Lobes model: inputs are decomposed in main *features*, represented by feature-specific groups of neurons within the input layer. Here a locally competitive topology is implemented, as suggested in Neurobiology [50]. This layer randomly projects connections to the second layer, which models the functionalities of the Mushroom Bodies, mainly constituted by Kenyon Cells (KCs layer). Each neuron in this layer is connected through fast excitatory synapses to its neighborhood and, within the same layer, through fast inhibitory synapses to the rest of the network. In order to have a symmetric set of connections, a toroidal shape was implemented. The KCs layer shows interesting clustering capabilities and represents the core of the system in terms of spatio-temporal pattern formation. Recurrent connections are present from the KCs to the ALs. The Lateral Horns model, as suggested from Neurobiology [49], has been thought as an input-triggered system that provides a delayed global inhibition to the Mushroom Bodies network. Moreover, the role of noise was assessed in a twofold aspect: the former is related to the clustering robustness, whereas the latter, more interesting, exploits the possibility to use the positive role of noise when no input activity is registered at the ALs layer. Noise produces a spontaneous learning activity, remainding the phenomenon of consolidation during sleep, well known as occurring in the fly, as well as in human beings.

5.2 Biological Background

The most deeply studied neural centers in the fly brain are the MBs, that, together with the LHs are widely recognized to play a fundamental role in processing the spatio-temporal information coming from the glomeruli of ALs. Mutual inhibitory connections among the ALs glomeruli have been found recently in neurobiological studies on the fruit fly, as discussed in [50]. This competitive topology allows the creation of odor-evoked patterns of excited and inhibited glomeruli that are sent out to the higher brain structures like MBs and LHs. MBs are a paired structure within the protocerebral hemispheres. They play a primary role in olfactory learning: this was unambiguously proven thanks to specific experiments with MB-defective mutant flies [16]. In the fly *Drosophila melanogaster*, each side of the MBs is constituted by 2500 Kenyon cells which run in parallel from the *calyx* through the *peduncle* and to the *lobes*. There is a prominent olfactory input from the Antennal Lobes into the calices. Input from other sensory modalities is not obvious in *Drosophila*, even

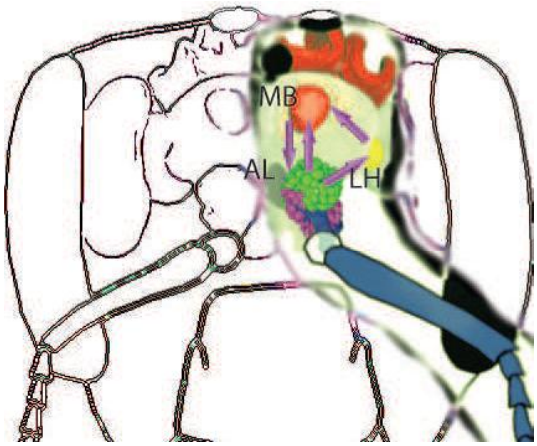

Figure 5.1: Circuit for olfactory processing. The Antennal Lobes (ALs) project olfactory information to the Mushroom Bodies (MBs) and Lateral Horns (LHs) through the Projection Neuron (PNs). In locusts, the LHs inhibits the MBs activity.

if high level tasks dealing with the choice behavior in front of contradictory visual cues and involving MBs are described for flies [39]. In other insect species MBs are a fundamental neural center where multimodal sensory integration for learning was found: for example honeybees MBs receive prominent visual [14], gustatory, and mechanosensory input [15]. There is also an output of the MBs to pre-motor areas of the brain. The information flow through MBs was formerly considered as prominently feedforward, i.e. from the Kenyon cells to the calyx and towards the lobes. Very recently, recurrent connections between MBs and ALs have been found. The presence of this functional feedback from the MBs to the ALs opened the way to suggest a model including top-down modulation of olfactory information processing in *Drosophila* [48]. The scheme of the architecture proposed is depicted in Fig. 5.1, where the different involved neural centers are outlined. Olfactory information flows in parallel from the ALs to the MBs and LHs. Connections from LHs to MBs have been found, but their entity in *Drosophila* is not well known. Further information comes from locusts, where LHs play an inhibitory effect to the MBs Kenyon Cells [49]. A model which takes into account this inhibitory role was implemented in [44]. In this model each Kenyon cell is strongly connected to the cells of its neighborhood, and in this architecture the Antennal Lobes layer randomly projects to the Kenyon cells layer. A coincidence detection mechanism allows the model to codify sequences of events in spatial patterns of firing neurons. No learning is implemented in the model proposed in [44], whereas the system architecture discussed in this paper includes also learning mechanisms to allow

pattern reconstruction and expectation capabilities.

5.3 Insect inspired neural model

The neural model here proposed (Fig. 5.2) combines behavioral evidences on attention capabilities in insects, including flies, with the state of the art on the neural structures responsible for these processes. It includes also a biologically relevant learning rule which boosts the system capabilities: expectation is the emergent aspect of this new architecture. The model is directly inspired to the olfactory system of the *Drosophila melanogaster*, including the new enhanced top-down connections from MBs to the ALs, and considering the global inhibitory role played by LHs. The overall neural structure is configured as a two layer recurrent network endowed with artificial spiking neurons. Presently the model capabilities are analyzed referring to the clustering, attention and expectation learning processes. Of course, a natural evolution of the model proposed could include an additional layer connected to the motor area for behavioral motion control. As previously outlined, the developed neural structure was inspired by the insect olfactory system. At the aim to build a computational model useful for a number of different applications, the same structure can be used for processing different sensorial artificial stimuli (e.g visual features can be easily used in robotic scenarios). In insects the MBs are involved in a huge number of tasks and completely different aspects of learning and memory [51]. For this reason in the rest of the chapter generic object features will be taken into consideration.

5.3.1 The Neuron and Learning Models

The neural network is built around a cluster of spiking neurons organized in layered lattices. Each unit is an Izhikevich spiking neuron [17]. The model is represented by the following differential equations:

$$\begin{aligned} \dot{v} &= 0.04v^2 + 5v + 140 - u + I \\ \dot{u} &= 0.02(-0.1v - u) \end{aligned} \tag{5.1}$$

with the spike-resetting

$$\texttt{if } v \geq 0.03\texttt{, then} \begin{cases} v \leftarrow -0.055 \\ u \leftarrow u + 6 \end{cases} \tag{5.2}$$

where v is the membrane potential of the neuron, u is a recovery variable and I

is the synaptic current. Izhikevich neural models are well-known in literature and offer many advantages from the computational point of view.

Neurons are connected through synapses. The synaptic model transforms the spiking dynamics of the pre-synaptic neuron into a current that excites the post-synaptic one. The mathematical response of the synapses to a pre-synaptic spike is reported below:

$$\varepsilon(t) = \begin{cases} Wt/\tau \exp(1 - t/\tau), & \texttt{if } t > 0 \\ 0 \ , & \texttt{if } t < 0 \end{cases} \tag{5.3}$$

where t is the time lasted from the spike, τ is the time constant and W is the efficiency of the synapse. This last parameter can be modulated with experience.

Hebbian learning, introduced by Donald Hebb in 1949, is a mechanism where the synaptic efficiency increases through coincident stimulations of the postsynaptic and presynaptic cell.

The Spike Timing Dependent Plasticity (STDP) can reproduce Hebbian learning in biological neural networks [26, 27]. The algorithm works on the synaptic weights, modifying them according to the temporal sequence of occurring spikes. The updating rule can be expressed by the following formula:

$$\Delta W = \begin{cases} A^+ \exp(\Delta t/\tau^+), & \texttt{if } \Delta t < 0 \\ -A^- \exp(\Delta t/\tau^-), & \texttt{if } \Delta t > 0 \end{cases} \tag{5.4}$$

where Δt is the time delay between pre and post synaptic spikes. In this way the synapse is reinforced if the pre-synaptic spike occurs before the post-synaptic one, it is weakened in the opposite situation. Parameters τ_+ and τ_- represent the slope of the exponential functions, whereas positive constants A_+ and A_- represent the maximum variation of the synaptic weight. Interesting applications in biorobotics of this learning paradigm, together with details on the parameters are reported in [45, 28].

5.3.2 Antennal Lobes Model

Inspired by the ALs of the *Drosophila melanogaster*, it is possible to assume having a layer able to codify the interesting *features* of objects. In the insect ALs each glomerulus is able to detect a peculiar component of an odor: in the model each neuron in this layer encodes a particular aspect related to a detected object. Neurons within the ALs model are organized in groups, as illustrated in Fig. 5.3. Each group codifies a kind of feature (examples of features could be color, shape, etc.), and neurons in the same group codify

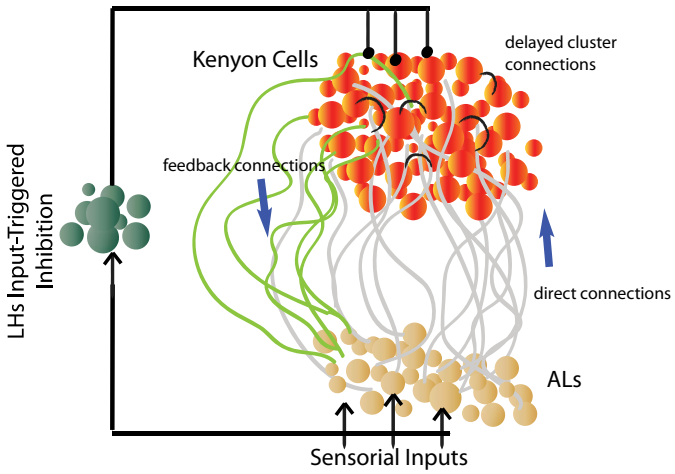

Figure 5.2: The Antennal Lobes (ALs) model is directly connected to the sensorial inputs (Antennas). We can assume that the activity of each AL neuron codifies a particular value for a specific feature. Neurons in the ALs are organized in groups. Synapses from the Antennal Lobes model to the Kenyon Cells (KCs) layer are randomly chosen, with a given probability of connectivity. The KCs layer is a toroidal lattice, with local excitatory and global inhibitory synapses. The Lateral Horns (LHs) periodically inhibit the KCs neurons. Feedback plastic connections link clusters in the MBs to the ALs neurons. Local connections within the ALs and within the KCs are not reported. The delayed plastic synapses in the KCs layer allow a temporal link between subsequent object presentations.

different values of that feature (i.e. different colors or shapes). Neurons in the same group are linked together through inhibitory synapses. This topology implies that, when the ALs layer is stimulated, after a short transient time, only one neuron in each group remains excited, according to a Winner-takes-all topology. Neurons in different groups are linked together through plastic synapses, reinforced when neurons are firing together, according to the Hebbian rule. This process reinforces organization among the neurons representing the different features of a presented object, leading them to reach a phase locked firing state. These mechanisms remind some way the Winnerless competition principle [52, 53], modelled after ALs studies. Therefore, when an object is presented to the network, the ALs model decomposes it in its relevant features, and the corresponding neuron of each group remains excited. The ALs model topology is inspired by the biological case [54], where excitatory and inhibitory connections allow the interaction between glomeruli in order to have the primary odors representation. The ALs layer projects excitatory

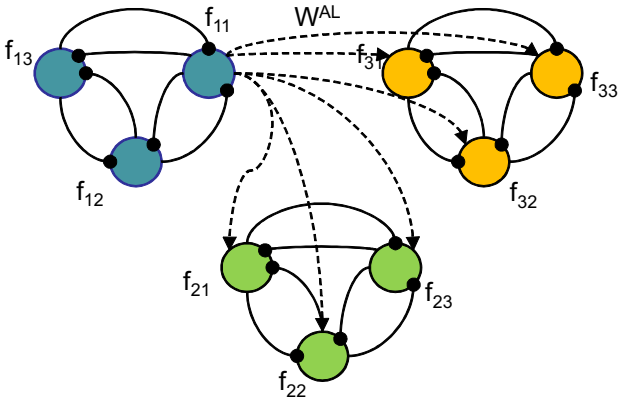

Figure 5.3: Connection scheme of the ALs neural model where three different features and three different classes within them are considered. The neurons associated to the same feature class are mutually inhibited whereas they excite neurons of other sets through plastic excitatory connections that are subject to learning (only the excitatory connections for neuron f_{11} are reported in figure).

direct connections to the MBs network, constituted by a number of neurons which represent the Kenyon Cells (KC) in the fly MBs. Each neuron of the ALs is connected to each KC model with a given probability of connection, recalling the sparseness of connections in the corresponding areas of the fly brain.

5.3.3 Mushroom Bodies and Lateral Horn Models

MBs model is configured as a complex recurrent neural structure. It is made up of a number of KCs which receive afferent input from the ALs and send feedback synapses back to the ALs. More in details, a competitive topology was designed for the KCs layer. Each KC is a spiking Izhikevich neuron and the whole KCs lattice, thanks to the connections among KCs and ALs neurons, undergoes a spatial temporal wave, which leads to the emergence of a cluster of neural activity. This spatial temporal activity represents the crucial aspect of the overall network. The KCs layer was conceived as a toroidal lattice where each neuron is connected through fast excitatory synapses to all the neurons of its neighborhood, and through fast inhibitory synapses to all the other neurons of the lattice, as shown in Fig. 5.4. The main capability of the KCs layer is a spontaneous clustering of spiking activity, driven by a Winner takes all-like structure. In this way, information coming from the ALs is compressed together into a cluster of neurons, spiking at a given frequency. In addition to this process, a slow and delayed diffusion of the neural activity within the KCs

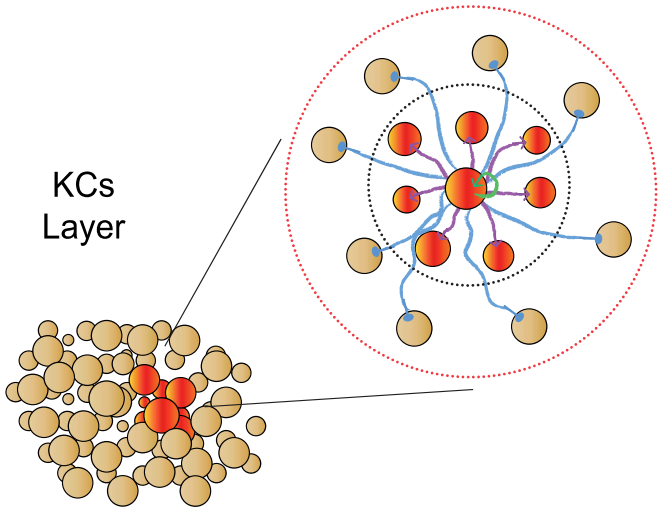

Figure 5.4: The KCs layer is a toroidal lattice, with local fast excitatory and global fast inhibitory synapses. Another set of plastic delayed synapses links each neuron of the KCs layer to the other neurons of the same lattice, in order to have the possibility to temporally link different clusters, allowing short term prediction and expectation capabilities of the neural architecture. In figure, the inner circle indicates the locally excitatory neighborhood, whereas the outer circle includes all the KCs layer network where a global inhibitory effect takes place.

layer is included in the model. More in details, another set of plastic delayed synapses links each neuron of the KCs layer to the other neurons of the same lattice, in order to have the possibility to temporally link different clusters. These synapses are subject to the STDP learning algorithm, that allows to discover and retain temporal causality among clusters. These connections have the interesting capability to generate, within the KCs layer, expectation and short term prediction capabilities. Plastic feedback connections are also present, as already outlined, from the MBs model to the ALs layer. These connections, recently discovered in Biology [48], were never considered in any MBs computational model up to now. Their role is precious to boost the model performance and two main functions have been identified: they are useful to create an expectation-based depolarization of the neurons in the ALs; they are also essential to reconstruct the expected object. When a cluster is elicited in the KCs layer, the synaptic connections between the neurons of the MBs cluster and those neurons which are firing in the AL (due to the synchronous presence of the corresponding input) are increased, according to the Hebbian paradigm.

In the fly brain, it is well known that Lateral Horns are connected to the MBs, whereas in the locust their inhibitory role for MB activity was emphasized [44]. Therefore, LHs have been here modeled modeled as an event-driven resetting system, that generates an inhibitory wave to the MBs, defining a processing time window for the system. In this way, the KCs layer integrates the information coming from the ALs in a given time window and, after the emergence of a cluster, the neural activity of the network is inhibited by the LHs wave.

5.4 Network design and simulation results

The behavior of the whole network is here analyzed through a series of simulations. The obtained results are useful to understand the basic principles that rule the network and its parameters.

5.4.1 Network Parameters

An important aspect of a multi-layer spiking network consists in the tuning of parameters. The guidelines used for this proposed model are here discussed. While the morphology of the insect brain structure is well known, the details of the topological organization and above all the peculiarities of the network connections are largely unknown. Only in some particular cases light is being shed and the features of specific neural structures were unraveled, thanks also to the support of behavioral Neurogenetics. Only very recently modern tools allowed reliable neurophysiological measurements in specific brain regions. This is the case of locust and, to a lower extent, of the fly. As a consequence, the network considered in this work was designed drawing considerations from a number of different cues. As regards the structure and the number of neurons in each subpart of the network, we know from Biology that the odorant components, through the olfactory glomeruli, stimulate 250 neurons for each AL, which project to 2500 KCs. In the presented model the same ratio has been roughly maintained, even if the actual architecture has a much scaled topology and connectivity with respect to the biological counterpart, and has to be considered as a proof of concept for the basic and enhanced capabilities ascribed to the olfactory insect neural architecture. In this case, 9 neurons in the ALs layer are connected to 81 KCs; each neuron in the ALs layer has a probability $P = 0.012$ of being connected to a KC neuron. The choice of the sparse connections between the first and the second layer is directly drawn by the sparse connections in the biological counterpart [49]. In the proposed simulations, the first layer is made by a 3x3 lattice. In particular, there are three groups

of neurons (f_1, f_2, f_3), and each group is made of three neurons (for instance, the neuron j in the group f_i will be called f_{ij}), as shown in Fig. 5.3. Neurons in the same group are connected each other through inhibitory synapses, with a synaptic efficiency $W^{AL} = -3$. Neurons in different groups that, after the presentation of an object, fire together, increment the efficiency of the synaptic link with a $\Delta W^{AL} = 2$. The initial value of such synapses is zero. When an object is detected, the neurons of the first layer that encode the features of that object are excited with an input current $I_{AL} = 70$. The synapses between the first and second layer have fixed efficiency of $W^{AL,KC} = 10$.

Concerning the KCs layer, a 9x9 lattice with a toroidal topology has been considered. The neurons in this layer are all connected each other according to the paradigm of local excitation and global inhibition. A neighborhood of radius $r = 1$ is defined. In this way, each neuron is connected to the neurons in its neighborhood and with itself through excitatory synapses with an efficiency of $W^{KC}_{near} = 50$. It is also connected to the other neurons of the lattice through inhibitory synapses with an efficiency of $W^{KC}_{far} = -30$. This set of connections gives the network its clustering capabilities. Moreover, a second set of synapses is implemented, which allows the linking of sequences of winning clusters. Each neuron is connected to each other neuron in the lattice through a time-delayed synapse, subjected to learning. In this case, the most active neurons of two clusters activated sequentially in time reinforce the synapses among them according to the STDP rule. Feedback connections are initially set to zero. When a cluster in the KCs layer is firing together with neurons in the AL layer, the corresponding synapses are raised, $\Delta W^{KC,AL} = 1$. The time constant used for fast excitatory and inhibitory synapses in the network is $\tau_{fast} = 1ms$. All the equations are solved using the Euler method with an integration time of 0.08 ms. Synapses time constants have been chosen in order to have a plausible matching with respect to the biological counterpart. Furthermore the learning coefficients for the network (e.g. ΔW, A^+ and A^-) are chosen in order to obtain a robust association after a few presentations of consecutive objects, similarly to the biological counterpart [55, 43]. In order to demonstrate the robustness of the structure and to mimic realistic situations, noise has been introduced during the simulations. In particular, each parameter has been altered adding a gaussian noise with zero mean and variance equal to the 10% of the mean value of the same parameter.

5.4.2 Analysis of the clustering properties

To test the clustering properties of the neural model an object with three different features is presented to the first layer of the network; three neurons are excited, one for each group of input neurons (Fig. 5.5). The ALs projects

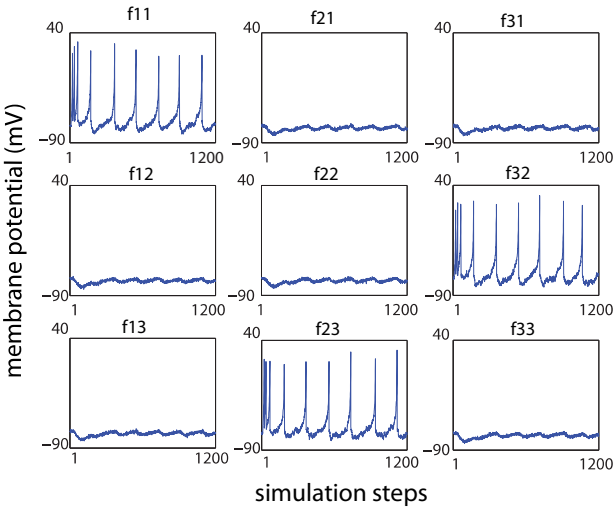

Figure 5.5: Evolution of the membrane potential of the neurons in the first layer, during the presentation of the first object. In this case, no competition is present between neurons, due to the absence of the contribution coming from the expectation feedback. However, it can be noticed the inhibitory effect of the excited neurons on the others. Input neurons project information to the KCs layer.

the information to the second layer (KCs layer), exciting its neurons. After a transient of 1200 simulation steps, the network is able to elicit a winning cluster. Fig. 5.6 depicts the trend of the mean potential of the KCs neurons in given time windows, clearly showing the arousal of the clustering effect. The emerged cluster tends to remain stable during time. It is important to notice that some of the main properties of the KCs layer model remain constant with respect to the variation of the dimensions of the lattice. For example, in Fig. 5.7, a simulation of a 20x20 lattice is presented. The behavior of the network is similar to the 9x9 one. The main difference stands in the time needed to elicit a winning neuron. A larger lattice needs longer to converge, since more connections are involved. However, the mean frequency of the oscillations in the membrane potential of the winning neuron remains within the same range. That is in line with the neurophysiological measurements performed in the locust ALs [56]. So the design of the neuron parameters, the input current amplitudes and the time constants have been conducted taking into consideration these guidelines from Biology. Also the mean membrane potential of the neurons remains unaffected from the network scaling. It is to be noticed that the transient time is also related to the connectivity level between the ALs and the KCs layer. The increase of wiring probability involves a longer transient

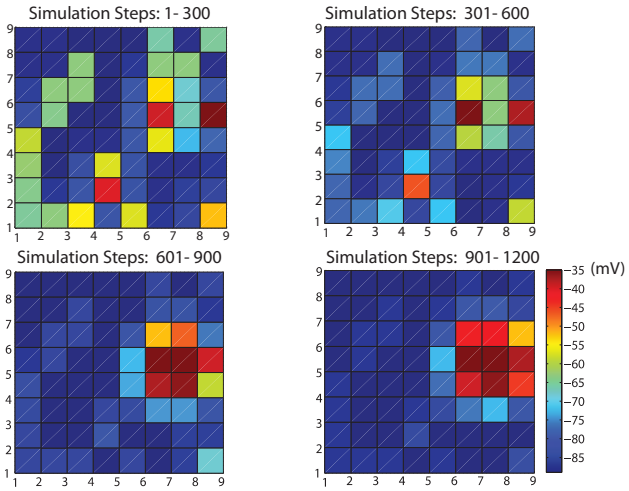

Figure 5.6: Evolution of the mean potential of the neurons in the 9x9 KCs layer. The network has been simulated for 1200 steps with an integration time of 0.08ms. The membrane potential is averaged every 300 simulation steps. At the end of the simulation, only one cluster of neurons remains active.

to reach a steady state condition in the KCs layer. In any case the clustering capabilities are preserved. It could be also noticed that the clustering capability of the network depends on the ratio between the efficiency of the local excitatory synapses and the inhibitory ones. In particular, maintaining the chosen ratio to about $5:3$, the clustering capabilities are preserved. However, high values of efficiency increase the robustness to noise. For example, with the parameters $W_{far}^{KC} = -3$ and $W_{near}^{KC} = 5$ the clustering performance decreases if a noise of 10% is introduced during the simulations. For this reason it is preferible to use larger weights, as already discussed, obtaining a more robust and stable clustering capability during the pattern formation process in the KCs layer. In the following the main capabilities of the proposed network are outlined through a series of key simulations.

5.4.3 Attention through top-down modulation

The network structure can be trained to show attentive capabilities, which consist in filtering out, from a previously presented and learned object, all the other stimuli, being them other objects or noise, that could be presented concurrently with the reference object. Such attention capability, recently discovered in the fly [47], is a simple emerging property of the presented structure which derives from the presence of recurrent top-down connections. In fact, if

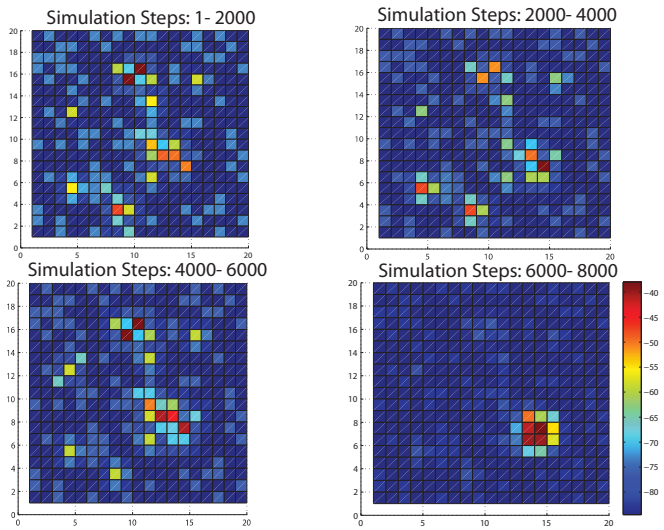

Figure 5.7: Evolution of the mean potential of the neurons in the 20x20 KCs layer. The network has been simulated for 8000 steps with an integration time of 0.08ms. The membrane potential is averaged every 2000 simulation steps. At the end of the simulation, only one cluster of neurons remains active.

a given object is repetitively presented to the network input, a particular cluster emerges, and concurrently, the feedback connections to the ALs neurons corresponding to the presented object are reinforced. If the presented object is disturbed by the presence of additional distracting inputs (being these noise or other objects), the feedback connections bias the ALs neurons associated to the current cluster, to be much more excited than those ones elicited by the distracter inputs. As a result, internal ALs connections, with the addition of the feedback ones, cooperate in such a way as to efficiently filter out the exogenous signals, enhancing the attentional process. If the top-down connections were absent, the WTA processing in the ALs layer would not be able, by itself, to filter out distracters and a new cluster would emerge, showing a clear example of distraction process, as found in cAMP-cascade learning mutant flies, which show attention deficits. If such an attentional process is extended to subsequently stimulated clusters, expectation-based processes emerge, as described and experimentally shown in the following.

5.4.4 Expectation through top-down modulation

The expectation capabilities of the MBs structure can be modeled exploiting the synaptic modulation of the feedback connections between the Kenyon Cells and the Antennal Lobes when objects are presented in sequence. To bet-

ter explain this process a simulation is here reported, where two subsequent objects are presented to the network. In particular, the first object is characterized by features that stimulate f_{11},f_{21},f_{31} ALs neurons whereas the second object is identified by other features (f_{11},f_{23},f_{32}). During the presentation, the KCs layer elicits two consecutive clusters and links them through the delayed synapses. Moreover, the connections between the two clusters and the corresponding input neurons at the ALs layer are learned. Several scenarios are presented in the following, to outline various interesting features of the proposed architecture.

1. A first simulation consists in the presentation of a first object, followed by another object with an incomplete feature set presented at the second step. In particular, information about the feature related to the second group of neurons in ALs (f_{2j}) is missing. In this case, thanks to the previous learning cycles, the KCs layer is able to reconstruct the lacking feature: feedback connections from the MBs excite the ALs neurons that codify that object and synaptic connections among neurons in different ALs groups allow the reconstruction of the complete object. No competition does take place in the ALs layer, but top-down connections allow the recalling of the lost information. An example of this reconstruction mechanism is shown in Fig. 5.8. The expectation capability herewith presented can be further exploited for modelling a simple sequence learning paradigm. In fact, if during the learning phase a short number (say three) of objects is presented, three winning clusters are subsequently elicited and the central neuron for each cluster reinforces its connection to the central neuron for the winning cluster associated to the subsequent object. So, during the testing phase the presentation of the first object is able to elicit the sequence of winning clusters in the KCs layer, which reconstruct at the AL layer, the sequence of corresponding objects. The sequence of formed clusters following this procedure is depicted in Fig. 5.9. At the end of each phase, the network is reset by the LHs.

2. In a second test, after the presentation of the first object, the second object is presented again. In this case, the feedback system acts as an expectation-based filter that enhances the response of the whole architecture. The cluster elicited by the first object stimulates, through the delayed connections, the second cluster and then the ALs neurons speeding up the response to the second object.

3. Finally the behavior of the network in case of unexpected situations is evaluated. After the presentation of the first object, a second object is

presented to the network, but it is different from the second object presented in the learning phase. In this case, a competition takes place. The top-down connections enhance the response of the neuron representing the common features between the object just presented (and unexpected) during the test phase and the second object shown in the learning phase. At the end of the competition, a new cluster is elicited in the KCs layer, as shown in Fig. 5.10. This cluster represents the new object, creating a new sequence. The network is then able to store multiple short competing sequences and the most reinforced one will be finally stored. It has to be considered that the structure is not conceived to act as a sequence generator, but it contains the basic ingredients and, suitably modified and scaled up, could be the starting point for an efficient bio-inspired sequence generator. From the biological point of view there is clear evidence for sequence learning in bees, but until now the neural circuits giving rise to such capability are unknown.

5.4.5 Consolidation during Sleep

An interesting property of the network can emerge, exploiting the presence of noise in the system. In fact the contribution of noise in can be useful to consolidate the acquired knowledge during a resting phase, when no sensorial inputs are given to the network. A simulation divided in two phases is prepared: the first one is a learning phase, in which the network creates the association between clusters and objects. In particular, four sequences of two objects have been presented to the network. At the end of the training phase no physical input is presented at the ALs layer, but it is assumed that the KCs layer is subject to noise which was supposed to be gaussian with zero mean and variance $\sigma_{noise} = 10$. This noisy disturbance will onset a dynamical transient in the KCs neurons until a cluster will emerge over the others, as shown in Fig. 5.11. If this cluster had formerly been trained to represent a given object, this will be recalled at the ALs layer, like an "imagined object". A new learning cycle will then arise, in which not only this object will be consolidated, but also all the other objects eventually expected after this one in an already learned sequence (see Fig. 5.12). New imagined solutions could also be experienced during this "sleeping phase" and, in more complex networks including also more environmental details, the system could discover new strategies to efficiently solve difficult situations starting from what already learned during the "awake phase".

5.5 Conclusions

Inspired by specific parts of the insects brain, it has been proposed a neural model for expectation-based learning. The neural architecture is a multi layer structure in which the first layer consists of sensory neurons inspired by the insect Antennal Lobes. The neurons of this layer are able to detect the presence of characteristic features in objects. The information coming from the sensorial system is then projected to the second layer, that is a self-organizing layer inspired by the insect Mushroom Bodies. The competitive topology of this network is focalized to the emergence of clusters, and it is periodically reset, simulating the LHs effect found in locusts. The basic principle of the architecture is that the expectation for objects can be translated into a sequence of winning clusters in the KCs layer, that projects back to the ALs. Simulation results show the suitability of the proposed network as a bio-inspired architecture, in which drawing inspiration by simple beings, emergent capabilities, like attention, expectation and simple sequence recalling tasks can be found. The network capabilities can be exploited in robotic applications like landmark recognition, behavioral choices in front of expected situations versus unexpected ones, and sequence learning for maze solving. Regarding the network topology, the random probability-based connections between the first and the second layer improves the clustering capabilities of the network. This enables the birth of new clusters in presence of slightly different objects, decreasing, on the other side, the memory capacity of the network that can be improved by scaling-up the network dimensions, reaching configurations similar to the biological case. Moreover, a really added value provided by this simple network is the possibility to reconstruct an expected object. In fact the top-down information stimulates the AL neurons that are considered as representative of the single features that constitute the expected object. The expected object represented in the KC layer, is then projected down at the sensing layer filtering out the other objects eventually present in the scene. So, in case of multiple presented objects, the network will "pay attention" only to the expected one. Finally, the network could learn even without a real input presented: if a suitable level of noise is added in the network in absence of input, for example simulating the overnight autonomous behavior, the noise will excite the KCs layer, which will give rise to sequences of network iterations. This phenomenon could suitably model the overnight memory consolidation effect, well known in insects. Of course the simulation results here presented have to further be refined, together with the model itself in a more and more strict accordance with the biological case.

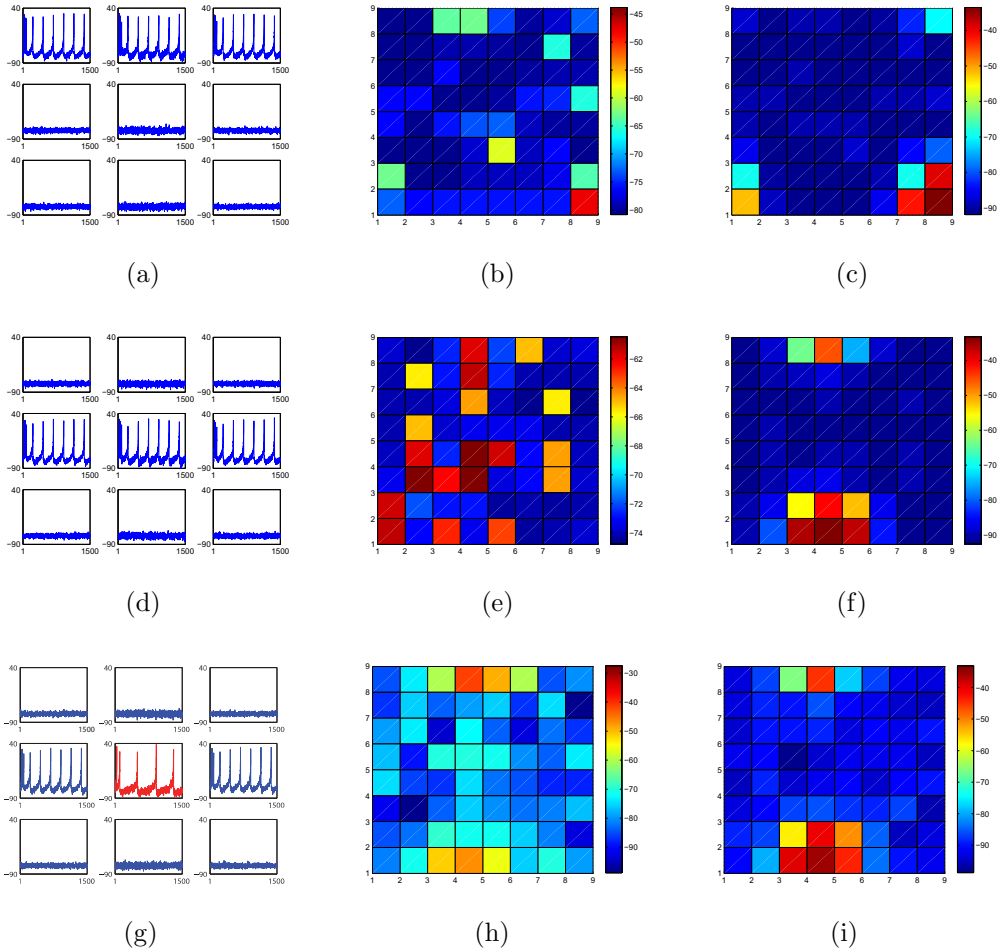

Figure 5.8: The network is able to reconstruct the missing feature using expectation mechanisms. When the first object is presented the ALs layer is stimulated (a) and a cluster emerges in the KCs layer. The mean of the KCs membrane potential at the beginning (b) and the end of the simulation (c) (for a total of 1500 simulation steps) is reported. During this process the plastic synapses in the ALs change according to the Hebbian rule as well as the feedback connections from KCs to ALs. When a second object is presented again, the ALs process the new features information (d) and the KCs layer converges to a new cluster (e)-(f). During this process the delayed connections in the KCs layer are modulated accordingly and the two consecutive clusters (c) and (f) will be linked together. Finally, after the learning phase, if the first object is presented, it is possible to reconstruct the missing feature (f_{22}) of the second object using the acquired knowledge (g) and the correct cluster emerges (h)-(i).

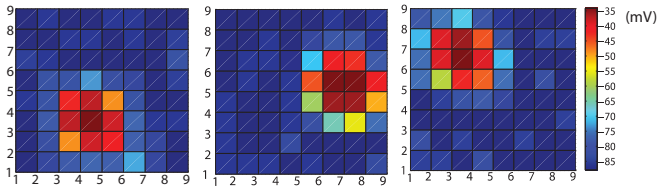

Figure 5.9: During the learning phase, three objects are presented to the network. In the test phase each cluster representing a given object excites the cluster that represents the following object in the sequence. Objects can be reconstructed thanks to the feedback connections from the KCs layer to the ALs.

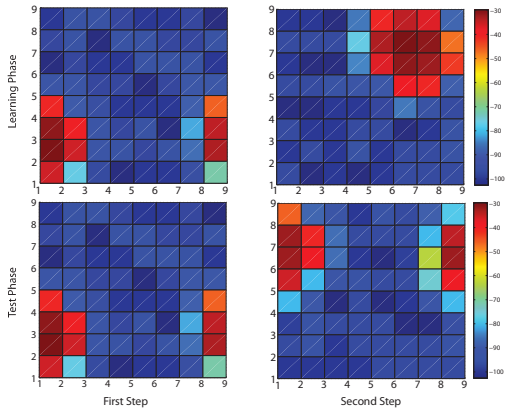

Figure 5.10: Behavior of the network in the case of non satisfied expectation. During the learning phase, after the presentation of two consecutive objects, the KCs layer elicits two clusters and links them through the delayed synapses. During the test phase, after the presentation of the first object, an object that does not follow the previous stored sequence is presented. In this case, at the second step the network tries to recall the second object, but the competitive topology in the first layer corrects the prediction and a different cluster is formed in the KCs layer.

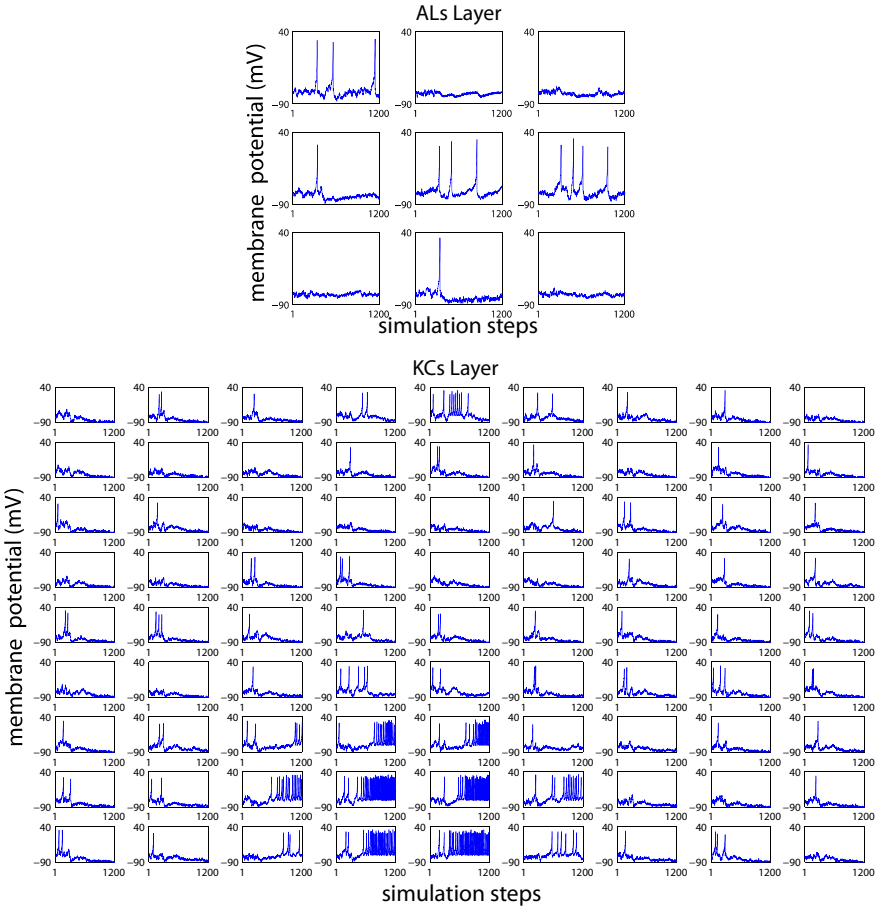

Figure 5.11: After the learning phase, noise can excite the KCs layer leading to the emergence of a cluster. It can be noticed the competition in the ALs layer during the transient in the KCs layer. The relative object features (f_{11}, f_{22}, f_{32}) are reconstructed in the ALs layer through the feedback connections.

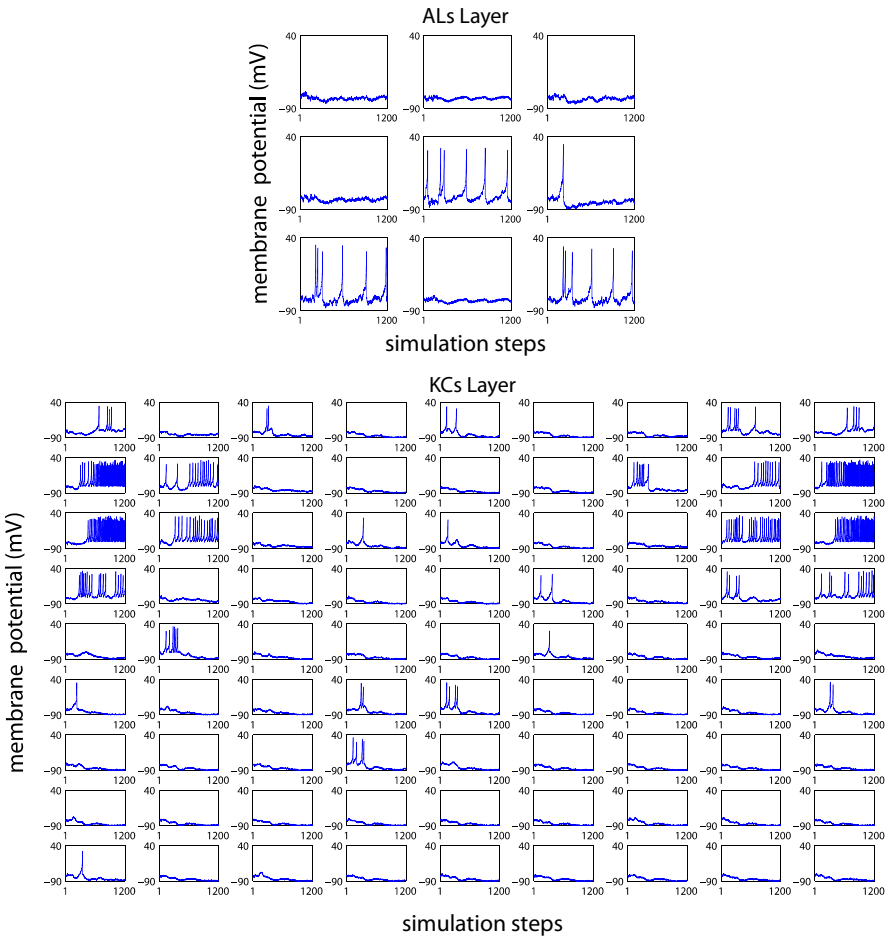

Figure 5.12: During the second step of the consolidation experiment the network autonomously recalls the second object. The connection between the two clusters is strengthened and the second cluster, in turn, stimulates the ALs layer, eliciting the corresponding object (f_{13}, f_{22} and f_{33}).

Chapter 6

Application to a Delayed Match-to-Sample Task

Insects, and in particular honeybees, demonstrate to be able to autonomously abstract complex associations and apply them in tasks involving different sensory modalities within the insect brain. Mushroom Bodies (MBs) are worth of primary attention for understanding memory and learning functions in insects. In fact, even if their main role regards olfactory conditioning, they are involved in many behavioral achievements and learning capabilities, as has been shown in honeybees and flies. Owing to the many neurogenetic tools, the fruit fly *Drosophila* became a source of information for the neuroarchitecture and biochemistry of the MBs, although the MBs of flies are by far simpler in organization than their honeybee orthologs. Electrophysiological studies, in turn, became available on the MBs of locusts and honeybees. In this chapter a novel bio-inspired neural architecture is presented, which represents a generalized insect MB with the basic features taken from fruit fly neuroanatomy. By mimicking a number of different MB functions and architecture, it is possible to replace and improve formerly used artificial neural networks. The model is a multi-layer spiking neural network where key elements of the insect brain, the antennal lobes, the lateral horn region, the MBs, and their mutual interactions are modeled. In particular, the model is based on the role of parts of the MBs named MB-lobes, where interesting processing mechanisms arise on the basis of spatio-temporal pattern formation. The introduced network is able to model learning mechanisms like olfactory conditioning seen in honeybees and flies and was found able also to perform more complex and abstract associations, like the delayed matching-to-sample tasks known only from honeybees. A biological basis of the proposed model is presented together with a detailed description of the architecture. Simulation results and remarks on the biological counterpart are also reported to demonstrate the possible appli-

cations of the designed computational model. Such neural architecture, able to autonomously learn complex associations is envisaged to be a suitable basis for an immediate implementation within an robot control architecture.

6.1 Introduction

Insects show interesting capabilities to learn, categorize and recall associations and contextual information in order to solve tasks that can, in the case of honeybees, even require a complex level of abstraction [60, 51, 89, 39]. Insect brains are becoming a primary source of inspiration for the design of powerful autonomous machine learning architectures and control algorithms. Within the insect brain the mushroom bodies (MBs) have attracted a lot of research attention regarding their architecture and behavioral functions for modeling artificial neural networks. MBs are well known in bees and flies for their role in performing associative learning and memory in odor conditioning experiments [61, 62, 16, 63, 43, 23], but they are also involved in the processing of different sensory modalities like for example visual tasks [62, 89, 39], other forms of learning, and in choice behavior (e.g. [14, 39]). We refer primarily to the architecture of the MBs in *Drosophila melanogaster* which is simpler than in the honeybee and can be divided into substructures, called *calyx, peduncle* and five *lobes* of the lobe system. The major intrinsic neuron type is the Kenyon cell and those cells make up the MBs, the substructures of which correspond to their dendritic regions, their axons and their axonal branches, respectively. Olfactory information is projected to the calyx regions of the MBs from the antennal lobes (ALs). Recently, also feedback connections from the MBs back to the ALs have been found [48]; a functional role of such connections in filtering input information is hypothesized here. MBs interact with the lateral horn region (LHs), presumably to provide a sparse representation of odors.

The ALs are modeled as a lattice of neurons, in which each neuron codifies a particular odor component. Moreover, a locally competitive topology is implemented here, as suggested by neurobiology [50]. The AL layer randomly projects connections to the MB calyx, which is composed of the dendritic arborizations of three different Kenyon cell types namely the $\alpha-/\beta-$neurons, the $\alpha^{'}-/\beta^{'}-$neurons and the γ-neurons. The $\alpha-/\beta-$ and the $\alpha^{'}-/\beta^{'}-$lobes are connected through plastic connections and demonstrate capabilities in clustering information. The LH model, as suggested by neurobiology [49], has been thought as an input-triggered system that provides a delayed global inhibition to the MB network.

The model here proposed is able to reproduce, beside the olfactory classical conditioning, more complex tasks, like delayed matching-to-sample tasks,

which represent capabilities found in honeybees [64].

The proposed artificial neural network of the MBs provides the possibility for modelling autonomous and complex decisions with application in controlling tasks which involve different sensory modalities within the insect brain, with particular attention to honeybees and flies. In honeybees prominent visual inputs to the MBs are anatomically evident and behaviorally most relevant [62]; in flies there is behavioral evidence for the involvement of the MBs in visual tasks like visual context generalization and resolving contradictory visual cues [89, 39].

6.2 Biological Background - *Drosophila* as an Example

Classical aversive or reward odor conditioning experiments in the fruit fly *Drosophila* [65, 66] have shown that acquisition of a memory, its stabilization and retrieval all require intact MBs [67, 23]. Their neuroarchitecture, their input/output relations and biochemistry are worked out in quite some detail (e.g. [55, 23]). Over the years, behavioral evidences accumulated for additional pivotal roles of the MBs in non-olfactory behaviors. [89] reported a function in discriminating between visual background and objects to be avoided in classical aversive conditioning experiments. The visual pathway to the MBs of flies is not anatomically known to date.

Mutations affecting olfactory and visual memory formation in *Drosophila* are also affecting short-term visual processes relevant to selective attention. A common component of these systems appears to be the MBs that might be involved in generating oscillatory brain activity required for attention-like processes in the fly brain [47, 57]. The chapter will therefore concentrate on the neuroanatomical details of the olfactory learning and memory pathway of the fruit fly assuming that the MBs, first serving olfaction, had turned out in evolution to be a "universally useful" learning network. Thus other sensory modalities may have been fitted into a very similar neuroanatomical structure preexisting for olfaction-related behaviors.

The computational MB-model shown in Figure 6.1 takes into account the actual biological organization of the olfactory pathway in flies consisting of the antennal lobes (AL), projection neurons of the antennal lobes (AL-PNs), the lateral horn (LH), the MB intrinsic Kenyon cells (KC), and extrinsic MB neurons (MB-EN1-4) as well as octopaminergic neurons (OAN) and dopaminergic Neurons (DAN). Olfactory sensory neurons (ORN) are excited by different odorant components and project, depending on their odor-receptor type, to

one of the about 62 glomeruli of the AL [68].

About 150 excitatory projection neurons (cholinergic) emerge from the AL [69], and deliver their preprocessed information to the calices (the input region of the MBs) and the lateral horn region (responsible for congenital behavior and direct responses to olfactory stimuli). At the level of the AL excitatory and inhibitory interneurons interact in the first preprocessing of olfactory information and the AL-PNs convey this pattern of activation. On average, each of the 2500 KCs receives input from ten AL-PNs [70] so that single KCs represent different combinations of odorants.

Detailed studies on the post- and presynaptic organization of the KCs at the level of the calices revealed that $\alpha - /\beta -$ and $\gamma-$neurons can form post- and presynaptic areas, whereas $\alpha' - /\beta'-$neurons exhibit just postsynaptic sites at their dendritic branches [71]. Synaptic input and output areas are organized in calycal microglomerular elements. Claw-like postsynaptic endings of several KCs enclose a given presynaptic projection neuron bouton. Therefore, one projection-neuron is able to contact different classes of KCs in perfect synchrony [72]. For instance, two copies of the same information might exist in different systems for differential processing. [71] suggested that the synaptic organization is suited for dendro-dendritic (i.e. bi-directional) communication between different KCs at the level of the calyx. [49] reported inhibitory input from the lateral horn into the calyx in locusts. This input leads to 20Hz-oscillations within the calyx and seems to shut off projection neuron input every 50ms [44]. In addition to the sparseness in time there is a sparse code implemented in the way how projection neurons converge onto individual KCs [70]. Respective connections between the lateral horn and MB calices are known also in *Drosophila*, but their direction is up to date undetermined. According to [70] sparse activity is useful in structures involved in memory in part because sparseness tends to reduce representation overlaps.

Neuroanatomical studies in *Drosophila* revealed arborizations of extrinsic and intrinsic MB neurons across the peduncle and mainly the lobe system. KCs have their dendritic specializations in the calyx, their axons run through the peduncle of the MB and bifurcate at its end into different MB-lobes. The γ-neurons run into the medial γ-lobe (and some bifurcate into a very small "heel"), α-/β-neurons bifurcate into the medial β- and the vertical $\alpha-$lobe. The $\alpha'-/\ \beta'$-neurons bifurcate into the medial β'- and the vertical $\alpha'-$lobe [73]. The lobes are the output region of the MBs and also a region for modulatory inputs [74, 75].

Intrinsic neurons provide an alternative modulation pathway between different KCs and/or KCs and other protocerebral brain areas. Extrinsic neurons, on the other side, may be able to bind sensory information processed earlier in

different lobes before or after any kind of modulation (see Fig. 6.1 EN-MB1-4).

MB modulation is one of the most interesting computational features for understanding olfactory-memory formation, consolidation and retrieval. To this end the MB model by [69] offers a possible explanation by allocating MB substructures to different modulation units. The model takes the three different KC types and their specific neuroanatomy into account and considers the organization of the MB-lobes into segments. Those segments are defined by the arborization of extrinsic MB neurons. The $\beta-$ and β'-lobes are subdivided into two and the $\alpha-$ and $\alpha'-$lobes into three segments per strata. Via these functional units the behavioral output of the MBs can be modulated. From here, for example, specific extrinsic MB neurons arborise, which are involved in the formation of a labile aversive memory [76], whereas some others help to integrate the internal state of hunger and appetitive memory in the fashion of a motivational switch [74].

Some of the MB-ENs specified as octopaminergic neurons (OAN; [77]) and others as dopaminergic neuron (DAN; [78]). The OANs are known to mediate the unconditioned stimulus in the reward processing [65, 66]. The reward neuron orthologous to the well-known VUMmx1-neuron in honeybees is the OA-vUMa2 neuron in flies [77].

The DANs play important roles in the acquisition of aversive and appetitive olfactory memory in flies (Fig.6.1 OAN and DAN; [79]). Their input to the MB subdivisions is weighing the processed information in the KCs, so that the behavioral outcome differs depending on the association of the stimulus with punishment or reward.

And last but not least KCs of the $\beta-$ and $\gamma-$lobes give rise to a functional feedback from these lobes centrifugally out to the antennal lobes via extrinsic MB neurons as shown in Fig. 6.1: EN-MB3 [48]. [48] reported a gain increase in the antennal lobes caused by this modulatory influence which may account for the formation of expectations.

Up to date there is no information on the extrinsic neurons connecting the MBs with premotor areas of the fly brain. Evidence comes from behavioral studies. Flies with ablated MBs show neither olfactory conditioned avoidance nor conditioned appetitive locomotor behavior and abnormal variations in their locomotor activity, suggesting premotor pathways which can be strengthened by learning and a general regulation of premotor areas by the influence of the MBs [80, 81].

Taking inspiration primarily from the fly system and from the different computational and learning capabilities of insect MBs, here a neural architecture is proposed which is useful also for visual tasks to be integrated with models of the Central Complex responsible for visual orientation. Involvement

of the fly MBs in respective tasks is based on behavioral evidence. However, the much more elaborate honeybee MB system does have known visual inputs to the calyces [82]. Also the organization of the visual inputs to the fly MB might be not so dissimilar to the olfactory system, as parallels in the glomerular organization of the visual input at the transition from the optic lobes to the lateral protocerebrum of flies are described [83].

The dimension of the network of the proposed computational model, in terms of a specific number of neurons and connections, does not match one to one with its biological counterpart. It indeed represents a scaled version ready for direct implementation in hardware for robot control applications [84, 85]. However, the neural architecture and biological structure have been maintained.

For the learning algorithms here it is proposed that information reaching the $\alpha^{'} - /\beta^{'}-$lobes is delayed during the path, so that the neural activity within the two lobe systems represents the current input ($\alpha - /\beta-$lobes) and the previous one ($\alpha^{'} - /\beta^{'}-$lobes). The whole neural network is modeled using lattices of spiking neurons. Moreover, learning mechanisms based on the Spike-Timing Dependent Plasticity (STDP) are used to associate the KCs activity to a premotor area. Similar structures Central Pattern Generators have been already developed and can be integrated for a complete control of legged robots [87, 88].

6.3 The Proposed Neural Architecture

The spiking networks used to model the insect brain blocks are based on the Izhikevich spiking neuron, proposed in [17]. The value used for the parameters are different between ALs and MBs. In the first case the Tonic Spiking model has been used, whereas to model the KCs the parameters have been optimized to guarantee an efficient and robust clustering formation capability as explained in the next sections.

Neurons are connected through synapses; the synaptic model transforms the spiking dynamics of the pre-synaptic neuron into a current that excites the post-synaptic one. The mathematical response of the synapses to a pre-synaptic spike is ruled by the following equation:

$$\varepsilon(t) = \begin{cases} Wt/\tau \exp\left(1 - t/\tau\right), & \texttt{if } t > 0 \\ 0 \ , & \texttt{if } t < 0 \end{cases} \tag{6.1}$$

where t is the time lasted from the emitted spike, τ is the time constant and W is the efficiency of the synapse. This last parameter can be modulated

with experience. The STDP has been used to reproduce Hebbian learning in biological neural networks [26, 27]. All the equations are solved using the Euler method with an integration time of 0.08 ms.

6.3.1 Antennal Lobe Model

Inspired by the insects' ALs, we can assume to have a layer able to codify the odor components (i.e. odorants) or, moving to the visual domain, the extracted *features* of objects. As in the insect ALs each glomerulus is able to detect a specific odorant (or a specific side chain of different odorants), in the model each neuron in this layer encodes a particular aspect related to a detected object. Neurons within the AL model are organized in groups. Each group codifies a kind of feature or odorant, and neurons in the same group codify different values or intensity of that feature. Neurons in the same group are linked together through inhibitory synapses. This topology implies that, when the AL layer is stimulated, after a short transient time, only one neuron in each group remains excited, according to a winner-takes-all topology. Neurons in different groups are linked together through plastic synapses, reinforced when neurons are firing together, according to the Hebbian rule. Therefore, when an odor is presented to the network, it is decomposed within the AL in its relevant odorant features, and the corresponding neuron of each feature group remains excited.

In the proposed simulations, the AL layer is constructed of a 4x4 lattice. In particular, there are four groups of neurons (f_1, f_2, f_3 and f_4), and each group is made of four neurons (for instance, the neuron j in the group f_i will be called f_{ij}). Neurons in the same group are connected to each other through inhibitory synapses, with a synaptic efficiency $W^{AL} = -3$. Neurons in different groups that, after the presentation of an object, fire together, are increasing the efficiency of the synaptic connection with a $\Delta W^{AL} = 2$. The initial value of such synapses is zero. When an object is detected, the neurons of the first layer encoding the features of that object are excited with an input current $I_{AL} = 70pA$.

The AL model topology is inspired by the biological case [54], in which excitatory and inhibitory connections allow the interaction between glomeruli in order to realize the primary odors representation. Each neuron in the AL layer has a probability P = 0.25 of being connected to the KCs. The choice of the sparse connections between the first and the second layer is directly drawn from the sparse connections in the biological counterpart [49]. The main issue is related to the design of connections within each layer. The synapses between the first and second layer have a fixed efficiency of $W^{AL,KC} = 10$.

6.3.2 Mushroom Body Lobes and Lateral Horn

Like in the biological counterpart, and as outlined previously, the KCs of the MBs project, through the peduncle, to five main appendices, called lobes. They possess roughly the same topology, but were shown to serve different functions. The architecture is restricted to model the structure and functions of the $\alpha-/\beta-$lobes, and the $\alpha^{'}-/\beta^{'}-$lobes, divided into two main networks. The two networks representing the KCs, project random dendritic arborizations to the ALs. Each network is designed so as to show a cooperative-competitive dynamics: if excited, the neurons in the AL layer begin a competition and, after a transient, only one cluster of neurons will remain active and stable. The LH model resets both the networks each 120 ms.

In the architecture each lobe is a 9x9 lattice of neurons with a toroidal topology. The neurons in this layer are all connected to each other according to the paradigm of local excitation and global inhibition. A neighborhood of radius $r = 1$ is defined. In this way, each neuron is connected to the neurons in its neighborhood and with itself through excitatory synapses with an efficiency of $W_{near}^{KC} = 50$. It is also connected with the other neurons of the lattice through inhibitory synapses with an efficiency of $W_{far}^{KC} = -30$. This set of connections gives the network its clustering capabilities. The time constant used for fast excitatory and inhibitory synapses in the network is $\tau_{fast} = 1ms$.

The lobes are connected to each other through two sets of plastic synapses, one from the $\alpha - /\beta-$lobes to the $\alpha^{'} - /\beta^{'}-$lobes and the other set from the $\alpha^{'}-/\beta^{'}-$ to the $\alpha-/\beta-$lobes. It is known from neurobiology that the neurons belonging to the two clusters are morphologically different. Moreover, whereas $\alpha - /\beta-$ neurons give information back to the ALs, generating feedback at the sensory stage, the $\alpha^{'} - /\beta^{'}-$ neurons provide no output signals back into the system, at the level of the calices. So we can assume that the information which arrives to these lobes is retained there and used as a kind of backup copy for memory purposes. In particular this is analogous to hypothesize that the signals coming from the ALs through the calices are delayed while arriving in the $\alpha^{'} - /\beta^{'}-$lobes. The implementation of this concept implies that the winning cluster in the $\alpha-/\beta-$lobes represents the odor presented to the ALs at the actual step, whereas the winning cluster in the $\alpha^{'}-/\beta^{'}-$lobes represents the odor presented to the ALs at the previous time step. The synapses between the lobe systems are reinforced when two clusters in different lobes are concurrently active. This structure can be used to detect whether the object presented to the ALs remains the same in two subsequent steps. In fact, if this is true, the plastic synapses between the lobe systems create a positive loop between the clusters in the two lobe systems: this allows the networks to increase the spiking rate of the active neurons. It is assumed also to have a neuron

sensitive to the firing activity of the $\alpha - /\beta-$lobes network. The sequence of the network evolution is schematically shown in Fig. 6.2 where, in the first step, two subsequent presentations of the same object generate a positive loop between the two lobe systems and a corresponding increase of spiking rate, whereas during the following presentation, a different object is identified as a consequence a loop is no longer generated and the spiking activity within the lobes is no longer boosted. During the first 1000 integration steps, the winning clusters are able to emerge independently in the two lobe systems. Soon after the synaptic connections between the winning clusters are strengthened and the effect of the connections is evaluated for another 500 integration steps. Only if the cluster associated with the first object in the $\alpha' - /\beta'-$lobes and that one associated with the second object in the $\alpha - /\beta-$lobes are the same (see Fig. 6.2 second column, the yellow and red dot indicating the winning clusters are in the same position), a positive loop can be created. If the two active clusters in the two lobe structures are not associated with the same object, the positive recurrent connections are not able to create a loop as shown in the last case examined in Fig. 6.2. In the presented model the mean spiking activity of the $\alpha-/\beta-$lobes is encoded in a neuron used to discriminate the matching/no-matching events.

6.3.3 Premotor Area

Biological experiments revealed that context generalisation, visual attention, salience based fixation and decision making are all MB mediated behaviors [89, 57, 39, 90, 91]. Furthermore, aspects of the control of motor activity are also linked to the MBs. For example, initial motor activity in MB-ablated flies is high, whereas long-term measurements show a decrease in motor activity [81, 80].

In the proposed model the activity of the KCs in the MB-lobes is finally used to control the system behavior, making a link to the Premotor Area primarily useful for robot control purposes. Let us consider a simple choice: the agent can decide if the presented object is attractive and worth to be followed or not. The MBs and the Premotor Area are connected via an associative structure that uses the STDP paradigm for a positive/negative-based reinforcement learning. In particular, four different neurons were considered: the *Reinforcement Neuron* (RN), the *Matching Neuron* (SN), the *No-Matching Neuron* (DN) and the *Premotor Neuron* (PmN). The network topology is depicted in Fig. 6.3. When the reward signal is active, an input current of $I_{RN} = 100pA$ is provided to the RN. The RN is connected to the PmN through a fixed synapse, $W_{RN} = 40$, representing the unconditioned response to the reward. The SN is a special neuron that it is assumed to be sensitive to the

mean spiking activity of the $\alpha - /\beta -$lobes. In particular, if the activity of these lobes is larger than a given threshold, the SN is active, excited through a constant current $I_{SN} = 40pA$. The SN is connected to the PmN through a plastic synapse, as well as the DN that is spontaneously active but can be inhibited by the SN. Moreover, another set of plastic STDP synapses links the $\alpha - /\beta -$ neurons to the PmN for a classical associative learning purpose.

6.4 Simulation Results

Inspired by the biological background, a set of experiments on learning in MBs are proposed in the following. The setup is able to learn to associate a targeting behavior to specific odors, depending on the specific odorant features, using a classical conditioning mechanism. At the same time, a more complex kind of learning, based on the delayed matching-to sample task has been considered.

In a first experiment the capability of the network to solve a classical conditioning task is shown. The simulation is divided into two phases, a learning and a test phase, and it has been repeated with two different testing setups. In particular, in the learning phase a sequence of ten odors (here simulated through abstract objects) is presented to the network. Here it is assumed to have three different odors: A, B and C. In particular, odor A is represented by odorant features associated with neurons f_{11}, f_{21}, f_{31} and f_{41} of the AL layer, odor B is represented by neurons f_{12}, f_{22}, f_{32} and f_{42} and odor C by the neurons f_{13}, f_{23}, f_{33} and f_{43}. A positive reinforcement signal is associated to odor A and so, whenever odor A is presented, the reinforcement neuron is also excited. The STDP is then used to establish the correlation between odor A, represented by a cluster in the $\alpha - /\beta -$lobes, and the PmN. During the subsequent test phase, no reward is given and the network must use the stored experience to make a choice that is visible in terms of level of activation of the PmN. In a second experiment the capability of the architecture to implement a more sophisticated kind of learning is investigated. In this case, the architecture should learn to activate the PmN only if two matching objects are presented in sequence, according to the matching-to-sample paradigm. In order to avoid possible ambiguities, here it is indicated as *simulation step* the interval between two different presentations of objects (1500 integration steps), whereas the integration step corresponds to 0.08 ms. The STDP is then used to establish the connection between the SN, active only when the loop interaction between lobes indicates the presence of a persistent object, and the PmN. As it is possible to notice from Fig. 6.4, the presence of loop connections between the lobes increases the spiking activity. In particular, Fig. 6.5 indicates

that it is possible to find a threshold in the neural activity of the $\alpha-/\beta-$lobes to distinguish the activity in the case of loop and no-loop connection between the lobe systems.

Fig. 6.6 shows the evolution of the membrane potential of the PmN and reward signal provided during the learning phase in the first and second experiment. During the learning phase the PmN follows the reward: in the first case associated with odor A and in the second case associated with the Matching event. The evolution of the synaptic weights subject to STDP is shown in Fig. 6.7 where only the trend of the winning neurons in the $\alpha-/\beta-$lobes is shown. It is evident from the weights evolution: in the first case the system learns the correlation between the reward and the odor A, whereas in the second case the initial ambiguity between odor A and a Matching event due to the particular sequence of presented objects is solved around the end of the simulation, when the correlation between reward and Matching event is well established. However the STDP learning rule is not only applied to the winning neuron (i.e. the most active one) but also to the other active neurons in the winning cluster of the $\alpha-/\beta-$lobes lattice. Finally, the behavior of the network was tested after the learning phase, without presenting a reward signal (see Fig. 6.8). The knowledge, acquired in the form of synaptic weights, is able to correctly activate the PmN either when the preference for odor A is learned or when the preference for Matching is formed. In this last case the network is able to identify Matching events even if odors never presented before are given as input (i.e. new odor C).

6.5 Discussion and Conclusions

Insects are a point of reference in neuroscience and their autonomous learning capabilities are amazing considering their tiny brain dimensions and their neuronal connectivity. Physiology and biochemistry of these intriguing architectures have been deeply investigated in these last years both to understand the sources of these astonishing capabilities and to design powerful autonomous machines and control algorithms. Inspired by biological evidences in honeybees and flies, a neural architecture has been designed and tested in simulations. The architecture derives from the olfactory and learning system primarily of flies and was found able to solve classical conditioning but also more complex tasks, not yet discovered in flies, like the delayed matching-to-sample tasks. The network was suitably scaled, in terms of dimensions, with respect to the biological counterpart, to provide both an efficient and rapid design using conventional computer architectures, and a direct shortcut to an efficient hardware implementation. Furthermore the system is based on the generation of spatio-

temporal patterns of activities within neural lattices and this approach was previously investigated in robot control applications [92, 53].

To understand neural circuits in insect brains, several approaches can be followed concurrently: both behavioral and neurophysiological experiments, and the realization of computational models at different levels of complexity.

Interesting examples of MB modeling are available in the literature. A well-known model for olfactory associative learning was proposed by [43]. This model addresses the larval stage, reproducing the effect of positive and negative reinforcements in olfactory conditioning. On the basis of these biological evidences, other ideas were developed to design biologically plausible models of the MBs. A more detailed analysis was performed by [70] who addressed the olfactory representation in *Drosophila* on the basis of KC in-vivo recordings.

[94] designed a high-level computational model of MBs for associative learning using simplified models of neurons and synapses and a learning rule based on activity dependent pre-synaptic facilitation. The developed model, in order to fill the gaps in existing knowledge, acquired some information from invertebrate studies and in particular the synaptic mechanisms underlying learning and memory in *Aplysia*. This procedure has been followed also in the present study, where knowledge on the MB functions was taken from bees and other insects and transferred to *Drosophila*. The feedback mechanisms used in [94] to stabilize the learning procedure allow to increase synaptic strength at an initial level appropriate for an association and to prevent strength increase for established associations. The model uses STDP and Hebbian learning to create associations between stimuli and it has been hypothesized that the matching of similar samples can be obtained through resonance using a positive feedback loop. However, the feedback mechanisms used in [94] to avoid the further increase of synaptic weights for established associations will be considered to further refine the proposed model at the level of the pre-motor area for behavior selection.

Self-organization properties of the MBs are discussed in [93]. Their model is based on spiking neurons and synaptic plasticity, distributed through different layers. It is able to show consistent recognition and classification of odors. In their study the MBs are assumed to be multi-modal integration centers combining olfactory and visual inputs. As in the presented model, their system capabilities are independent of the type and source of information processed in the MBs.

[95] investigated the interaction of MBs and ALs in non-elemental learning. Different levels of learning and reinforcement mechanisms were considered at the stage of the KCs to create a coincidence detector and non-elemental learning. The present study considers learning at the KC layer and also plasticity

at the level of the AL as suggested by [50]. They had applied important filtering mechanisms to reduce noise and reconstruct missing features directly at the input level. Moreover, the different roles of specific lobes in the MBs, not considered in [95], has been addressed in the current computational model.

The learning capacity of the model by [95], which is a simplification of the fly MBs, seems to be larger than the capacity shown by flies in shock-odor association experiments. The current model has not been compared to fly experiments, which do not exist to date. However, the model shows that the MB structure is well suited for performing matching-to-sample tasks.

In the actual model, as previously outlined, single objects are consecutively presented to the network, which has to decide if the actually presented object matches or not the previously presented one. The model does neither take notice of the type of features shown by the objects, nor of the fact that multiple objects could be contemporarily present in the environment, but considers the object presented to the network as the results of a segmentation. Moreover, the network parameters were designed to allow a learning convergence within a few reward cycles. This last choice was adopted in view of a robotic implementation of the network. However, the network reported here shows the key ingredients for modeling a generalization of the matching-to-sample task: the concept of sameness. In fact, biological experiments in honeybees present learning campaigns involving much longer series of presentations and reward cycles before the animals grasp the concept of sameness. Moreover, several sensory modalities are commonly involved. All these aspects could be considered in a generalization of the network, which therefore could be useful to model the concept of sameness.

In conclusion, the model architecture discussed here represents a fundamental building block toward an artificial neural processing structure unifying different functionalities, and performing different behaviors, that biological counterparts are able to show.

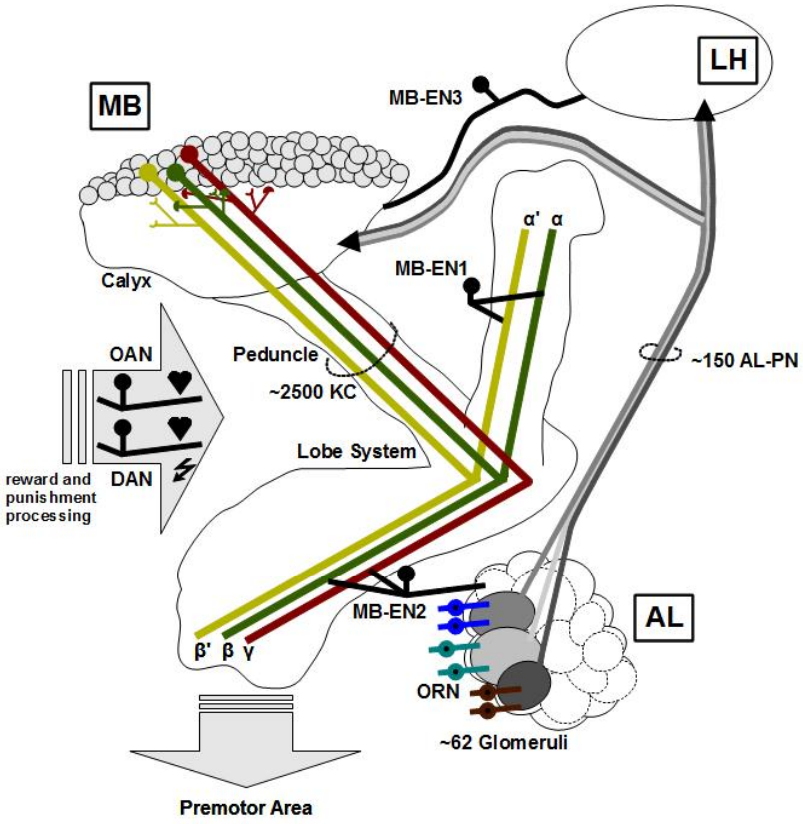

Figure 6.1: Block scheme of the processing of odor stimuli in insects. Olfactory receptor neurons (ORN) transfer information to the Antennal Lobes (AL). Each of the 62 glomeruli there is specific for a particular odor receptor. The ALs' activity is transferred through the Projection Neurons (AL-PN) to the Kenyon Cells (KC) in the Mushroom Body (MB) and to the Lateral Horn (LH) region. The calyx of the MB is the KC input region for PN odor information, but KCs have also mixed synaptic terminalia (postsynaptic (open semicircle) and presynaptic (full semicircle) allowing for inter-KC traffic. The peduncle of the MB is composed of KC axons which project into five different lobes of the lobe system: ($\alpha - /\beta-$neurons (green) bifurcate in the $\alpha-$ and $\beta-$lobe, $\alpha' - /\beta'-$neurons (yellow) bifurcate in the $\alpha'-$ and $\beta'-$lobe, γ-neurons (red) project in the γ-lobe. The KCs, through axo-axonal connections lead to the formation of spatio-temporal patterns at the level of the lobes (MB-EN1). Projections from the lobes to the AL would be well suited for controlling filtering of sensory information there (e.g. expectation driven selective gain control). MB extrinsic neurons (MB-EN3) coming from the LH are resetting the MB activity with inhibitory input to the calyx. Octopaminergic Neurons (OAN) mediate the unconditioned stimulus in the reward processing, whereas dopaminergic Neurons (DAN) play important roles in the acquisition of aversive and appetitive olfactory memory. The Premotor Areas of the insect brain are modulated by the MBs, but a direct neuronal link is unknown to date.

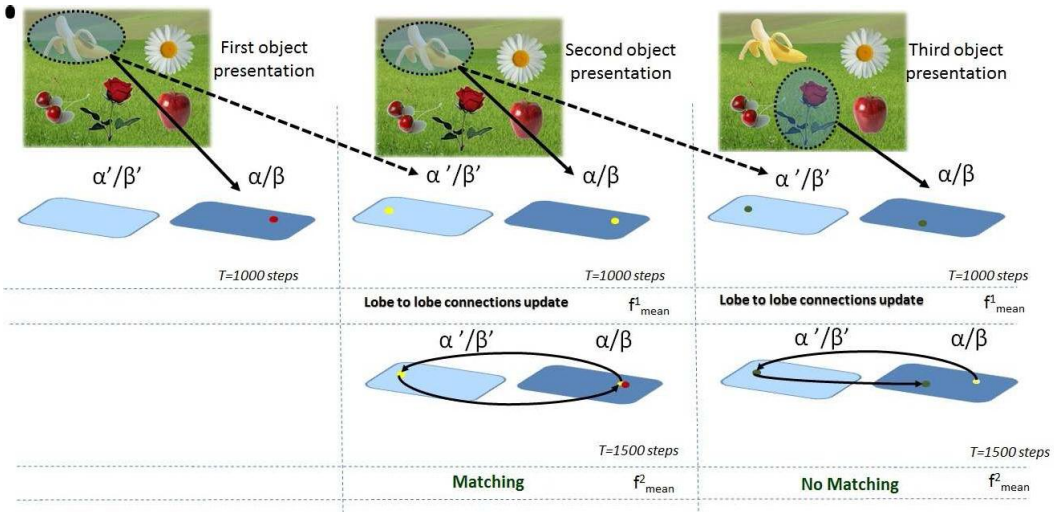

Figure 6.2: Processing steps executed by the network during the presentation of a series of odors (here presented through objects). When the first object is presented information about its characteristics are transferred to the $\alpha - /\beta-$lobes of the MBs and a cluster arises in the lattice (represented here by objects). During the presentation of a second object the same process for the $\alpha - /\beta-$lobes is performed whereas the $\alpha^{'} - /\beta^{'}-$lobes are exited by the previously presented object. These presentations lead to the emergence of two clusters in both of the lobe systems (i.e. after T=1000 simulation steps) and the plastic synaptic lobe-to-lobe connections are increased: the connection between the previously winning neuron of the $\alpha - /\beta-$lobes and the current winning neuron of the $\alpha^{'} - /\beta^{'}-$lobes is strengthened together with the synapses between the current $\alpha^{'} - /\beta^{'}-$ winner and the current $\alpha - /\beta-$winner. The mean spiking activity of the $\alpha - /\beta-$lobes (f^2_{mean}) computed in the interval [1000 - 1500] integration steps is then compared with the activity without the lobe-to-lobe connection (f^1_{mean}). If a loop has been created (i.e. the winning neuron in the $\alpha - /\beta-$lobes is in the same position) a relevant increase in the spiking rate is obtained allowing the matching/no-matching discrimination.

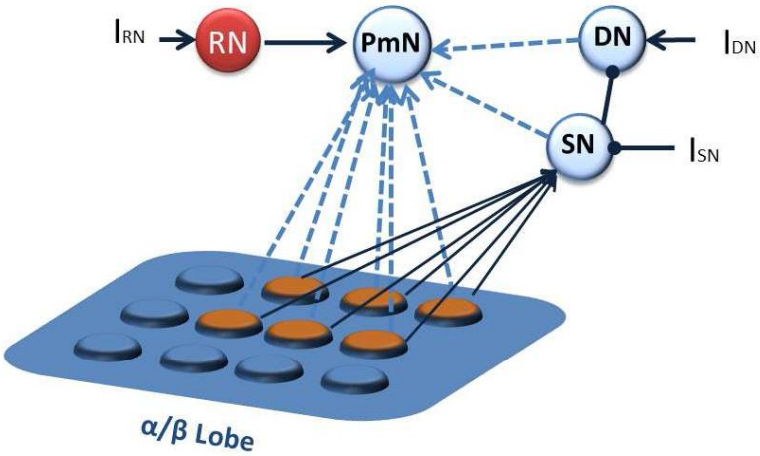

Figure 6.3: Scheme of the interaction between the $\alpha - /\beta-$lobe layer in the MBs and the Premotor Area. Plastic synapses (dashed lines) connect the lobe layer with the Premotor Neuron (PmN) as well as the Matching/No-Matching Neurons (SN and DN) with PmN. Fixed synapses are shown as solid lines (for the sake of clarity only a subset of connections coming from the $\alpha - /\beta-$lobe layer is visible in the scheme). If the spiking activity of the lobe layer is high enough, the generated current is able to activate the SN that otherwise is inhibited by the current I_{SN}. The SN inhibits the DN that is excited by a constant current I_{DN}.

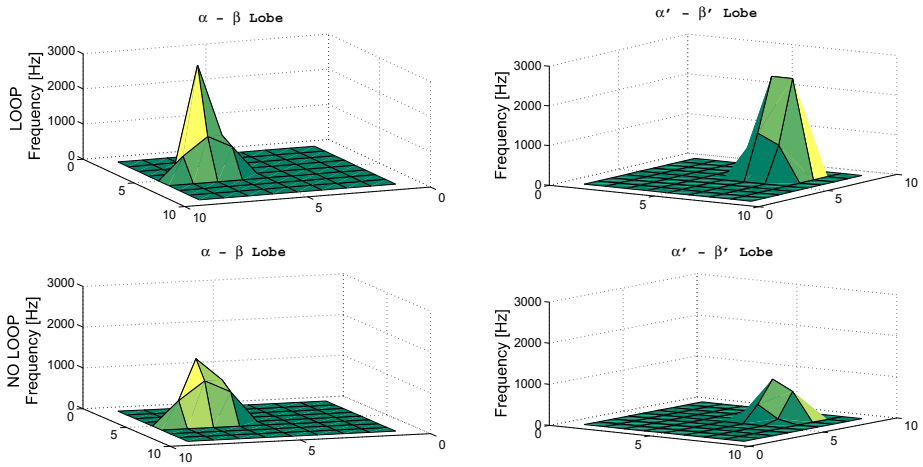

Figure 6.4: Clusters of spiking activity in the $\alpha - /\beta -$ and $\alpha^{'} - /\beta^{'} -$lobes in the case of loop and no loop connection between lobes. In the first case the activity of the networks is raised. The color indicates the level of activity in terms of frequency following the level reported in the frequency axis; warmer colors represent higher activity.

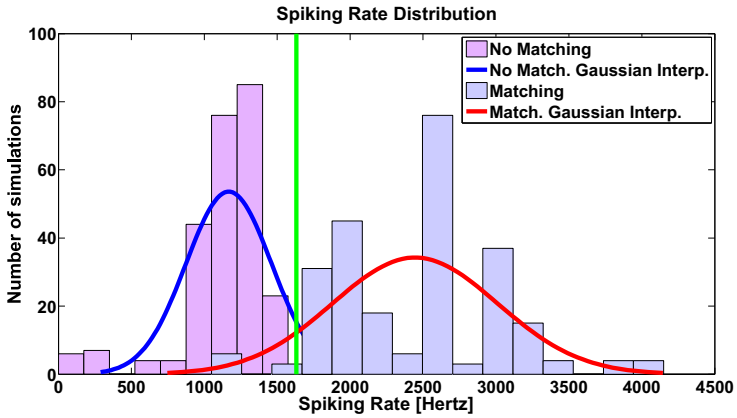

Figure 6.5: Statistical distribution obtained over 500 simulations of the mean spiking activity of the $\alpha - /\beta -$lobes after the increase of the feedback connections between lobes. When a loop arises, the spiking rate is significantly increased and choosing a threshold at f = 1632 Hz it is possible to distinguish the Matching/No-Matching of two consecutive presented objects, with an error of about 3%.

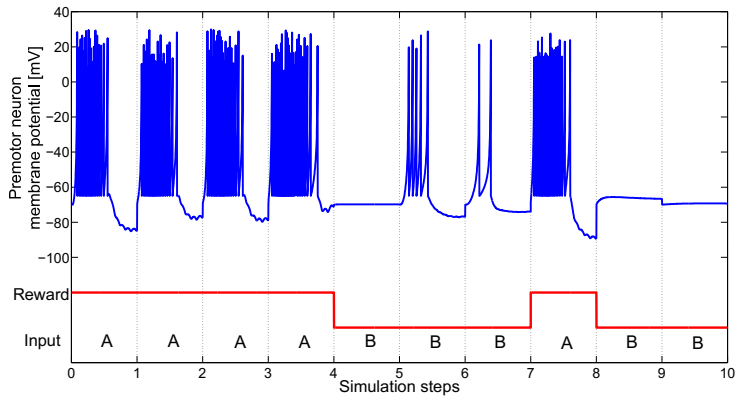

(a)

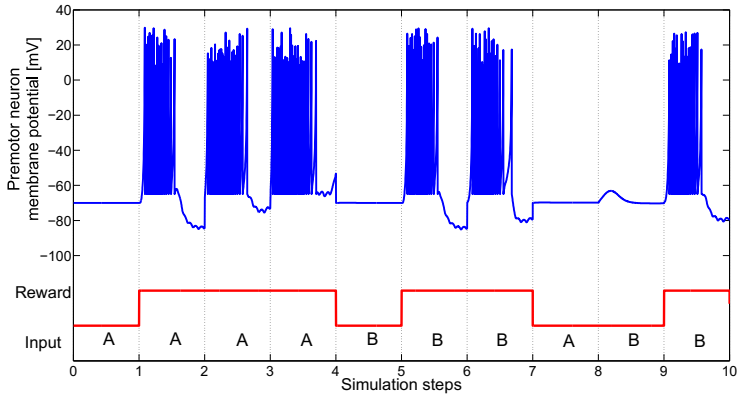

(b)

Figure 6.6: Evolution of the membrane potential of the PmN and reward signal provided during the learning phase. In simulation (a) the object A is rewarded whereas in (b) the same sequence of objects is presented as in simulation (a), but the Matching is reinforced. When the PmN is active the system indicates its preference for the presented object and a following behavior is elicited.

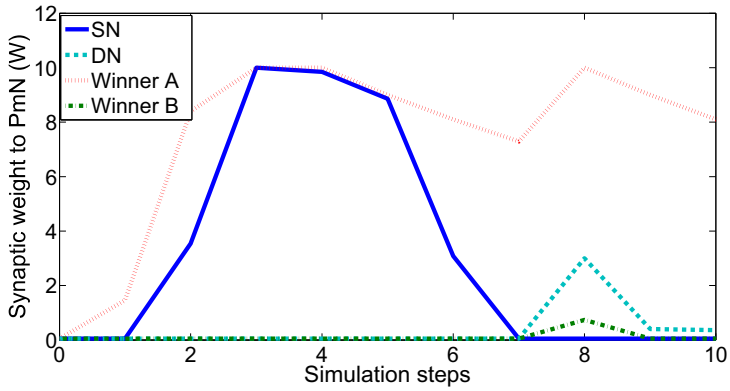

(a)

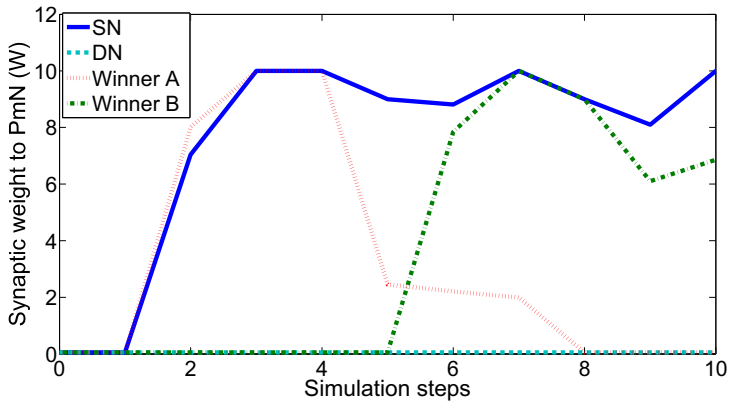

(b)

Figure 6.7: Evolution of the synaptic weights to the PmN, when the object A is rewarded (a) and when the Matching event is reinforced (b). Only the weights associated with the winner neuron (i.e. the most active one) are shown even if all the active neurons in the winning cluster are subject to the STDP learning.

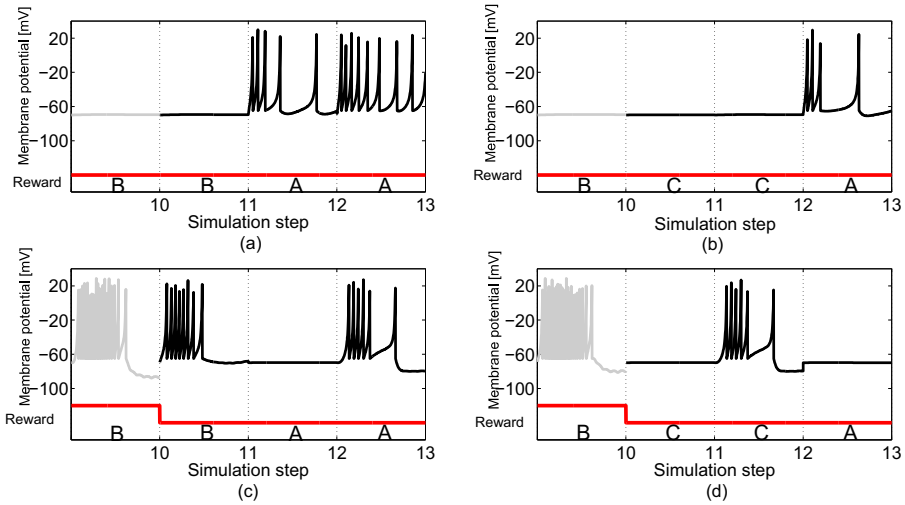

Figure 6.8: Results of the testing phase when the reward in no longer provided to the system and an autonomous decision has to be taken. The last simulation step of the learning phase (grey lines) and three new steps for the test phase (black lines) are shown. After learning, in which object A was rewarded (Fig. 6.6(a)), the system is able to follow A also during the test phase (a) and does not show any preference when new objects are presented (b). After learning, during which each Matching event is reinforced (Fig. 6.6(b)), the system is able to recognize autonomously successive presentations of the same object (c) even if it was never shown before to the network (d).

Chapter 7

Modeling attentional loop in the insect Mushroom Bodies

In this chapter a novel bio-inspired neural architecture is presented, in which the MBs role in attention tasks is focused. In particular, it is a multilayer spiking neural network where the MBs and their direct and or indirect interactions to other key elements of the insect brain, the Central Complex (CX) and the Lateral Horns (LHs), are modeled. The biological background of the proposed model is presented together with a detailed description of the architecture; simulation results and remarks on the biological counterpart are also reported.

7.1 Introduction

In this chapter a particular case of behavioral alteration is considered, supposedly linked to MBs in *Drosophila*, that regards the filtering of the sensorial inputs coherently with the attention towards a visual stimulus. In fact, recent works have shown that mutations affecting olfactory memory formation in *Drosophila* also produce distinct defects in visual attention-like behaviors [47, 57, 58]. In this chapter a model inspired by the *Drosophila* brain is presented. The model is a multilayer spiking neural network. The first layer is a visual sensorial layer and it has been modeled as a lattice of neurons, in which each neuron codifies a particular feature of the visual input. A locally competitive topology is here implemented. It can be noticed that biological evidences indicate the CX as the place of high visual processing and visual memory in *Drosophila* brain, and that no direct connection is found between CX and MBs. However, indirect connections that can involve other neural assemblies are commonly considered plausible in Neurobiology [59]. The first

layer of our model can be considered as a simplification of such interactions. The input layer randomly projects connections to the MBs model, which is composed of two distinct subnetworks, namely the $\alpha - /\beta -$ lobes layer and the $\alpha' - /\beta' -$ lobes layer. Feedback connections are present from the MBs layers to the input layer. The LHs model, as suggested from neurobiology [49], has been thought as an input-triggered system that provides a delayed global inhibition to the MBs network. The model here presented is an extension of the work described in the previous chapter, used to model expectation-based processes in the insect olfactory system.

7.2 Biological Remarks

The CX resides at the midline of the insect brain, between the protocerebral hemispheres. It is composed of four main regions [11]. The *fan-shaped body* (FB) is the largest neuropil which possesses eight fans in the latero-lateral extent, six layers in the dorso-ventral direction and four shells in the anterior-posterior direction. The *ellipsoid body* (EB) has a perfect toroid shape and possesses 16 segments and it has two radial zones. The paired *noduli* reside ventral to the FB just dorsal to the oesophagus. The *protocerebral bridge* (PB) is a rod-like neuropil composed of a chain of 16 glomeruli just posterior to the FB. Because there are no known projections from primary sensory areas to the CX, the input into the CX seems to be highly preprocessed. Experimental evidences from many different insect species demonstrate that primarily visual information is processed in the CX [12, 13]. The MBs are a paired structure of the insect protocerebral hemispheres. The MBs "frame" the CX without known direct connections. In flies, there is a prominent olfactory input from the antennal lobes into the calices. In fact, MBs and LHs are neural structures of the insect brain able to codify the spatio-temporal information coming from the glomeruli of ALs. Connections from LHs and MBs have been found; the entity of these connections in *Drosophila* are not well known, but in locusts, LHs offer an inhibitory effect to the MBs neurons [49]. Input from other sensory modalities is not obvious in *Drosophila*, but tasks related to vision, where MBs are involved, were identified for fly experiments. In honeybees, MBs receive prominent visual [14], gustatory, and mechanosensory [60] input. In flies and bees, the MBs lobe region receives information on sugar reward or electric shock. There is an output of the MBs to pre-motor areas of the brain. Inside the MBs the flow of information is through the MBs cells from the calyx towards the lobes. Very recently, recurrent connections between MBs and ALs have been found [48]. The presence of this functional feedback from the MBs to the ALs suggests top-down modulation of olfactory information processing in

Drosophila. The presence of dynamically changing conditions in the environment leads animal to develop attention process. Changing environments have lead animals to evolve attention-like processes. Attention facilitates to focus on the attended events, while filtering out irrelevant information. These interesting processes have been studied in *Drosophila* [47, 57, 58, 59], where mutations affecting olfactory memory formation also affects the visual attention-like behavior. In particular, results in [59] suggest that MB in flies behaves like a sensory gain controller, allowing the processing of salient signals, filtering out the background noise and distracting signals.

7.3 The Proposed Neural Architecture

Taking inspiration from the insect brain and from the different behavioral aspects and learning capabilities of the MBs, here a neural architecture mainly based on spiking neurons is proposed. This architecture is mainly constituted by three interacting lattices. The input lattice is derived from the capabilities of the CX. It is able to decompose and represent visual stimuli through features. The input layer randomly projects to the MBs $\alpha - /\beta -$ and $\alpha^{'} - /\beta^{'} -$ lobes. Each lobe is modeled as a spherical lattice with clustering capabilities. Delayed feedback synapses are present from the $\alpha - /\beta -$ lobes to the input layer. These connections act as a filter for the sensory inputs on the basis of the previously followed object. A block diagram of the architecture is shown in Fig. 7.1, where the different networks, their interactions and the main role are summarized.

7.3.1 The Neural Model and Learning Algorithm

The spiking networks used to model the insect brain blocks are based on the Izhikevich spiking neuron, proposed in [17]. The value used for the parameters are different between the ALs and MBs. In the first case the Tonic Spiking model has been used whereas to model the KCs the parameters have been optimized to guarantee an efficient and robust clustering formation capability as better explained in the next sections. Neurons are connected through synapses. The synaptic model transforms the spiking dynamics of the pre-synaptic neuron into a current that excites the post-synaptic one. The mathematical response of the synapses to a pre-synaptic spike is ruled by the following equation:

$$\varepsilon(t) = \begin{cases} Wt/\tau \exp\left(-t/\tau\right), & \texttt{if } t > 0 \\ 0 \ , & \texttt{if } t < 0 \end{cases} \tag{7.1}$$

where t is the time lasted from the emitted spike, τ is the time constant and

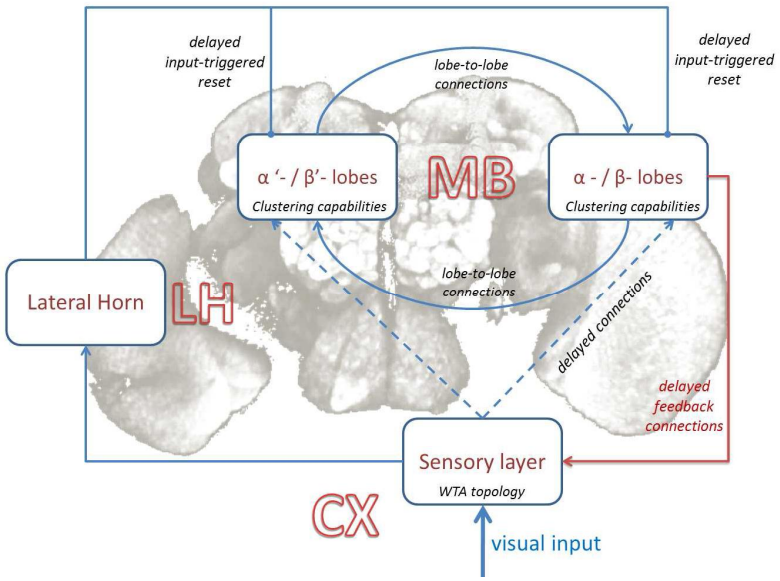

Figure 7.1: The proposed neural architecture. MBs lobes interact each other to detect the persistence of a visual stimulus. Feedback connections from the $\alpha -/\beta -$ lobes to the Sensory Layer act as a filter for the visual input. The Lateral Horn provides an input-triggered reset to the MBs lobes.

W is the efficiency of the synapse. This last parameter can be modulated through experience. The Spike-Timing Dependent Plasticity (STDP) can reproduce Hebbian learning in biological neural networks [26, 27]. Interesting applications of this learning paradigm to biorobotics, together with details on the parameters, are reported in [28].

7.3.2 The Sensory Layer

The CX resides in all insect brains and it is composed of four main regions [11]. In this chapter, the functionalities of one of these areas, the FB body, have been focused. Experimental evidences from *Drosophila* and many other different insect species demonstrate that primarily visual information is processed in the FB. In our model the *Drosophila* FB directly inspired the input layer. Even though direct connections between CX and MBs are not documented in biology, indirect connections are plausible [59]. Each neuron in the sensorial layer encodes a particular aspect related to a detected visual stimulus. Neurons within the input layer are organized in groups. Each group codifies a kind of feature, and neurons in the same group codify different values or intensity of that feature. Neurons in the same group are linked together

through inhibitory synapses. This topology implies that, when the layer is stimulated, after a short transient time, only one neuron in each group remains excited, according to a winner-takes-all topology. Therefore, when an object is presented to the network, it is decomposed in its relevant features, and the corresponding neuron of each feature group remains excited. Neurons in different groups are linked together through plastic synapses, instantly reinforced for neurons encoding different features of the same object. The input layer projects excitatory direct connections to the MBs. Each neuron of this layer is connected to each KC with a given probability of connection, recalling the sparseness of connections in the corresponding areas of the insect brain.

7.3.3 Mushroom Body Lobes and Lateral Horn interactions

Like in the biological counterpart, the KCs of the MBs project, through the peduncle, to specific appendices, called lobes. They possess roughly the same topology, but were shown to serve different functions. In our model, one network represents the $\alpha - /\beta -$ lobes, whereas another one represents the $\alpha^{'} - /\beta^{'} -$ lobes. The two networks are connected randomly with the input layer. Each network was designed to show a cooperative-competitive dynamics: if excited, the neurons in this layer begin a competition and, after a transient, only one cluster of neurons will remain active and stable. The LH model resets both the networks each 120 ms. The lobes are connected to each other through two sets of plastic synapses, one from the $\alpha - /\beta -$ lobes to the $\alpha^{'} - /\beta^{'} -$ lobes and the other set from the $\alpha^{'} - /\beta^{'} -$ to the $\alpha - /\beta -$ lobes. It is known from Neurobiology that the neurons belonging to the two clusters are morphologically different. Moreover, whereas $\alpha - /\beta -$ neurons give information back to the ALs, generating a feedback at the sensory stage, the $\alpha^{'} - /\beta^{'} -$ neurons were found to provide no output signals back into the system, but they just receive sensory input in the last place at the level of the calices. So it was assumed in the previous chapter that the information which arrives to these lobes is retained there and used as a kind of backup copy for memory purposes. The synapses between the lobe systems are reinforced when two clusters in different lobes are concurrently active. This structure was used in the previous chapter to detect whether the object presented to the input layer remains the same in two subsequent steps. In fact, under these conditions, the plastic synapses between the lobe systems create a positive loop between the clusters in the two lobe systems: this allows the networks to increase the spiking rate of the active neurons. We assumed also to have a neuron sensitive to the firing activity of the $\alpha - /\beta -$ lobes network to detect this situation. Two

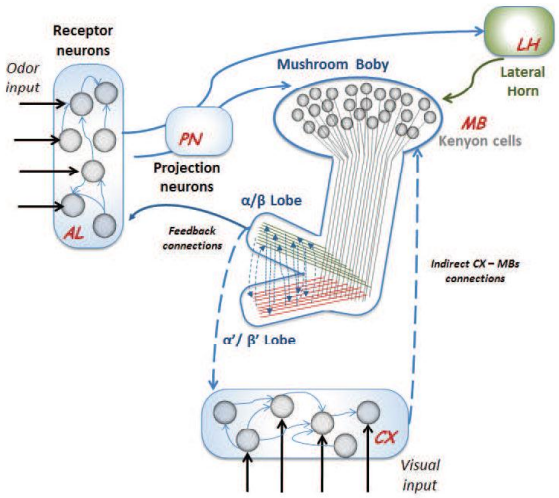

Figure 7.2: MBs and their interactions with the insect brain centers. MBs, together with the ALs and LHs, are the place for odor representation and learning. Biological evidences give MBs also a role in behavior adaptation on the basis of visual stimuli. Dashed lines represents indirect connections that involve other brain centers. Direct CX to MBs connections have not been found in biology until now.

subsequent presentations of the same object generate a positive loop between the two lobe systems and a corresponding increase of spiking rate, whereas the successive presentation of a different object is identified due to the missing loop that does not boost the spiking neural activity in the lobes. We will assume that the feedback synapses are activated by the increase of the synaptic activity in the lobes. A biologically plausible scheme of the architecture is shown in Fig. 7.2; the MBs are responsible for the gating of preprocessed visual inputs coming from CX even if the identification of direct connections between the two centers is still missing in Neurobiology. The dynamical evolution of the neural architecture is shown in Fig. 7.3. The features presented are acquired by the first layer and used as input for the $\alpha-/\beta-$ lobes in the MBs, where a cluster arises. The second presentation of the same object leads to the detection of the sameness through the positive feedback among the $\alpha-/\beta-$ and $\alpha^{'}-/\beta^{'}-$ lobes. In the third step the presentation of multiple concurrent objects is managed by the system that, through the descending feedback connections between the $\alpha-/\beta-$ lobes and the sensory layer is able to devote its attention to the previous detected object, filtering out the disturbing input. The main part of the proposed architecture was carefully studied together with Neurobiologists in [**?**] and was found able to show emergent capabilities to cope with the

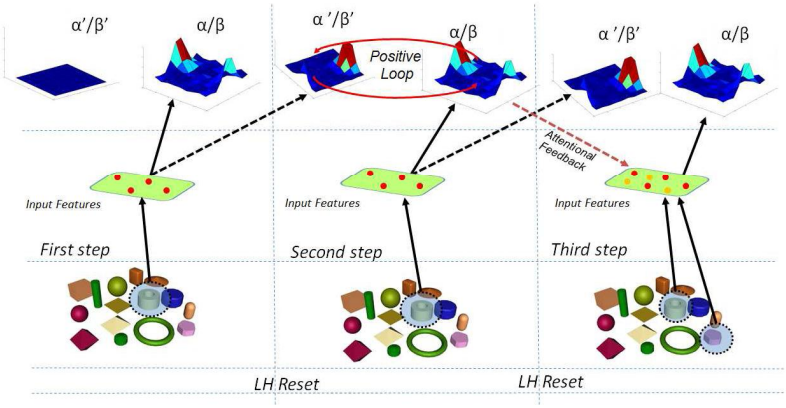

Figure 7.3: Attentional loop scheme: two subsequent presentations of the same object increase the activity of the lobes and activate the loop synapses between them. This event triggers the delayed activation of feedback connections back to the input layer, enhancing the top-down attentional loop towards that object (third step), even in presence of multiple concurrently presented objects or noise. Notice that the positive loop between the lobes appears also during the third step due to the cluster formation in the lobes. It is not reported to emphasize the presence of the attentional feedback.

"delayed match-to-sample" issue, well known in insects. This network did not take into account the presence of feedback synapses from the lobes to the input layer. The introduction of this loop enables to elicit attentional capabilities, the main theme of this paper.

7.3.4 The role of the feedback synapses

A set of feedback synapses, from the $\alpha - /\beta -$ lobes lattice to the input layer has been implemented in this augmented version of the MB network. These connections produce a pre-polarization of the input layer and act as a filter for the sensorial input, based on an attention-like paradigm. Feedback synapses are updated according to the STDP learning algorithm. The role of feedback connections in the insect olfactory system model has been analyzed on the basis of the biological evidences in [48]. In this chapter two major important differences are reported with respect to previous models: the first one is that the spatial temporal dynamics that was assumed to link the different object internal representations in time is modeled as a specific function of the lobes, and the second aspect is that the output of the feedback synapses is delayed; the postsynaptic current influences the input layer only after the lobes resetting via LHs. This is equivalent to assume that the action of these

feedback connections, being focussed to enhance attentional loops, is able to persist also after the inhibition from LHs.

7.4 Simulation Results

In this section the parameters of the network and the simulation results are presented.

7.4.1 Network Parameters

In the proposed simulations, the input layer consists of a 4x4 lattice of neurons. In particular, there are four groups of neurons (f_1, f_2, f_3 and f_4), and each group is made of four neurons (e.g. the neuron j in the group f_i will be called f_{ij}). Neurons in the same group are connected to each other through inhibitory synapses, with a synaptic efficiency $W^{FB} = -3$. Neurons in different groups that, after the presentation of an object, fire together, instantly increase the efficiency of the synaptic connection with a $\Delta W^{FB} = 7$. The initial value of such synapses is zero, and the synapses are reset each step. When an object is detected, the neurons of the first layer encoding the features of that object are excited with an input current $I_{FB} = 70pA$. Each neuron in the input layer has a probability P = 0.25 of being connected to KCs. The choice of the sparse connections between the first and the second layer is directly drawn from the sparse connections in the biological counterpart [49]. The main issue is related to the design of connections within each layer. The synapses between the first and second layer have a fixed efficiency of $W^{FB,KC} = 10$. In our architecture each lobe is a 9x9 lattice of neurons with a toroidal topology. The neurons in this layer are all connected to each other according to the paradigm of local excitation and global inhibition. A neighborhood of radius $r = 1$ is defined. In this way, each neuron is connected to the neurons in its neighborhood and with itself through excitatory synapses with an efficiency of $W^{KC}_{near} = 50$. It is also connected with the other neurons of the lattice through inhibitory synapses with an efficiency of $W^{KC}_{far} = -30$. This set of connections gives the network its clustering capabilities. The time constant used for fast excitatory and inhibitory synapses in the network is $\tau_{fast} = 1ms$. All the equations are solved using the Euler method with an integration time of 0.08 ms (i.e. one simulation step). A gaussian noise with zero mean and variance equal to the 10% of its nominal value is applied to each parameter of the architecture.

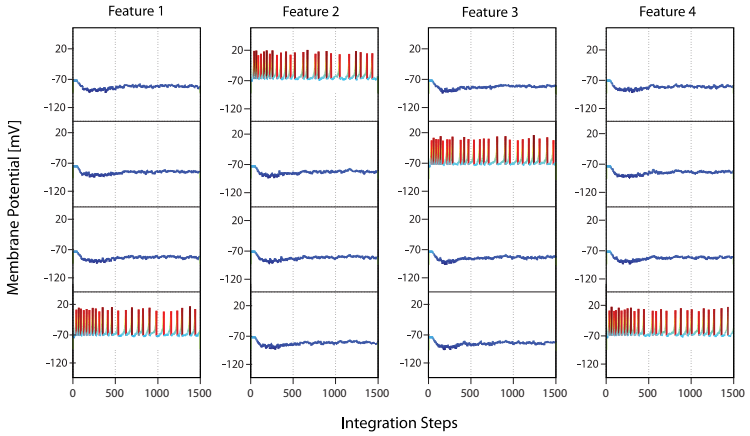

Figure 7.4: Expectation-like behavior. After two subsequent presentation of the same object, no input is present at the third step. The evolution of the input layer is shown. The expected features are reconstructed through the feedback connections coming from the MBs $\alpha-/\beta-$ lobes.

7.4.2 Experimental Results

In this section some simulation results are illustrated, in order to demonstrate how the proposed model works. In particular, three tests have been conducted. The first one aims at showing the arousal of expectation-like effects in this model. This kind of feature was already presented. The same test is here presented to show that the upgraded model introduced in this paper retain the old capabilities, and extend its performance including new ones, based on a more strict biological background. The other simulations aim to show the capabilities of the model in filtering the input stimuli according to the attention paradigm.

Expectation-like test

This simulation can be considered a preliminary test, in which the role of the feedback connections is introduced. After two subsequent presentations of the same object, no input is presented at the third step. As shown in Fig. 7.4, the feedback connections allow the reconstruction of the features of the object expected in the input layer.

Reinforcing the same object

After two subsequent presentations of the same object, again the same object is presented at the third step. In this case the feedback synapses reinforce

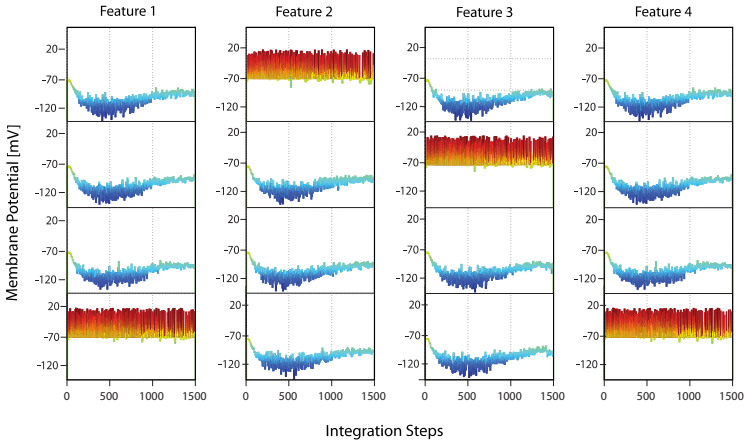

Figure 7.5: Reinforcement test. The feedback connections reinforce the activity of the neurons associated to the features of the presented object if it correspond to the expected one.

an already present stimulus. The spiking rate of the neurons in the first layer representing the features of the reinforced object is increased (Fig. 7.5).

Attention test

After two subsequent presentations of the same object, two objects are contemporarily presented at the third step. In particular, we assume that one of the objects is the expected one, whereas the other one is a distractor. In this case a competition between the neurons representing the features of the objects occurs in the first layer. The feedback synapses act as a bias on the expected features. The evolution of the membrane potential of neurons representing expected and unexpected features are shown in Fig. 7.6. After a transient, the winner-takes-all topology allows the network to filter out the unexpected object.

7.5 Remarks and Conclusions

Insects are a very interesting case of study both in Neuroscience and in Robotics. It is very useful to analyze simple insect brains that can solve complex tasks and process advanced sensorial data. Here an artificial neural network has been proposed, which consists in a multi layer network, inspired by neural structures of the *Drosophila* brain, the Central Complex and the Mushroom Bodies. These structures are involved in visual processing and visual memory, and in behavioral adaptation and olfactory learning, respectively.

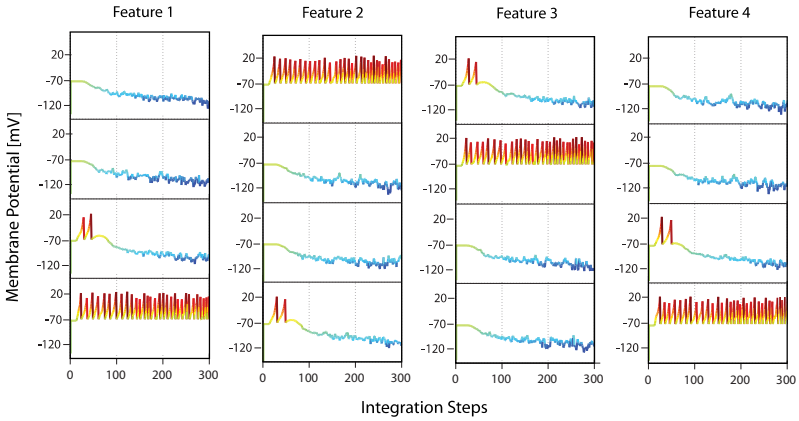

Figure 7.6: Attention test. The evolution of the membrane potential of neurons representing expected $f_{14}, f_{21}, f_{32}, f_{44}$ and unexpected features $f_{13}, f_{24}, f_{31}, f_{43}$ are shown here. After a transient, the winner-takes-all topology allows the network to filter out the unexpected object.

Even if no direct connection between these two neural centers was found in the Drosophila brain, we supposed from behavioral evidence that even the presence of an indirect link would suffice to reproduce some of the interesting capabilities involving multimodal integration. In this paper, the proposed model is able to reproduce an attention-like filtering of the sensorial input, which results to be of primary interest in mobile robotics, if visual inputs are taken into account. In fact simulation results show the robustness of the proposed architecture in presence of competing objects at the input layer, which could be used to enhance the capabilities of roving robots in the analysis of specific objects in cluttered environments, minimizing the effect of noise. The integration of this structure within the main blocks described in Chapter 1, will allow the realization an insect brain inspired neural architecture for applications in perceptual robotics.

Bibliography

[1] B. Webb, T.R. Consi, *Biorobotics : methods and applications*, Menlo Park, CA : AAAI Press/MIT Press, 2001.

[2] M. Dorigo, T. Stützle, *Ant Colony Optimization*, MIT Press. ISBN 0-262-04219-3, 2004.

[3] M.V. Srinivasan et al, "Honeybee Navigation: Nature and Calibration of the Odometer", Science 287, 851, 2000.

[4] F. Rind, R. Santer, J. Blanchard, P. Verschure, *Sensors and sensing in biology and engineering*, springerwiennewyork ed. Barth, Humphrey, Secomb, ch. *Locust's looming detectors for robot sensors*, 2003.

[5] B. Webb, T. Scutt, "A simple latency dependent spiking neuron model of cricket phonotaxis," *Biological Cybernetics*, vol. 82(3), pp. 247-269, 2000.

[6] P. Arena, L. Fortuna, M. Frasca, L. Patané, M. Pavone, "Realization of a CNN-driven cockroach-inspired robot", *International Conference on Circuits and Systems (ISCAS)*, 2006.

[7] J. Watson, R. Ritzmann, S. Zill, A. Pollack, "Control of obstacle climbing in the cockroach, Blaberus discoidalis, I. Kinematics", *J. Comp. Physiol. A*, vol. 188, pp. 39-53, 2002.

[8] H. Cruse, T. Kindermann, M. Schumm, J. Dean, J. Schmitz, "Walknet a biologically inspired network to control six-legged walking", *Neural Networks*, vol. 11, pp. 1435-1447, 1998.

[9] R. Strauss, C. Berg, "The Central Control of Oriented Locomotion in Insects - Towards a Neurobiological Model", *International Joint Conference on Neural Networks*, 2010.

[10] R. Strauss, "The Central Complex and the genetic dissection of locomotor behaviour", *Curr. Opin. Neurobiol.*, vol. 12, pp. 633-638, 2002.

[11] U. Hanesch , K.F. Fischbach, M. Heisenberg, "Neuronal architecture of the Central Complex in *Drosophila melanogaster*", *Cell Tissue Res.*, vol.257, pp.343-366, 1989.

[12] G. Liu, H. Seiler, A. Wen, T. Zars, K. Ito, R. Wolf, M. Heisenberg, L. Liu, "Distinct memory traces for two visual features in the *Drosophila* brain", *Nature*, vol. 439, pp. 551-556, 2006.

[13] K. Neuser, T. Triphan, M. Mronz, B. Poeck, R. Strauss, "Analysis of a spatial orientation memory in *Drosophila*", *Nature*, vol. 453, pp. 1244-1247, 2008.

[14] W. Gronenberg, G.O. Lopez-Riquelme, "Multisensory convergence in the Mushroom Bodies of ants and bees", *Acta. Biol. Hung.*, vol.55, pp.31-37, 2004.

[15] U. Schröter, R. Menzel, "A new ascending sensory tract to the calyces of the honeybee Mushroom Body, the subesophageal-calycal tract", *Journal of Comparative Neurology*, vol. 465, no.2, pp. 168-178, 2003.

[16] J.S. de Belle, M. Heisenberg, "Associative odor learning in *Drosophila* abolished by chemical ablation of Mushroom Bodies" *Science*, vol.263, pp.692-695.

[17] E.M. Izhikevich, "Simple Model of Spiking Neurons", *IEEE Transactions on Neural Networks*, vol. 14, n°6, pp. 1569-1572, 2003.

[18] S. Chernova, R.C. Arkin, "From Deliberative to Routine Behaviors: A cognitively inspired action-selection mechanism for routine behavior capture", *Adaptive Behavior*, vol. 15, n°2, pp.199-216, 2007.

[19] M. Mronz, R. Strauss, "Visual motion integration controls attractiveness of objects in walking flies and a mobile robot", *International Conference on Intelligent Robots and Systems, Nice*, pp. 3559-3564, 2008.

[20] L. Alba, P. Arena, S. De Fiore, L. Patané, R. Strauss, G. Vagliasindi, "Implementation of a Drosophila-inspired orientation model on the Eye-Ris platform", to appear in proceedings of Int. Conf. on Cellular Non linear Networks and their Applications, 2010.

[21] R. Möller, H. Hoffmann, "An extension of Neural Gas to local PCA", *Neurocomputing*, vol. 62, pp. 305-326, 2004.

[22] G. Hartmann, R. Wehner, "The ant's path integration system: a neural architecture". *Biol. Cybern.* vol. 73, pp. 483-497, 1995.

[23] X. Liu, R.L. Davis, "Insect olfactory memory in time and space", *Curr. Opin. Neurobiol.*, vol. 6, pp. 679-685, 2006.

[24] C. Margulies, T. Tully, J.Dubnau, "Deconstructing memory in *Drosophila*", *Curr. Biol.*, vol.15, pp.700-713, 2005.

[25] M. Mronz, "Die visuell motivierte Objektwahl laufender Taufliegen (*Drosophila melanogaster*). - Verhaltensphysiologie, Modellbildung und Implementierung in einem Roboter. *PhD thesis*, University of Wuerzburg, 2004.

[26] S. Song, K.D. Miller, L.F. Abbott, "Competitive Hebbian learning through spike-timing-dependent synaptic plasticity", *Nat Neurosci* vol.3, pp.919-926, 2000.

[27] S. Song, L.F. Abbott, "Cortical development and remapping through Spike Timing-Dependent Plasticity", *Neuron*, vol. 32, pp. 339-350, 2001.

[28] P. Arena, L. Fortuna, M. Frasca, L. Patané, "Learning anticipation via spiking networks: application to navigation control", *IEEE transactions on neural networks*, vol. 20, n. 2, pp. 202-216, February 2009.

[29] L. Seugnet, Y. Suzuki, L. Vine, L. Gottschalk, P.J.Shaw, "D1 receptor activation in the mushroom bodies rescues sleep-loss induced learning impairments in Drosophila", *Curr. Biol.*, vol. 18, pp. 1110-1117, 2008.

[30] K.G. Götz, R. Biesinger,"Centrophobism in Drosophila melanogaster. Physiological approach to search and search control", *J. Comp. Physiol. A*, vol. 156, pp. 329-337, 1987.

[31] S. De Belle, M. B. Sokolowski, "Heredity of rover/sitter: Alternative foraging strategies of Drosophila melanogaster larvae", *Heredity*, 5 9, pp. 73-83, 1987.

[32] M. Besson, J.R. Martin, "Centrophobism/thigmotaxis, a new role for the mushroom bodies in Drosophila", *J. Neurobiol.* 62: 386-396.

[33] B. Webb, "Can robots make good models of biological behaviour?", *Behavioral and Brain Sciences*, vol. 24, pp. 1033-1050, 2001.

[34] R.D. Beer, R.D. Quinn, H.J. Chiel, R.E. Ritzmann, "Biologically-inspired approaches to robotics", *Communications of the ACM*, vol. 40, pp. 30-38, 1997.

[35] N. Franceschini, J.M. Pichon, C. Blanes, "From insect vision to robot vision", *Phil. Trans. R. Soc. Lond. B.* , vol. 337, pp. 283-294, 1992.

[36] B. Webb, "Using robots to model animals: A cricket test", *Robots and Autonomous Systems*, vol. 16, pp. 117-134, 1995.

[37] D. Lambrinos, R. Moller, T. Labhart, R. Pfeifer, R. Wehner, "A mobile robot employing insect strategies for navigation", *Robotics and Autonomous Systems*, vol. 30, n° 1, pp. 39-64, 2000.

[38] M. B. Reiser, M. H. Dickinson, "A test bed for insect-inspired robotic control", *Phil. Trans. R. Soc. Lond.*, vol. 361, pp. 2267-2285, 2003.

[39] S. Tang, A. Guo, "Choice behavior of Drosophila facing contradictory visual cues", *Science*, vol. 295, pp. 1543-1547, 2001.

[40] P. Arena, S. De Fiore, L. Patané, P.S. Termini, R. Strauss, "Visual learning in Drosophila: application on a roving robot and comparisons", *Proc. SPIE* Microtechnologies for the new millennium, Prague (2011).

[41] P. Arena, M. Cosentino, L. Patané, A. Vitanza, "SPARKRS4CS: a software/hardware framework for cognitive architectures", *Proc. SPIE* Microtechnologies for the new millennium, Prague (2011).

[42] R.N. Huerta, T.Nowotny, "Fast and Robust Learning by Reinforcement Signals: Explorations in the Insect Brain". *it Neural Computation*, vol. 21, pp. 2123-2151, 2009.

[43] S. Scherer, R.F. Stocker, B. Gerber, "Olfactory learning in individually assayed *Drosophila* larvae", *Learn. Mem.*, vol. 10, pp. 217-225, 2003.

[44] T. Nowotny, M.I. Rabinovich, R.N. Huerta, H.D.I. Abarbanel, "Decoding temporal information through slow lateral excitation in the olfactory system of insects", *J. Comput. Neurosci.*, vol. 15, pp. 271-281, 2003.

[45] P. Arena, L. Patané, "Simple sensors provide inputs for cognitive robots", *Instrumentation and Measure Magazine*, vol. 12(3), pp. 13-20, 2009.

[46] P. Arena, S. De Fiore, L. Patané, M. Pollino, C. Ventura, "Insect inspired unsupervised learning for tactic and phobic behavior enhancement in a hybrid robot", *International Joint Conference on Neural Network*, 2010.

[47] B. van Swinderen, "Attention-like processes in *Drosophila* require short-term memory genes", *Science*, vol. 315, pp. 1590-1593, 2007.

[48] A. Hu, W. Zhang, Z. Wang, "Functional feedback from mushroom bodies to antennal lobes in the *Drosophila* olfactory pathway", *Proc. Natl. Acad. Sci. USA*, vol. 107(22), pp. 10262-10267, 2010.

[49] J. Perez-Orive, O. Mazor, G.C. Turner, S. Cassenaer, R.I. Wilson, G. Laurent, "Oscillations and sparsening of odor representations in the mushroom body", *Science*, vol.297, pp. 359-355, 2002.

[50] S. Sachse, C.G. Galizia, "Role of inhibition for temporal and spatial odor representation in olfactory output neurons: a calcium imaging study", *J. Neurophysiol.*, 87, 1106-1117, 2002.

[51] L. Chittka, J. Niven, "Are bigger brains better? ", *Current Biology*, vol. 19, pp. 995-1008, 2009.

[52] M.I. Rabinovich, A. Volkovskii, P. Lecanda, R. Huerta, H.D.I Abarbanel, G. Laurent, "Dynamical Encoding by Networks of Competing Neuron Groups: Winnerless Competition", *Phys.Rev.Lett.*, 2001.

[53] P. Arena, L. Fortuna, D. Lombardo, L. Patané, M. Velarde, "The WinnerLess Competition paradigm in Cellular Nonlinear Networks: Models and Applications, *Int. J. Circ. Theor. Appl.*, vol. 37, pp. 505–528, 2009.

[54] N.Y. Masse, G.C. Turner, G.S.X.E. Jefferis, "Olfactory information processing in *Drosophila*", *Curr. Biol.*, vol. 19, pp. 700-713, 2009.

[55] B. Gerber, S. Scherer, K. Neuser, B. Michels, T. Hendel, R.F. Stocker, M. Heisenberg, "Visual learning in individually assayed *Drosophila* larvae", *J. Exp. Biol.*, vol. 207, pp. 179-188, 2004.

[56] M.P. Nawrot, S. Krofczik, F. Farkhooi, R. Menzel, "Fast dynamics of odor rate coding in the insect antennal lobe", arXiv:1101.0271 v1 [physics.bio-ph], 2011.

[57] B. van Swinderen, K.A. Flores, "Attention-like processes underlying optomotor performance in a *Drosophila* choice maze", *Dev Neurobiol.*, vol. 67, n° 2, pp. 129-145, 2007.

[58] B. van Swinderen, B. Brembs, "Attention-Like Deficit and Hyperactivity in a *Drosophila* Memory Mutant", *The Journal of Neuroscience*, vol. 30, n° 3, pp. 1003-1014, 2010.

[59] W. Xi, Y. Peng, J. Guo, Y. Ye, K. Zhang, F. Yu, A. Guo, "Mushroom bodies modulate salience-based selective fixation behavior in *Drosophila*", *European Journal of Neuroscience*, vol. 27, pp. 1441-1451, 2008.

[60] U. Schrter, R. Menzel, "A new ascending sensory tract to the calyces of the honeybee Mushroom Body, the subesophageal-calycal tract", *Journal of Comparative Neurology*, vol. 465, no. 2, pp. 168-178, 2003.

[61] R. Menzel, U. Muller, "Learning and memory in honeybees: from behaviour to neural substrates", *Annu. Rev. Neurosci.*, vol. 19, 379-404, 1996.

[62] R. Menzel, "Searching for the memory trace in a mini-brain, the honeybee", *Learn. Mem.*, vol. 8, pp. 53-62, 2001

[63] P. Szyszka, M. Ditzen, A. Galkin, C.G. Galizia, R. Menzel, "Sparsening and temporal sharpening of olfactory representations in the honeybee mushroom bodies", *J. Neurophysiol.*, vol. 94(5), pp. 3303-3313, 2005.

[64] M. Giurfa, S. Zhang, A. Jenett, R. Menzel, M.V. Srinivasan, "The concepts of sameness and difference in an insect", *Nature*, vol. 410, pp. 930-933, 2001.

[65] M. Schwaerzel, M. Monastirioti, H. Scholz, F. Friggi-Grelin, S. Birman, M. Heisenberg, "Dopamine and octopamine differentiate between aversive and appetitive olfactory memories in *Drosophila*", *J. Neurosci.*, vol. 23, pp. 10495-10502, 2003.

[66] C. Schroll, T. Riemensperger, D. Bucher, J. Ehmer, T. Voller, K. Erbguth, B. Gerber, T. Hendel, G. Nagel, E. Buchner, A. Fiala, "Light-induced activation of distinct modulatory neurons triggers appetitive or aversive learning in *Drosophila* larvae", *Curr. Biol.*, vol. 16, pp. 1741-1747, 2006.

[67] J. Kasuya, H. Ishimoto, T. Kitamoto, T. (2009), "Neuronal mechanisms of learning and memory revealed by spatial and temporal suppression of neurotransmission using $shibire^{ts1}$, a temperature-sensitive dynamin mutant gene in *Drosophila melanogaster*", *Frontiers in Molec. Neurosci.*, vol. 2(11), pp. 1-6, 2009.

[68] E. Fishilevich, L.B. Vosshall, "Genetic and functional subdivision of the *Drosophila* antennal lobe", *Curr. Biol.*, vol. 15, pp. 1548-1553, 2005.

[69] N. Tanaka, H. Tanimoto, K. Ito, "Neuronal assemblies of the *Drosophila* mushroom body", *J. Comp. Neurol.*, vol. 508, pp. 711-755, 2008.

[70] G.C. Turner, M. Bazhenov, G. Laurent, "Olfactory representations by *Drosophila* mushroom body neurons", *J. Neurophysiol.*, vol. 99, pp. 734-746, 2008.

[71] F. Christiansen, C. Zube, T.F.M. Andlauer, C. Wichmann, W. Fouquet, D. Owald, S. Mertel, F. Leiss, G. Tavosanis, A.J. Farca Luna, A. Fiala, S.J. Sigrist, "Presynapses in kenyon cell dendrites in the mushroom body calyx of *Drosophila*", *J. Neurosci.*, vol. 31, pp. 9696-9707, 2011.

[72] Leiss, F., Groh, C., Butcher, N.J., Meinertzhagen, I.A., & Tavosanis, G. (2009). Synaptic organization in the adult *Drosophila* mushroom body calyx *J. Comp. Neurol.*, 517, 808–824.

[73] J.R. Crittenden, E.M.C. Skoulakis, K.A. Han, D. Kalderon, R.L. Davis, "Tripartite mushroom body architecture revealed by antigenic markers", *Learn. Mem.*, vol. 5, pp. 38-51, 1998.

[74] M.J. Krashes, S. DasGupta, A. Vreede, B. White, J.D. Armstrong, S. Waddell, "A neural circuit mechanism integrating motivational state with memory expression in *Drosophila*", *Cell*, vol. 139, pp. 416-427, 2009.

[75] T. iemensperger, G. Isabel, H. Coulom, K. Neuser, L. Seugnet, K. Kume, M. Iche-Torres, M. Cassar, R. Strauss, T. Preat, J. Hirsh, S. Birman, "Behavioral consequences of dopamine deficiency in the *Drosophila* central nervous system", *Proc. Natl. Acad. Sci.*, vol. 108, pp. 834-839, 2011.

[76] Y. Aso, I. Siwanowicz, L. Bracker, K. Ito, T. Kitamoto, H. Tanimoto, "Specific dopaminergic neurons for the formation of labile aversive memory", *Curr. Biol.*, vol. 20, pp. 1445-1451, 2010.

[77] S. Busch, M. Selcho, K. Ito, H. Tanimoto, "A map of octopaminergic neurons in the *Drosophila* brain", *J. Comp. Neurol.*, vol.513, pp.643-667, 2009.

[78] Z. Mao, R.L. Davis, "Eight different types of dopaminergic neurons innervate the *Drosophila* mushroom body neuropil: anatomical and physiological heterogeneity", *Frontiers in Neural Circuits*, vol. 3(5), 2009.

[79] Y.C. Kim, H.G. Lee, K.A. Han, "D1 dopamine receptor dDA1 is required in the mushroom body neurons for aversive and appetitive learning in *Drosophila*", *J. Neurosci.*, vol. 27, pp. 7640-7647, 2007.

[80] J.R. Martin, R. Ernst, M. Heisenberg, "Mushroom bodies suppress locomotor activity in *Drosophila* melanogaster", *Learn. Mem.*, vol. 5, pp. 179-191, 1998.

[81] C.N. Serway, R.R. Kaufman, C.N. Serway, R.R. Kaufman, R. Strauss, S.J. de Belle, "Mushroom bodies enhance initial motor activity in *Drosophila*, *J. Neurogenet.*, vol. 23, pp. 173-184, 2009.

[82] B. Ehmer, W. Gronenberg, "Segregation of visual input to the mushroom bodies in the honeybee (*Apis mellifera*)", *J. Comp. Neurol.*, vol. 451, pp. 362-373, 2002.

[83] N.J. Strausfeld, I. Sinakevitch, J.Y. Okamura, "Organization of local interneurons in optic glomeruli of the Dipterous visual system and comparisons with the antennal lobes", *Dev. Neurobiol.*, vol. 67, pp. 1267-1288, 2007.

[84] P. Arena, L. Fortuna, M. Frasca, L. Patané, L., C. Sala, "Integrating high-level sensor features via STDP for bio-inspired navigation", *ISCAS 2007*, 2007.

[85] P. Arena, S. De Fiore, L. Fortuna, M. Frasca, L. Patané, G. Vagliasindi, "Reactive navigation through multiscroll systems: from theory to real-time implementation", *Autonomous Robots*, vol.25(1-2), pp. 123-146, 2008.

[86] P. Arena, S. De Fiore, L. Patané, M. Pollino, M., C. Ventura, "STDP-based behavior learning on TriBot robot. *Proceedings of SPIE - the International Society for Optical Engineering*", 2009.

[87] P. Arena, L. Fortuna, M. Frasca, L. Patané, "Sensory feedback in CNN-based central pattern generators", *International Journal of Neural Systems*, vol. 13(6), pp. 469-478, 2003.

[88] P. Arena, L. Fortuna, M. Frasca, L. Patané, "A CNN-based chip for robot locomotion control", *IEEE Transactions on Circuits and Systems I: Regular Papers*, vol. 52(9), pp. 1862-1871, 2005.

[89] L. Liu, R. Wolf, R. Ernst, M. Heisenberg, "Context generalization in *Drosophila* visual learning requires the mushroom bodies", *Nature*, vol. 400, pp. 753-756, 1999.

[90] W. Xi, Y. Peng, J.Z. Guo, K. Ye, K. Zhang , J. Yu, "Mushroom bodies modulate salience-based selective fixation behavior in *Drosophila*", *Europ. J. Neurosci.*, vol. 27, pp. 441-451, 2008.

[91] K. Zhang, J.Z. Guo, Y. Peng, W. Xi, A. Guo, "Dopamine-mushroom body circuit regulates saliency-based decision-making in *Drosophila*", *Science*, vol. 316, pp. 1901-1904, 2007.

[92] P. Arena, L. Fortuna, D. Lombardo, L. & Patané, "Perception for action: Dynamic spatiotemporal patterns applied on a roving robot", *Adaptive Behavior*, vol. 16(2-3), pp. 104-121, 2008.

[93] T. Nowotny, R. Huerta, H.D.I. Abarbanel, M.I. Rabinovich, "Self-organization in the olfactory system: one shot odor recognition in insects", *Bio.l Cybern.*, vol. 93, pp. 436-446, 2005.

[94] D. Smith, J. Wessnitzer, B. Webb, "A model of associative learning in the mushroom body", *Biol. Cybern.*, vol. 99, pp. 89-103, 2008.

[95] J. Wessnitzer, J.M. Young, J.D. Armstrong, B. Webb, "A model of non-elemental olfactory learning in *Drosophila*", *J. Comput. Neurosci.*, vol. 32, pp. 197-212, 2012.